RHEINISCHE
FRIEDRICH-WILHELMS-
UNIVERSITÄT BONN

Microglial Activation in Alzheimer's Disease

Dissertation

Zur

Erlangung des Doktorgrades (Dr.rer.nat.)

der

Mathematisch-Naturwissenschaftlichen Fakultät

der

Rheinischen Friedrich-Wilhelms-Universität Bonn

vorgelegt von

Herrn Darío Tejera

aus

Montevideo, Uruguay

Bonn

2018

Angefertigt mit Genehmigung der Mathematisch-Naturwissenschaftlichen Fakultät der Rheinischen Friedrich-Wilhelms-Universität Bonn

1.Gutachter: Prof. Dr. Michael T. Heneka

Klinik für Neurodegenerative Erkrankungen & Gerontopsychiatrie (Univertitätsklinikum Bonn)

Deutsches Zentrum für Neurodegenerative Ekrankungen

2. Gutachter: Prof. Dr. Walter Witke

Institut für Genetik

Universität Bonn

Tag der Promotion: 21.11.2018

Erscheinungsjahr: 2019

Para Andrea, que me enseño amar….y a esta profesion.

“Que poderia ser mais difícil de conhecer que conhecer como conhecemos?” Antonio Damasio.

O sentimento de Si

TABLE OF CONTENTS

List of publications related to the thesis

1) *Microglia in Alzheimer's disease: the good, the bad and the ugly.* **Dario Tejera** & Michael T. Heneka. **Current Alzheimer's Research**. 2016;13(4):370-80.
2) *Microglia-derived ASC specks cross-seed amyloid-β in Alzheimer's disease.* Venegas C, Kumar S, Franklin BS, Dierkes T, Brinkschulte R, **Tejera D**, Vieira-Saecker A, Schwartz S, Santarelli F, Kummer MP, Griep A, Gelpi E, Beilharz M, Riedel D, Golenbock DT, Geyer M, Walter J, Latz E, Heneka MT. **Nature.** 2017 Dec 20;552(7685):355-361
3) *United Again: Sting and the Police.* **Dario Tejera** & Michael T. Heneka. **Neuron**. 2017 Dec 20;96(6):1207-1208
4) *Microglia modulation through external vagus nerve stimulation in a murine model of Alzheimer's disease*. Kaczmarczyk R, **Tejera D**, Simon BJ, Heneka MT. **Journal of Neurochemistry.** 2017 Dec 21

List of abbreviations

2PLSM	2-Photon Laser Scanning Microscopy
Aβ	Amyloid Beta
APP	Amyloid Precursor Protein
AD	Alzheimer's Disease
ASC	Apoptosis-associated speck-like protein containing CARD
BBB	Blood Brain Barrier
CNS	Central Nervous System
Con	Control
DREADD	Designer Receptor Exclusively Activated by Designer Drug
DBH	Dopamine Beta-hydroxylase
DSP4	N-(2-chloroethyl)-N-ethyl-2-bromobenzylamine hydrochloride
IL-1β	Interleukin 1-Beta
i.p	Intraperitoneally
LPS	Lipopolysaccharide
LC	Locus Ceruleus
LOAD	Late-onset Alzheimer's disease
MCI	Mild Cognitive Impairment
MXO4	Methoxy-XO4
mo	Month old
NLRP3	NACHT-,LRR-and pyrin-domain-containing protein 3
NA	Noradrenaline
NpHR	Halorodopsin
nNOS	Neuronal Nitric Oxide Synthase
NF-κB	Nuclear factor-κB
Psen	Preselin
PYD	Pyrin Domain
ROI	Region of Interest
ThT	Thioflavin-T
TLR	Toll like Receptor
TGF-β	Transforming Growth Factor-Beta
TNF-α	Tumor Necrosis Factor-alpha

TACE	TNF-α converting enzyme
TH	Tyrosine Hydroxylase
WT	Wild-Type

1. Summary

Alzheimer's disease (AD) is the most prevalent type of dementia and characterized by the deposition of extracellular amyloid-beta (Aβ) and tau hyper-phosphorylation. Over the past decade, neuroinflammation has emerged as an additional pathological component. In the brain, microglia, representing the brain major innate immune cells, play an important role during AD. Once activated, microglia show substantial changes in their morphology, characterized by a retraction of cell processes and concomitant increase of soma volume. Systemic inflammation is known to increase the risk for cognitive decline in humans including AD, however the mechanism remains elusive. In the first part of this dissertation, microglial changes upon a transient peripheral immune challenge in the context of aging and AD are assessed in vivo, using 2-photon laser scanning microscopy (2PLSM). CX3CR1-EGFP-positive microglia were monitored at 2 and 10 days post immune challenge by lipopolysaccharide (LPS). Microglia exhibited a significant reduction of branches and the area covered by those at 2 days after LPS, a phenomenon that had been resolved at 10 days. Importantly, morphology changes were concomitant to changes in the inflammatory response.

Transient systemic inflammation reduced microglial phagocytic clearance of Aβ in APP/PS1 mice, increasing amyloid deposition. Importantly, NACHT-,LRR- and pyrin (PYD)-domain-containing protein 3 (NLRP3) inflammasome deficiency blocked many of the observed microglial changes upon peripheral immune challenge, including alterations of microglial morphology and amyloid pathology. NLRP3 inhibition may thus represent a novel therapeutic strategy for brain protection during systemic inflammation.

In patients with AD, deposition of amyloid-β is accompanied by activation of the innate immune system, particularly microglial NLRP3 inflammasome activation. Activation of the NLRP3 inflammasome involves the recruitment of the adaptor protein apoptosis-associated speck-like protein containing CARD (ASC). This process ultimately is leading to the formation of an ASC speck. The spreading of pathology within and between brain areas is a hallmark of neurodegenerative disorders. Although neuroinflammation is currently accepted as a hallmark of AD, its contribution to the spreading of the pathology has not been investigated. In the second part of this dissertation the involvement of microglial activation in spreading of Aβ pathology is investigated. Here it was found that ASC specks released by microglia bind rapidly to Aβ in AD patients and AD murine models. This release increased the formation of Aβ oligomers and aggregates, acting as an inflammation-driven cross-seed for Aβ pathology. Together these

results support the hypothesis that inflammasome activation is connected to seeding and spreading of amyloid pathology.

One of the features of AD is the degeneration of the Locus Ceruleus (LC) neurons, early in the disease. The LC is the major source of noradrenaline (NA) in the brain. Besides its role as a neurotransmitter, NA has been found to be a potent immunosuppressor acting through β-adrenoreceptors expressed by microglia cells. The strong correlation between LC degeneration, NA depletion and severity of AD in patients has prompted multiple studies of the contribution of LC dysfunction to AD progression and neuroinflammation through the use of animal models. However, current approaches to study LC degeneration rely on the use of pharmacological toxins or by using genetic knockout. These approaches carry the risk of misinterpretation due to confounding factors including modulation or loss of peripheral NA. Additionally, these approaches do not reflect the progressive nature of LC degeneration in the context of AD. Based on these observations, the third part of this dissertation it is based on the establishment of an inducible model that allows transient silencing of LC activity in response to optogenetic modulation in transgenic mice. The results presented in this part of the dissertation showed that LC silencing was successfully achieved. Additionally, simultaneous LC optogenetic modulation and *in vivo* imaging revealed that microglia was transiently activated by LC silencing. These results indicate that optogenetic modulation is suitable tool to study LC degeneration and highlight the importance of NA in the microglial activation process.

In summary, this dissertation focuses on the role of microglial activation in the context of AD. The first part, particularly bring light to how microglial activation triggered by systemic inflammation influences the progression of AD in a NLRP3-dependent manner. In the second part, it is uncovered how microglial activation contributes to the spreading of AD pathology. Finally, the third part of this dissertation highlights the importance of LC degeneration regulating microglial activation in the context of AD. In conclusion, the work presented here shows that microglial activation is not only a consequence but also a cause for AD.

2 Introduction

For decades the brain has been viewed as an immune-privileged organ, meaning that inflammation is provoked either through direct infection or after the breakdown of the blood–brain barrier (BBB) with subsequent infiltration of peripheral immune cells (1). It is now widely accepted that systemic infection, aging and neurodegenerative disease can trigger an immune response in the central nervous system (CNS) (2–4) which can subsequently lead to sustained neuroinflammation. Microglia, the resident innate immune cells of the brain, actively contribute to neuronal damage in the course of neuroinflammation, during which overactivation and dysregulation of microglia have disastrous and progressive neurotoxic consequences (5). There is now consensus over the occurrence of dynamic microglia turnover in the brain and that its phenotype may change depending on the context (6, 7).

2.1 Alzheimer's disease

AD is the most common type of dementia representing about 50-70% of the cases (8). By 2050 the disease prevalence is projected to reach higher epidemic levels, converting AD into a massive socio-economical problem (9). AD is clinically characterized by memory loss and cognitive deficits (figure 1) (10). Pathologically AD manifest at least two decades before the onset of cognitive symptoms, and includes extracellular Aβ deposition, tau hyper-phosphorylation and chronic neuroinflammation, which lately cause the loss of neuronal cells mainly in the cortex and hippocampus (11). In parallel, AD also involves the breakdown in BBB, astrocytosis and oligodendrogliosis exposing that AD is a systems disorder and the roles and interactions of different cell types in the decline of brain homeostasis and resultant dementia is a major research topic (12). Given the fact that after disease onset, treating symptoms it is extremely difficult, scientifically based strategies preventing AD are needed. Sporadic late-onset AD (LOAD) accounts for more than 99% of all cases (13). LOAD cases are constantly increasing aligned with aging of the world population, converting aging as the primary risk factor for developing AD. In contrast, early-onset AD is mostly familial, as a result of mutations in genes encoding the amyloid precursor protein (*App)* and presenilin 1 and 2 (*Psen)*.

Most of the familial mutations affect the proteolytic processing of APP by β-secretase and γ-secretase generating soluble Aβ fragments with different aggregation nature (9)

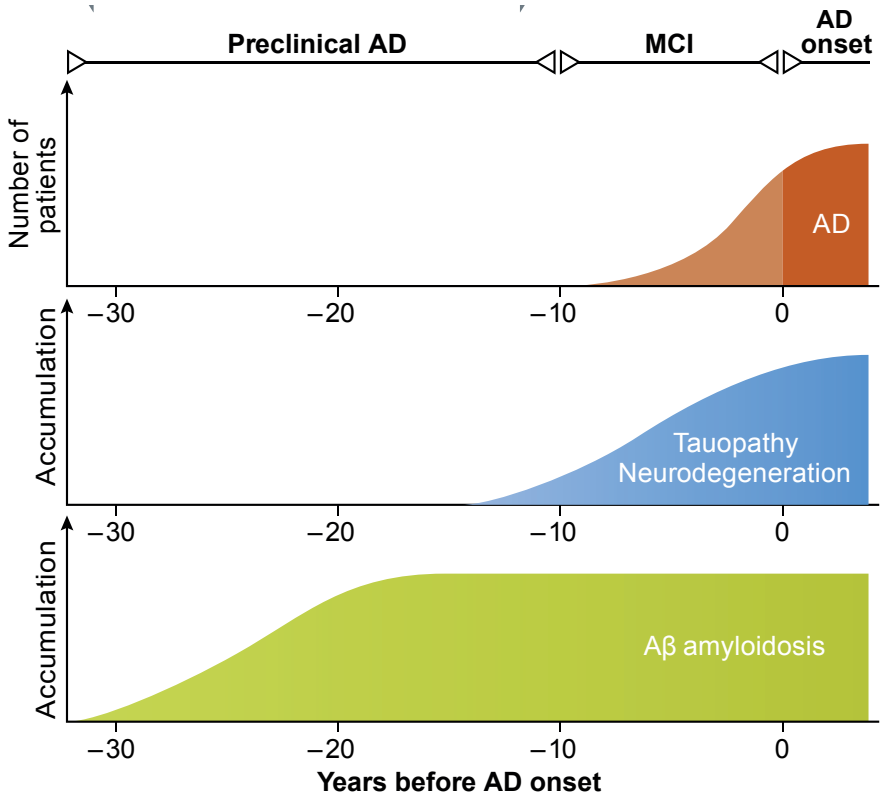

Figure 1. Neurological symptoms of AD. Three phases led to the onset of AD. The first one represents the preclinical phase of AD, characterized by Aβ accumulation without neurological manifestations. The second phase is mild cognitive impairment, characterized by tau hyper-phosphorylation and neuronal loss without dementia. The last phase corresponds to AD, where the irreversible loss of neuronal circuits leads to symptoms of dementia. Adapted from (9)

2.2 Murine models of AD

Mutations in *App* and *Psen genes* have been identified as causing AD (table 1). In this sense, the majority of murine AD models (first generation) have been focused on these mutations (14). Transgenic animals based on amyloid production typically express high levels of Aβ peptide usually through altering the processing of APP. This is generally achieved through introduction of human APP, or a PSEN mutation, altering γ-secretase enzyme activity, and subsequently, the cleavage of APP (15, 16). Cleavage of APP occurs by both β-secretase enzyme and the γ-secretase enzyme resulting in a 42 amino acid peptide. This peptide forms the fibrillar Aβ, which is found at the senile, compact deposits with dense cores. Neurofibrillary tangles are also a histopathological signature of AD, and are composed of hyper-phosphorylated forms of tau protein (15). Tau is a microtubule-associated protein that binds to the microtubules in the axon stabilizing them. However, during AD hyper-phosphorylation of tau triggers the dissociation of this protein from the microtubules and the generation of oligomeric and aggregated forms. (17).

Importantly Aβ oligomers have been reported to contribute to tau oligomerization (18) Transgenic mice that recapitulate tau pathology express either wild-type human tau or mutant one (15). In an attempt to closely mimic the overall pathological marks of AD, double and triple-transgenic mice have been generated. Of note, current AD transgenic murine models not only recapitulate the hallmarks of the disease, but also other neuropathological features associated with AD, such as astrogliosis and alterations of the vascular unit (14). To overcome intrinsic drawbacks of the APP processing paradigm, mouse models utilizing an App knock-in strategy were generated to overproduce pathogenic Aβ such as $A\beta_{1-42}$ without overexpressing APP. Single App knock-in mouse models were generated in which the murine Aβ sequence was humanized by changing three amino acids that differ between mice and humans into the endogenous mouse *App* gene (19). Table 1 summarizes the main murine AD models and their application for pre-clinical studies.

	Strain(s)	Genetic background	Promoter	Mutation(s)	General features	Suitable applications
Single transgenic APP-Tg	PDAPP	C57B6 x DBA2	PDGF-β	APP^{V717F}	Moderate behavioral phenotype Neuronal loss in some models	Analysis of Aβ production, deposition, and Aβ-associated neuroinflammation Drug development (targeting Aβ deposits and secretases) Analysis of behavior if caused by Aβ Identification of CSF biomarkers
	Tg2576	B6; SJL mixed background	hamster prion protein (PrP)	$APP^{KM670/671NL}$		
	APP23	C57BL/6	mouse Thy1	$APP^{KM670/671NL}$		
	J20	C57BL/6	PDGF-β	$APP^{KM670/671NL,V717F}$		
	TgCRND8	Hybrid C3H/He-C57BL/6	hamster prion protein (PrP)	$APP^{KM670/671NL,V717F}$		
Double transgenic APP-Tg x PSEN1-Tg or KI	APPPS1	C57BL/6J	mouse Thy1 (APP, PS1)	$APP^{KM670/671NL}$ $PS1^{I166P}$	Moderate behavioral phenotype Aβ accumulation from early stage Neuronal loss in some models	Analysis of Aβ production, deposition, and Aβ-associated neuroinflammation Drug development (targeting Aβ deposits and secretases) Analysis of behavior if caused by Aβ Identification of CSF biomarkers Analysis of cell death, in some cases
	5XFAD	C57BL/6J x SjL)F1 and C57BL/6J	mouse Thy1.2 (APP, PS1)	$APP^{KM670/671NL,I716V,V717I}$ $PS1^{M146L,L286V}$		
Triple transgenic	3xTg-AD	C57BL/6J	mouse Thy1.2 (APP, Tau) endogenous (PS1)	$APP^{K670N,M671L}$ $PS1M^{146V}$ $MAPTP^{301L}$	Moderate to severe behavioral phenotype NFT formation Neuronal loss	Analysis of Aβ production, deposition, and Aβ-associated neuroinflammation Drug development (targeting Aβ and tau) Analysis of behavior if caused by Aβ and tau Tau imaging Identification of CSF biomarkers Analysis of cell death
Single App knock-in	NL-F	C57BL/6J	endogenous APP	$APP^{KM670/671NL,I716F}$	Minor behavioral phenotype No overexpression of APP and byproducts except for CTF-β Endogenous *App* promoter-driven gene expression Presence of relevant control mice (NL mice) Two lines for differential purposes NL-F (wild-type Aβ) NL-G-F (Arctic Aβ) : Aβ accumulation from early stage	Analysis of Aβ production, deposition, and Aβ-associated neuroinflammation Analysis of molecular pathways Analysis of neural network Omics analysis Reverse genetic analysis using the knockout and knock-in mice Drug development (preventive) Additional gene manipulations (gene editing) Analysis of transcription and splicing of APP Identification of CSF and plasma biomarkers
	NL-G-F	C57BL/6J	endogenous APP	$APP^{KM670/671NL,E693G,I716F}$		

Table 1. Comparison of current AD models. Adapted from (9)

2.3 *Microglia in the developing and adult brain*

Comprising around 10% of the cells in the CNS, microglia represent the major principal cellular component of the immune system in the brain. They derive from precursors that express macrophage colony-stimulating factor receptor, found in the mesodermal yolk sac early in embryonic development between E8.5 and E9.5 in mice at a time before the blood–brain barrier restricts cell migration into the brain (20–22). Distributed throughout the CNS, the density of microglia varies between different areas of the brain (23). They constitute the first line of defense by constantly surveying both the white and grey matter for invading pathogens or injury (24). Previously, the ramified morphology of microglia was associated with a so-called “resting” phenotype. However, “resting” microglia cannot be considered to be quiescent or even dormant. Studies using in vivo two-photon laser scanning microscopy in transgenic mice expressing enhanced green fluorescent protein in the Cx3cr1 locus (encoding CX3CR1, a chemokine receptor) revealed that microglial processes are highly motile and flexible (25). These studies have led to a new definition of “resting” microglia, which actually survey their environment continually without disturbing neuronal networks (26). During development, it is thought that microglia contribute to the maturation of the neural network by stimulating vascularization and assisting the elimination of excess neurons and synapses, as well as facilitating cell differentiation (27, 28).

Beyond this role during development, increasing evidence indicates that microglia play a key role in maintaining homeostasis in the CNS by maintaining neuronal networks (29). More specifically, microglia appear to be important for the formation and control of synaptic plasticity (29), learning (30) and neurogenesis. In 2010, Tremblay et al. demonstrated that microglial cell bodies juxtaposed with synaptic-associated elements, including synaptic clefts. Moreover, via two-photon microscopy using the double CX3CR1-GFP/Thy1-YFP transgenic mouse model, it has been shown that microglial cells contact dendritic spines. These dendritic spines were smaller compared to those with no contact and also exhibited an increased rate of elimination over a time period of two days. This suggests that microglial cells may control the functional and structural states of synapses through interactions with dendritic spines (29). In line with these findings, recent reports have demonstrated an involvement of microglial cells in synaptic remodeling during postnatal stages, by which microglial cells actively phagocytize neuronal components in a process known as synaptic pruning (31). The developmental stages and the level of synaptic activity of the respective stub regulate this synaptic pruning. It has been shown that microglia are targeted to the synapse by the complement system proteins or by the fractalkine receptor CX3CR1 (31, 32). Genetic deficiency for the complement receptor 3

reduced the number of engulfed synapses (31). On the other hand, microglia from CX3CR1 knock out mice showed an increased synaptic pruning and altered synaptic activity (32). These findings are supported by the fact that genetic depletion of microglia causes a significant decrease in dendritic spine turnover (30). Parkhurst and colleagues showed that microglia are not only involved in the elimination but also formation of spines (30). These results point to an intimate role for microglia in maintaining neuronal networks, which ultimately could influence learning and memory in the adult brain.

2.4 *Microglial activation*

One of the characteristics of microglia is their activation at a very early stage in response to aging (6), obesity (33) systemic inflammation (2) acute brain injury (34) and neurodegenerative diseases (35, 36). Under physiological conditions microglia exhibit highly ramified and motile cell processes scanning the environment for tissue damage, cell debris or pathogens. Once microglia sense signals indicating such challenges, they react in order to maintain cerebral homeostasis (25, 29). During aging and neurodegeneration, microglia acquire an activated phenotype, morphologically characterized by a reduction in branch number accompanied by an increase in cell soma volume. This process is understood as a shift between the resting /surveying state towards an activated phenotype (figure 1).

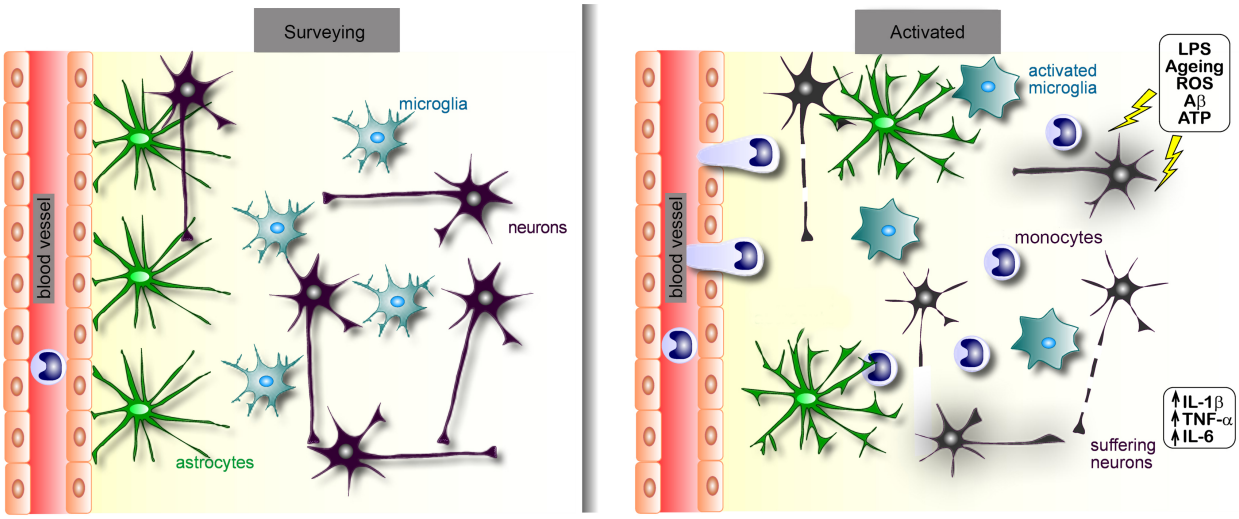

Figure 1. Phenotypic shift of microglia: In the left panel microglia exhibits a surveying phenotype searching for threats in the environment. Once the integrity of the CNS is compromised by different stimulants, the microglial phenotype shifts towards an activated state, which is accompanied, by cytokine secretion, astroglial reactivity and BBB disruption as well as infiltration by peripheral monocytes. Adapted from (37)

Microglia activation often precedes reactions of any other cell type in the brain. They respond not only to almost any changes in the brain structural integrity but also to very subtle alterations in their microenvironment, such as imbalances of ion homeostasis, which can precede histologically detectable pathological changes (38). In order to continually survey their neuronal environment and maintain tissue homeostasis and neuronal integrity, the microglial cell surface has been equipped with numerous transporters, channels and receptors known collectively as the microglia sensome (39). The microglia sensome includes receptors for neurotransmitters, neurohormones, neuromodulators, cytokines and chemokines, as well as pattern recognition receptors (figure 2) (39).

Outside the CNS, activated macrophages have been categorized as classically activated macrophages (or M1) respond to LPS plus IFN-γ, whereas alternatively activated macrophages "see" either IL-4/IL-13 (M2a); immune complexes along with IL-1 (M2b); or a variety of modulatory stimuli, such as glucocorticoids, TGF-β, or IL-10 (M2c) (40–42). Microglia are also likely to exist in a range of phenotypic states during chronic activation: these cells have a wide range of phenotypes that are indicative of their response to the local environment, including interaction with other cells and their physiological activity in the brain. Importantly, the ability to isolate or image subsets of unperturbed microglia to characterize their gene expression and mode of action as discriminated by physiological markers is restricted at present (11).

2.5 *Aging: a major priming factor for microglia*

Originally described for macrophages (43), microglia priming makes reference to an enhanced sensitivity to an inflammatory stimulus (44). Aging is associated with substantial alteration of the gene expression profile of the whole brain and has been defined as one of the major priming factors for microglia. On the transcriptome level, endogenous ligands are downregulated during aging, whereas factors for host defense and neuroprotection are upregulated (39). To what extent age-related microglia priming results from cell-autonomous cellular aging, rather than prolonged exposure to the aged neural environment is uncertain. In physiologically aged and senescence-accelerated mice, where telomere shortening (hallmark of aging) is accelerated, profound microglia priming was characterized by increased production of cytokines and reactive oxygen species, and enhanced phagocytic capacity (45). This model provided proof of principle that environmental effects, such as aging, can drive microglia priming.

2.6 *Neuroinflammation in Alzheimer's disease*

AD is the most prevalent type of dementia currently affecting approximately 45 million people worldwide (46). The incidence of AD increases with age and as the human life span continues to increase, so does the burden of this chronic illness (46). Pathologically, AD is characterized by the extracellular deposition of Aβ, the formation of neurofibrillary tangles and neuroinflammation (1). Over the past decade, the latter has evolved as an important contributor to AD pathogenesis (47). This is supported by human studies and murine models of AD showing that non-steroidal anti-inflammatory drugs reduced the risk of developing AD or $A\beta_{1-42}$ deposit load, respectively (48). Toll like receptor 4 (TLRs) and their co-receptors CD14 and CD36 play a major role in microglial Aβ recognition (49). It has been shown that aggregated Aβ elicits an initial, acute immune response by activating microglia via the cell surface receptor CD36. This ligation subsequently triggers the formation of a TLR4–TLR6 heterodimer which recruits the adaptor protein myeloid differentiation protein 88 (MyD88), resulting in augmented nuclear factor-κB (NF-κB) (figure 2) signaling. This causes transcription and expression of genes involved in the immune response including but not restricted to tumor necrosis factor alpha (TNF-α) and interleukin-1β (IL-1β) (50). The hypothesis that innate immune activation contributes to AD pathogenesis has recently been supported by genome-wide association studies which identified several immunity-related gene variants, including *Trem2* (51) and *Cd33* (52), that increase the risk of developing AD. CD33, also known as Siglec-3, is a 67-kDa transmembrane glycoprotein that is expressed on the surface of myeloid progenitor cells (53), mature monocytes (54) and macrophages (55). It functions as a lectin, a carbohydrate-binding protein, and it contains putative immunoreceptor tyrosine–based inhibitory motifs that are typically inhibitors of cellular activity (56). In support of this putative function, CD33 has been shown to constitutively repress monocyte-derived pro-inflammatory cytokines (54). Recent data showed that microglial cells in the human brain express CD33 (57). Additionally, increased CD33 protein levels and increased numbers of CD33-positive microglial cells have been reported in the AD brain. The increase in CD33-positive microglial cells was positively correlated with higher $A\beta_{1-42}$ levels (52, 56). TREM2 is expressed in the myeloid cell lineage and in the brain particularly by microglial cells (58). This is supported by recent data using direct RNA sequencing, which quantitatively defined the transcriptome from purified microglia. It was shown that TREM2 is highly enriched in microglial cells compared to macrophages and other glial cells such as astrocytes (39). Until now, the exact function of TREM2 in the brain is not well defined. Some reports indicate that TREM2 appears to negatively regulate the inflammatory and TLR-mediated response by paring with the signaling adapter DAP12 (59). This is based in part on

the fact that TREM2 deficient macrophages show increased TNF-α production (60). In addition, TREM2 has been found to serve as a positive regulator of phagocytic functions of myeloid cells. Thus, TREM2 may directly mediate clearance of apoptotic neurons and bacteria (61).

It is important to note that to date AD-associated TREM2 mutations are not well characterized. However, a current hypothesis proposes that mutations in TREM2 may lead to a pro-inflammatory state, which may promote Aβ production and compromise phagocytic clearance. Aβ accumulation activates microglia and astrocytes, which in turn exacerbates neurotoxicity by releasing pro-inflammatory mediators including complement factors, cytokines, chemokines and prostanoids (62). Interestingly, TREM2 has been shown to increase in murine AD models (Frank et al., 2008), possibly in a failed compensatory attempt to keep the inflammatory response controlled (63). Recent studies have shown that TREM2 deficient microglia undergo metabolic failure and apoptosis upon Aβ challenge resulting in a decreased microglia assembly at sites of Aβ deposition, and thus leading indirectly to reduced Aβ clearance (64, 65).

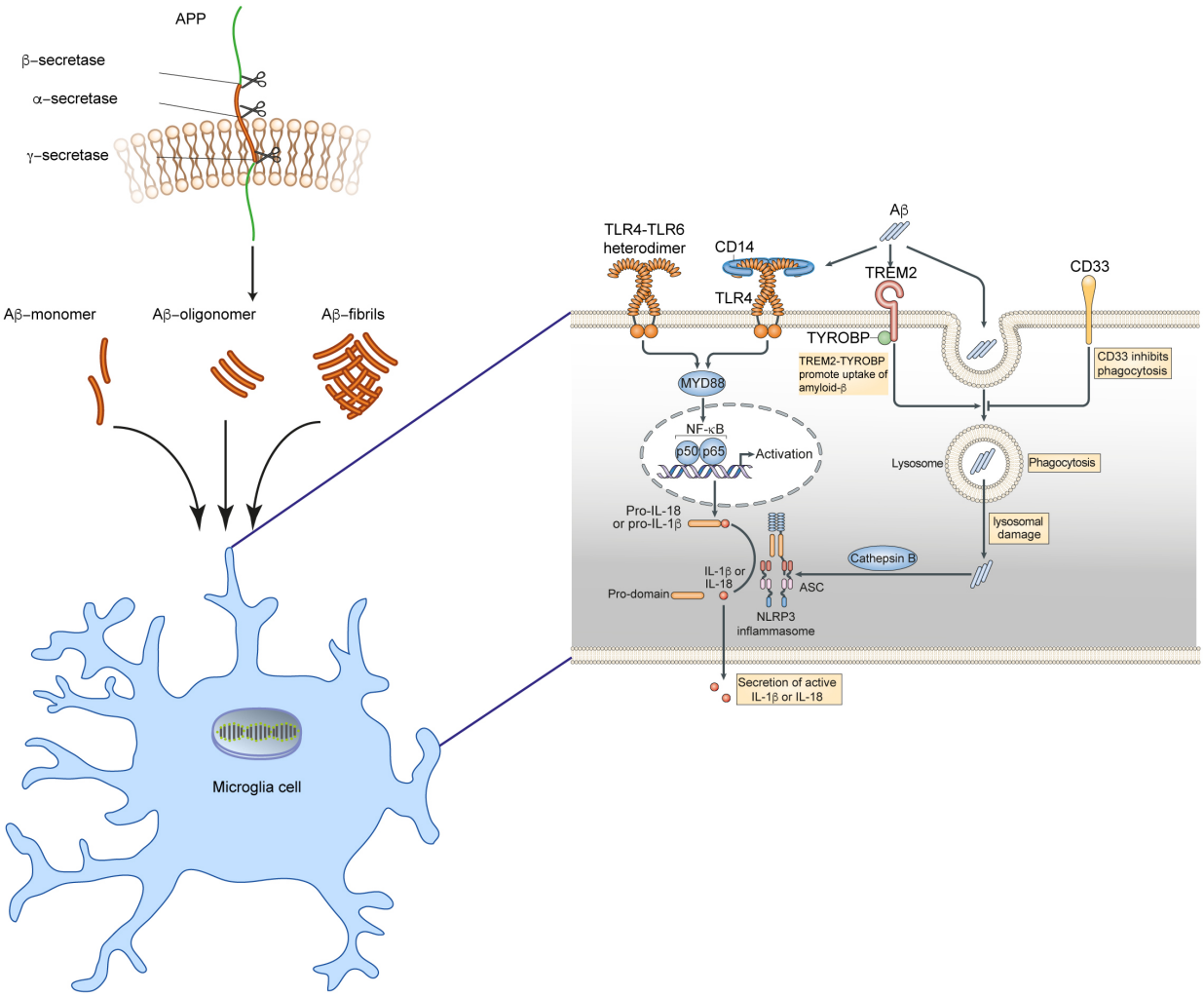

Figure 2. Microglia sensome involved in microglial activation: microglial cells are fully equipped with a range of pattern recognition receptors, such as CD36, TLR4, and TLR6. Binding of Aβ to CD36 triggers TLR4-TLR6 dimerization, which leads to subsequent activation of the NF-κB transcription factor leading to pro-inflammatory gene transcription. TREM2 and CD33 are receptors involved in the phagocytosis process. TREM2 increases phagocytosis of Aβ in AD pathology, however mutations in TREM2 have been associated as a risk factor in AD. CD33 inhibits Aβ phagocytosis. Aβ per se and the inflammatory response generated by microglial activation is producing neuronal damage. Adapted from (1, 11, 66)

2.7 *Cytokines and soluble factors in Alzheimer's disease*

Cytokines are small proteins ranging from 8000 to 40000 Da (67). They are secreted either by immune or non-immune cells (67). The biological effects of these proteins include stimulation or inhibition of cell proliferation, cytotoxicity/apoptosis, antiviral activity, cell growth and differentiation and inflammatory response (68). Since these molecules have diverse functions in the CNS, it is not surprising that the levels of many cytokines in neurodegeneration particularly in AD, increase (68). For convenience IL-1, TNF-α and IL-6 will be defined as pro-inflammatory cytokines, and IL-4, IL-13 and Transforming Growth Factor beta (TGF-β) as anti-inflammatory cytokines, but the reader should note that this is not an absolute definition. IL-1 is one of the major pro-inflammatory cytokines. This cytokine presents two different forms (IL-1 alpha and beta) whose biological effects are indistinguishable between each other. IL-1 affects nearly every cell type, often in concert with other pro-inflammatory cytokines such as TNF-α. Although IL-1 could trigger host defense mechanisms and functions as an immunoadjuvant, IL-1 is a highly inflammatory cytokine. The margin between clinical benefit and unacceptable toxicity in humans is exceedingly narrow (67). Increased IL-1β levels have been implicated in response to Aβ deposition (69, 70). Moreover, in murine models of AD treatment with the non-steroidal anti-inflammatory drug ibuprofen reduced the brain levels of IL-1β and Aβ deposition (71).

TNF-α is one of the main pro-inflammatory cytokines, which acts in combination with IL-1β to augment the inflammatory response through paracrine stimulation of further pro-inflammatory cytokine release (72). TNF-α is synthesized as a monomeric transmembrane protein that is inserted into the membrane as a homotrimer and cleaved by the matrix metalloprotease TNF alpha-converting enzyme (TACE; ADAM17) to a 51 kDa soluble circulating trimer (73). Due to its very low levels in the healthy brain, it has been difficult to determine its physiological function (74). In the context of inflammation or disease TNF-α is mainly produced by glial cells (50, 75). Furthermore, it has been shown that there is an increase in the levels of TNF-α at amyloid deposits, and this result was correlated with cognitive deficits in the Tg2576 transgenic mice (76). Moreover, there is a large body of evidence indicating that microglial cells release large amounts of TNF-α when stimulated with Aβ peptides (77). Furthermore, it has been

demonstrated that microglial stimulation with TNF-α produces a downregulation of receptors involved in Aβ binding and degradation as well as a reduction in the phagocytic ability to take up Aβ (49). In addition to this, it has been demonstrated that ablation of the TNF receptor in APP23 transgenic mice (APP23/TNFR1$^{-/-}$) inhibited Aβ generation and diminished deposit formation in the brain. These results were accompanied by a reduction in microglia activation as well as neuronal loss (78).

2.8 NLRP3 inflammasome: a central sensor for danger signals

The initiation of the inflammatory response by microglia involves the multiprotein complexes termed 'inflammasomes'. Comprising of a cytosolic multiprotein platform, the inflammasome enables the activation of pro-inflammatory caspases, mainly caspase-1 (79). Caspase-1 is critically involved in the inflammatory processes through the cleavage and release of pro-inflammatory cytokines such as IL-1β and IL-18. Additionally, caspase-1 also promotes pyroptosis (80), a form of programmed cell death where immune cells recognize danger signals, release pro-inflammatory cytokines, swell, burst and die (81).

Thus, inflammasomes are essential protein complexes that direct the response of the innate immune system to pathogenic stimuli (82). NLRP3 inflammasome is the best-recognized and most widely studied regulator of caspase 1 activation. Its N-terminal protein–protein interaction domain is a PYD, and thus, requires the adaptor ASC, which triggers ASC helical fibrillar assembly (figure 2) (83). ASC fibrils then recruit the effector caspase-1 via CARD interactions leading to autoproteolytic activation and subsequent assembly of ASC fibrils into a large paranuclear ASC speck (84). This complex reacts to a wide variety of activating stimuli, which include bacterial, fungal and viral components, endogenous danger signals such as extracellular ATP, amyloid-β and uric acid crystals (85–87). Recently it has been shown that IL-1β levels are regulated in a NLRP3 inflammasome-dependent manner in APP/PS1 transgenic mice.

In this work, Nlrp3 deficient mice were crossed into APP/PS1 animals to assess the contribution of the NLRP3 inflammasome to the pathogenesis of Alzheimer's disease. In APP/PS1/Nlrp3 deficient mice, caspase-1 cleavage of IL-1β was significantly reduced and total brain IL-1β levels were shown to be comparable to healthy wild-type animals. More importantly, APP/PS1/Nlrp3 deficient mice were largely protected from cognitive impairment and suppression of long-term potentiation (88). These results underline the importance of IL-1β as a driving force of neuroinflammation in AD.

2.9 *Chemokines.*

Like cytokines, chemokines, participate in the sterile immune response of AD. The major role of chemokines is to act as chemoattractants, allowing the migration of other immune cells to sites of injury and disease (89). These cells, which are attracted by chemokines, follow a signal of increasing chemokine concentration towards the primary source. In addition to act as chemotactic mediators of the immune system, it is now recognized that chemokines also play multiple roles in the regulation of homeostasis (89) and an increased glial or neuronal expression can be detected in both, acute or chronic CNS disorders (90–92). In mouse models of AD, the involvement of several chemokine receptors such as CCR2 (93), CXCR1 (94, 95) and CXCR3 (96) has been described. In the case of CCR2, deficiency of this chemokine in the Tg2576 transgenic AD model showed accelerated disease progression and impaired microglial accumulation around Aβ deposits, resulting in an overall increase in Aβ levels (93). These results suggest that CCR2-dependent microglial accumulation could play a protective role at some stages of the disease. Regarding to CXCR1 and CXCR3, experimental data show a gene dose-dependent reduction of Aβ deposition in the APPPS1 mouse model of AD. Importantly, in the respective models, no changes of APP processing were detected. Moreover, a significant reduction in microglial activation, neuronal loss and cognitive impairment were found, suggesting that these chemokine receptors are intimately involved in disease development (94–96).

2.10 Systemic inflammation: a risk factor for Alzheimer's disease

Systemic inflammation is defined as a whole-body inflammatory state and the occurrence of a suspected or diagnosed infection. This is a major leading cause of mortality among ICU patients, accounting for 10-50% of deaths (97). It has been shown that the peripheral immune system has a strong effect on the brain as exemplified by the high incidence of delirium and cognitive decline experienced by patients who suffer from systemic infections (98). In rodent experiments, peripheral challenge with components of the outer membrane of gram-negative bacteria, LPS, were shown to trigger neuroinflammation and neurodegeneration (99, 100). This is reflected by a sustained increase in pro-inflammatory cytokines, not only in serum, but also in the brain (2, 99, 101). Concomitantly with these observations, microglial activation has been extensively reported in the context of systemic inflammation, either in rodents or humans (2, 99, 102, 103). Under certain circumstances microglia cells can acquire a chronically activated phenotype, which may contribute to the initiation or progression of neurodegenerative disease. This chronic activation that occurs in microglia following systemic infection might account for

why neurobehavioral manifestations can persist in elderly patients even after they recover from sepsis and cytokine levels have reduced. This information inspired the formulation of a neuroinflammatory hypothesis explaining the association of systemic infection and neurodegenerative diseases such as AD. This connection between the periphery and the brain may place the microglia as a central player allowing us to try and decipher how these cells contribute to brain degeneration. Although microglia-driven neuroinflammation has been identified as a key process during systemic inflammation, aging and neurodegenerative diseases, its in vivo dynamics and mechanisms remain poorly understood

2.11 Microglial modulation through Noradrenaline

A neurotransmitter is defined as a chemical messenger released by a neuron and that affects a specific target in a specific manner. The target can either be another neuron or a non-neuronal cell, such as astrocytes and microglia (104). NA belongs to the catecholamine transmitter family and it is synthetized from the essential amino acid tyrosine (104). The LC is the small brain stem nucleus located at the tegmentum of the 4th ventricle. Approximately 90% of LC neurons are tyrosine hydroxylase positive noradrenergic neurons (105). Ten percent of all LC neurons express the neuronal nitric oxide synthase (nNOS) and do not contribute directly to the noradrenergic supply of the targeted brain regions (106). The LC represents the major source of cerebral NA which projects to several brain regions. The majority of axons arising from the LC terminate in the neocortex and hippocampus (107–109). Half of all LC terminals end by contacting neurons, while the remaining half ends at microglial and astroglial cells forming non-synaptic contacts. It has been shown that neurotransmitter receptors on microglia act as modulators of microglial function (110). Thus, NA acts, besides its role as a classical neurotransmitter, as a potent immunosuppressor (111). LC-derived NA and β-adrenoreceptors have been implicated in the physiological modulation of memory formation and retrieval (109, 112–115). In the past decade NA has been shown to act as a potent suppressor of the microglia-mediated inflammatory response. Indeed, stimulation of mouse microglia with NA abrogated Aβ-induced cytokine and chemokine production (116). This effect is mediated by the binding of NA with β-adrenoreceptors on microglia. In line with this, stimulation with the β-adrenoreceptor agonist, Isoproterenol, mimicked the anti-inflammatory response observed with NA (116, 117). Research dating back to the 1960s implicated LC degeneration in aging and the pathogenesis of AD (118–120). Indeed, it has been shown for AD patients a 70% reduction in the LC neuronal population and NA levels (121). The drop in NA concentration tightly correlates with the progression and extent of memory dysfunction and cognitive impairment (121).

Degeneration of LC neurons has been observed in patients exhibiting “mild cognitive impairment” (MCI), an early form of AD, with 80% of MCI patients eventually succumbing to full AD (122). In addition, lesions or ablation of LC neurons in murine models of AD increased neuroinflammation, amyloid deposition and cognitive impairments (116, 123, 124). Thus, these data suggest that NA may suppress brain inflammation and therefore a reduction in NA could contribute to the pathogenesis of AD and other neurodegenerative diseases. However, it is worth noting that most of these studies have been performed by either using pharmacological agonists or antagonists or by using genetic knockout animals lacking dopamine β-hydroxylase ($DBH^{-/-}$). These approaches carry the risk of misinterpretation due to confounding factors including modulation or loss of peripheral NA function, since the pharmacological substances used were almost exclusively administered systemically, and their action therefore was not restricted to the brain. Likewise, $DBH^{-/-}$ animals may have developed compensatory mechanisms, since they were lacking central and peripheral NA since birth (prenatally, *in utero*, NA levels are being replenished by treatment of pregnant dams with the NA precursor L-threo-DOPS) (118). Therefore, new tools to study LC neurodegeneration in the context of neurodegeneration are needed.

3 Materials and Methods

3.1 Reagents

Product	Catalog number	Application	Comments	Provider
6E10	SIG-39320	Western blot	1:1000 dilution	Covance (San Diego, USA)
ASC antibody (polyclonal rabbit anti mouse)	AG-25B-0006-C100	Immunohistochemistry	1:300 dilution	AdipoGen (Liestal, Switzerland)
Beclin 1 antibody (polyclonal rabbit anti mouse)	3738	Western blot	1:1000 dilution	Cell Signaling (Frankfurt, Germany)
Buprenorphin hydrochloride	RBP-6300	Surgery	0,1mg/Kg	Indivior (Slough, UK)
Caprofen		Surgery	5mg/kg	Pfizer (Berlin, Germany)
CD11b antibody (polyclonal rat anti mouse)	MCA711	Immunohistochemistry	1:300 dilution	Bio-Rad (Munich, Germany)
CD169 antibody (monoclonal rat anti mouse)	MCA884	Immunohistochemistry	1:50 dilution	Bio-Rad (Munich, Germany)
c-fos antibody(polyclonal rat anti mouse)	ab190289	Immunohistochemistry	1:250 dilution	Abcam (Cambridge, UK)
Cyanoacrylate glue		Surgery		UHU (Brühl, Germany)
CT-20 antibody (polyclonal rabbit anti mouse)	171610	Western blot	1:20000 dilution	Millipore (Darmstadt, Germany)
Dental cement		Surgery		Heraeus Kulzer (Hanau, Germany)

Dexamethasone		Surgery	6mg/Kg	Jenapharm (Jena, Germany)
Dextran Red	9004-54-0	Two-photon imaging	20mg/Kg	Sigma-Aldrich (Darmstadt, Germany)
Iba-1 antibody (polyclonal goat anti mouse	NB100-1028	Immunohistochemistry	1:50 dilution	Novus Biologicals (Wiesbaden, Germany)
Iba-1 antibody (polyclonal rabbit anti mouse)	019-19741	Immunohistochemistry	1:500 dilution	Wako chemicals (Neuss, Germany)
Ketamine		Surgery	1,5mg/Kg	Ratiopharm (Ulm, Germany)
Ki-67 antibody (polyclonal rabbit anti mouse)	ab15580	Immunohistochemistry	1:500 dilution	Abcam (Cambridge, UK)
LPS (Ultrapure from *Salmonella typhimurium)*	L6143	Systemic inflammation treatment	1mg/Kg	Sigma-Aldrich (Darmstadt, Germany)
Methoxy-XO4	4920	Two-photon imaging Immunohistochemistry	10mg/Kg 10µM	Tocris biosciences (Bristol, UK)
Tyrosine hydroxylase antibody (monoclonal mouse anti mouse)	MAB7566	Immunohistochemistry	1:100	R&D systems (Wiesbaden, Germany)

Table 2. List of reagents and their applications

3.2 Human tissue samples

Post-mortem brain material from patients with histologically confirmed AD, vascular dementia, fronto-temporal dementia and corticobasal degeneration as well as age-matched controls who had died from non-neurological disease, were derived from the Neurological Tissue Bank of the Biobank of the Hospital Clínic-IDIBAPS. All patients had signed an informed consent and agreed to the use of their brain material for medical research. Ages as well as post-mortem times were similar between controls and AD cases. Post-mortem times varied from 3.5 to 5 h. After explantation, brain specimens were immediately snap-frozen and stored at −80 °C until further use. Patients and controls were 75 ± 6 years old.

3.3 Animals

C-X3-C motif, receptor 1-GFP (CX3CR1/GFP) transgenic mice (125) exhibiting a microglia-specific expression in CNS and APP/PS1 transgenic animals (126) were purchased form The Jackson Laboratory (Bar Harbor, ME) on a C57BL/6N background. NLRP3-deficient animals (127) were also backcrossed onto C57BL/6. All mice were housed under standard conditions at 22°C and a 12h light/dark cycle with free access to food and water. Animal care and handling was performed according to the declaration of Helsinki and approved by the local ethical committees (animal experimentation project number: 84.02.04.2013.A101). The following animal groups were analyzed: CX3CR1GFP/$^{+}$, CX3CR1GFP/$^{+}$/ *Nlrp3*$^{-/-}$, CX3CR1GFP/$^{+}$/ APP/PS1, CX3CR1GFP/$^{+}$ /APP/PS1/*Nlrp3*$^{-/-}$ at 5 and 15 months of age (table 3).

For ASC seeding experiments APP/PS1 transgenic mice and Asc$^{-/-}$ mice (Millennium Pharmaceuticals, Cambridge, MA) were both on the C57BL/6 genetic background.

Tissues of the following animal groups were analyzed: wild type, Asc$^{-/-}$, APP/PS1, APP/PS1;Asc$^{-/-}$ (table 3).

For optogenetic modulation of LC 12 month-old mice with selective expression of the inhibitory opsin halorhodopsin (eNpHR3.0) only in noradrenergic LC neurons were generated. This was achieved by cross breading of B6;129S-*Gt(ROSA) 26So*$^{rtm39.1(CAG-HOP/EYFP)Hze}$/J mice (H-ROSA) and B6.Cg-Tg(TH-cre)1Tmd/J mice (TH-cre). The H-ROSA mice are heterozygous for the Rosa-CAG-LSL-eNpHR3.0-EYFP-WPRE allele. A *loxP*-flanked STOP cassette prevents transcription of the downstream eNpHR3.0-EYFP fusion gene. Because the CAG promoter driven reporter construct was targeted for insertion into the *Gt(ROSA)26Sor* locus, eNpHR3.0-EYFP expression is determined by which tissue(s) express Cre recombinase. When bred to mice that express Cre recombinase, the resulting offspring has the STOP cassette deleted in the *cre*-expressing tissues, resulting in expression of the eNpHR3.0-EYFP fusion protein. By using Th-cre mice the eNpHR3.0-EYFP was expressed in tyrosine hydroxylase positive neurons (TH-Cre/H-ROSA). In order to image microglia under the two-photon microscope, these mice were crossbred with the CXCR1GFP/$^{+}$ mice (table 3).

Experiment	Genotype	Age (months old)	Application
Systemic inflammation	CX3CR1GFP/$^{+}$ CX3CR1GFP/$^{+}$/*Nlrp3*$^{-/-}$ CX3CR1GFP/$^{+}$/APP/PS1 CX3CR1GFP/$^{+}$/APP/PS1/*Nlrp3*$^{-/-}$	5; 15	Two-photon microscopy Flow cytometry
	Wild-type *Nlrp3*$^{-/-}$ APP/PS1 APP/PS1/*Nlrp3*$^{-/-}$	5; 15	Immunohistochemistry Western blot ELISA
ASC cross-seeding Aβ	Wild-type APP/PS1 ASC$^{-/-}$ APP/PS1/ASC$^{-/-}$	4; 8; 12; 24	Immunohistochemistry
LC optogenetic modulation	CX3CR1GFP/$^{+}$/TH-cre/H-ROSA CX3CR1GFP/$^{+}$/H-ROSA	12	Two-photon microscopy
	TH-cre/H-ROSA H-ROSA	12	Immunohistochemistry

Table 3. The list of the genetically modified animals and their applications

3.4 Animal treatment and surgery

For the systemic inflammation experiments, animals were intraperitoneally (i.p.) injected with a single dose of LPS (1mg/kg body weight). For cranial window surgery animals were anesthetized with 1,5mg/kg ketamine (Ratiopharm, Ulm, Germany) and 0,1mg/kg xylazine (Serumwerk Bernburg, Bernburg, Germany). Mice were additionally injected subcutaneously with a mixture of 0,1mg/kg Buprenorphin hydrochloride (Indivior, Slough, UK), 6mg/kg dexamethasone (Jenapharm, Jena, Germany) and 5mg/kg caprofen (Pfizer, Berlin, Germany) to reduce pain and inflammation. Mice were placed on a heating blanket connected to a rectal probe for maintaining body temperature at 37°C. The head was fixed in a stereotaxic frame (Narishige, London, UK) and craniotomy was performed as previously described (128) with some minor modifications. Briefly, the hair was removed using a hair removing cream; a midline incision was made and the periosteum was gently removed by scraping. A 3 mm window over

the somatosensory cortex area was generated using a dental driller (Schick, Schemmerhofen, Germany) with a 0,4mm drilling head. A 5mm coverslip was attached to the skull using cyanoacrylate glue (UHU, Brühl Germany). A customized titanium ring was attached to the skull using dental cement (Heraeus Kulzer, Hanau, Germany). The mice were imaged after a 2 weeks recovery period.

For optogenetically silence LC a 400µm-diameter mono fiber optic cannula (Doric Lenses Inc. Quebec, Canada) was stereotaxically introduced into LC. Briefly, after mice were anesthetized (as previously described), an optic cannula was unilaterally introduced adjacent to LC (anteroposterior -5,45mm, mediolateral +1,28mm, dorsoventral 3,65mm) (129). The cannula was attached to the skull using dental cement (Heraeus Kulzer, Hanau, Germany). Once cannula was implanted and a craniotomy was performed as previously described.

The mice were allowed to recover for a two-week period before imaging was carried out.

3.5 In vivo two-photon laser scanning microscopy

A Nikon A1R MP microscope and a titanium–saphire laser (Chameleon Ultra, Coherent, Santa Clara, CA) were used for mouse brain *in vivo* imaging. For the systemic inflammation experiments the same five separate region of interest (ROIs) were imaged per mouse successively, before (Base), two days and ten days after LPS injection (figure 4).

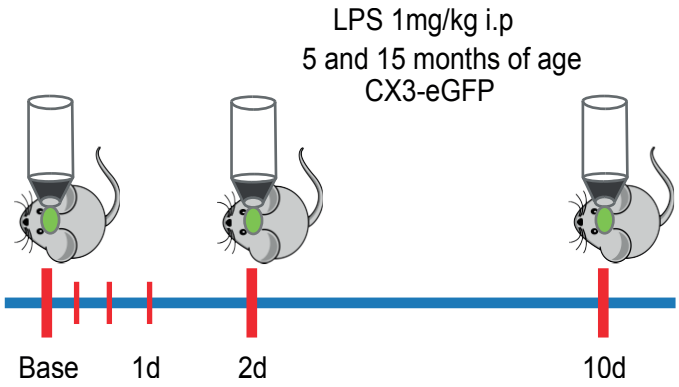

Figure 4. Two-photon imaging experimental design for systemic inflammation experiments

For optogenetic experiments the same five separate ROIs were imaged per mouse successively, before (preinhibition), 24 hours and one week after LC optogenetic inhibition (figure 5). Optogenetic modulation was performed according to Carter and colleagues (130). In brief, unilateral continuous light delivered by the implanted cannula achieved inhibition of the LC by laser with 593nm wavelength. A continuous photostimulation protocol for 1 hour was applied.

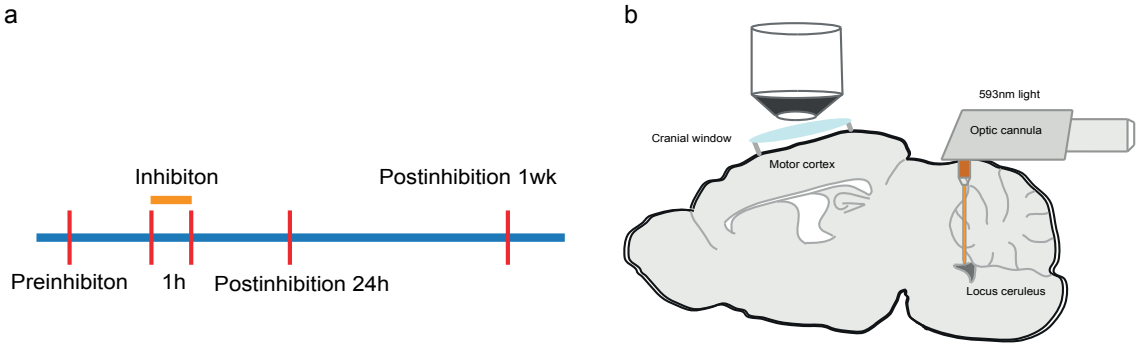

Figure 5. Experimental design for LC optogenetic modulation experiments. a) Two-photon experimental paradigm representation. b) Cannula and cranial window implantation scheme.

During all imaging sessions the laser power did not exceed 30mW. Three-dimensional Z-stacks (40μm length; 0,5μm step between optical planes) were acquired using a Nikon 25X objective (1,1 NA). For visualization of blood vessels, 20mg/kg body weight dextran red 70KDa (Sigma-Aldrich, Darmstadt, Germany) was injected intraperitoneally, 30 minutes before the imaging session. To visualize Aβ deposits, 10mg/kg of methoxy-XO4 (Tocris Bioscience, Bristol, UK) in 50% DMSO/50% NaCl (0.9%), pH 12, was also injected intraperitoneally 3 hours before the imaging session (131).

For quantitative analysis two-photon Z-stacks were automatically reconstructed using a self-customized python-based script. Reconstructions were visually checked using the ImageJ plugin “simple neurite tracer” (figure 6). Each cell was individually extracted, and all the individual files were analyzed using the open source software L-measure (132).

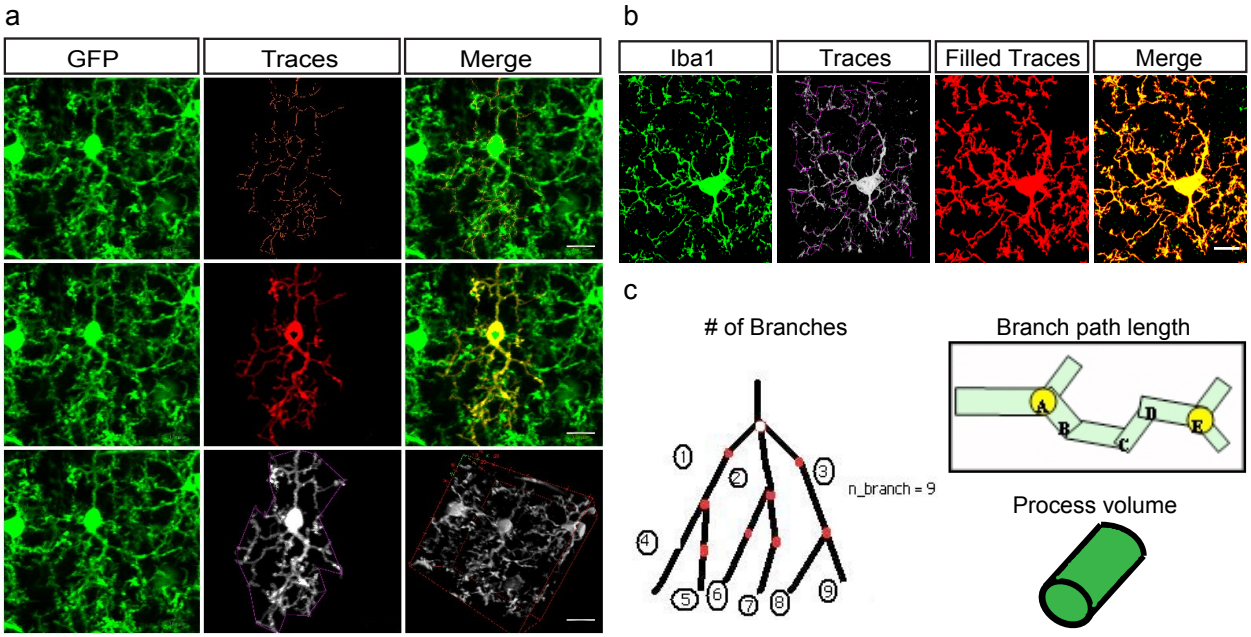

Figure 6. Automatic 3D microglia reconstruction script for confocal and two-photon microscopy. a) Representative two-photon images of a *CX3cr1*-eGFP mouse and its automatic 3D reconstruction. Scale bar: 10µm. b) Representative confocal image form an Iba1 staining (green) and its automatic reconstruction. Scale bar: 10µm. c) Example of morphological parameters analysis and quantification.

3.6 Histology and immunohistochemistry

Mice were anesthetized with 100mg/kg (body weight) of ketamine and 16mg/kg (body weight) of xylazine and then were transcardially perfused with ice cold PBS (30ml), following perfusion the brain, lung, liver, spleen and kidney were removed. One hemisphere of the brain and the organs were flash frozen in liquid nitrogen and stored at -80°C. The other hemisphere was fixed with 4% paraformaldehyde for 24h at 4°C, washed 3 times with cold PBS and stored in PBS-NaN_3. 40µm coronal, virbratome sections were then stained using the free-floating method. For free-floating staining, sections were washed 3 times for 5 mins with PBS, triton X-100 0.1% (PBS-T), blocked for 1h with BSA 1% and incubated overnight with primary antibodies. Next day the sections were washed 3 times for 5 mins in PBS-T, incubated with secondary antibody conjugates (1:500) (Invitrogen, Darmstadt, Germany) for 60 mins and washed 3 times with PBS for 5 mins. For visualization of amyloid Aβ deposits, sections from APP mice were incubated with 10µM methoxy-XO4 for 10 mins and then washed 3 times in PBS. Sections were mounted using Immu-Mount (Thermo Scientific, Bonn, Germany).

3.7 Epifluorescence microscopy

Images were acquired using an Olympus BX61 epifluorescence microscope equipped with a disc-spinning unit. Aβ deposits were imaged using a 4X (0,16 NA) objective. For Ki-67 and CD169, Z-stacks were taken with an oil immersion 40X (1,0 NA) and 60X (1,35 NA) respectively. For quantitative image analysis of hippocampal and cortical immunostaining, serial coronal sections of five animals from each group were examined. For each animal, 10 parallel sections, with a defined distance of 40µm and showing both the hippocampus and cortex were analyzed. Quantification of the number of Aβ deposits and size were determined using the ImageJ plugin 3D object counter (133). Quantification of microglia proliferation was conducted by manual cell counting using merged images of Iba1 and Ki67 staining. Proliferative microglia were normalized to the total number of microglia cells counted. TH and c-fos staining were analyzed taking 5 parallel sections with 40µm separation from the LC and motor cortex. Images were acquired using a 40X (1,0 NA) objective. C-fos immunofluorescence was quantified using ImageJ software. Quantification of intra- and extracellular ASC specks was performed for human subjects in 10 controls and 10 cases of patients with AD. From each patient, six hippocampal brain sections with a defined distance to each other were evaluated. Intra- and extracellular ASC specks were counted in 10 randomly chosen fields per section at a magnification of 40X. Similarly, hippocampal sections of wild-type and APP/PS1 mice were analyzed at 2, 4 and 8 months of age. The proportion of intra- or extracellular ASC specks was given as intracellular or extracellular ASC speck per microglia or percentage of all ASC specks detected.

3.8 Protein extraction and Western blot

Brains of 5 and 15-month-old mice were homogenized in PBS containing 1 mM EDTA and 1mM EGTA and protease inhibitor mixture, further extracted in RIPA buffer [25mMTris·HCl (pH 7.5), 150mM NaCl, 1% Nonidet P-40, 0.5% NaDOC, 0.1% SDS], and centrifuged at 20,000 × g for 30 min, and the pellet was solubilized in 2% SDS, 25 mM Tris·HCl (pH 7.5). Samples were separated by NuPage and immunoblotted using antibodies Anti-CT20 (1:20000, Millipore, Darmstadt, Germany, Cat. No. 171610), 6E10 (1:1000, Covance, San Diego, CA, USA, Cat. No. SIG-39320) and anti-beclin-1 (1:1000, Cell signaling, Frankfurt, Germany, Cat. No. 3738) followed by incubation with appropriate secondary antibodies. Immunoreactivity was detected using an Odyssee CLx imager (LICOR, Bad Homburg, Germany) and pictures were analyzed using Image Studio (LICOR, Bad Homburg, Germany).

3.9 ELISA quantification of cerebral Aβ concentration

Quantitative determination of amyloid-β was performed using an electrochemoluminescence ELISA for $A\beta_{38}$, $A\beta_{40}$ and $A\beta_{42}$ according to the protocol (see section 3.10) of the supplier (Meso Scale Discovery, Rockville, MD, USA). Signals were measured on a SECTOR Imager 2400 reader (Meso Scale Discovery, Rockville, MD, USA).

3.10 ELISA pro-inflammatory response quantification

Pro-inflammatory response was determined in brain lysates using the V-PLEX Plus Pro-inflammatory Panel 1 (mouse) Kit for 10 cytokines (IFN-γ, IL-1β, IL-2, IL-4, IL-5, IL-6, KC/GRO, IL-10, IL-12p70 and TNF-α) following the protocol provided by the supplier (Meso Scale Discovery, Rockville, MD, USA). Briefly, 50µl of diluted sample, calibrator, or control were added per well. The plate was sealed with an adhesive plate seal and incubated at room temperature with shaking for 2 hours. Later, the plate was washed 3 times and the detection antibody was added. The plate was sealed and incubated at room temperature with shaking for 2 hours. Finally, the plate was washed and the read buffer was added. Signals were measured on a SECTOR Imager 2400 reader (Meso Scale Discovery, Rockville, MD, USA).

3.11 Isolation of microglia from adult mouse brains

Neural Tissue Dissociation Kit (P), Myelin Removal Beads II and CD11b (Microglia) MicroBeads were all obtained from Miltenyi Biotec, (Bergisch Galdbach, Germany) were used for magnetic isolation of microglial cells from adult APPPS1/ CX3CR1/GFP$^{-/+}$, APPPS1, APPPS1/NLRP3$^{-/-}$ /CX3CR1/GFP$^{-/+}$ and APPPS1/NLRP3$^{-/-}$ mice brains, in accordance to the manufacturer's guidelines. Briefly, brains were dissected after perfusion with PBS; enzymatically digested using the Neural Tissue Dissociation Kit. Cells were incubated for 15 min at 4°C with Myelin Removal Beads II (Miltenyi Biotec, Bergisch Galdbach, Germany) and separated from myelin in a magnetic field using LS columns, MACS MultiStand and QuadroMACS (Miltenyi Biotec, Bergisch Galdbach, Germany). Cells were incubated with CD11b (Microglia) MicroBeads (Miltenyi Biotec, Bergisch Galdbach, Germany) for 15 min followed by separation of CD11b positive cells in a magnetic field using MS columns and OctoMACS (Miltenyi Biotec, Bergisch Galdbach, Germany).

3.12 Flow cytometry

To detect cell death, microglia were incubated with LIVE/DEAD Fixable Far Red Dead Cell Stain Kit (ThermoFisher Scientific, Waltham, MA, US). Cells were labeled with the microglial cell surface antigen antibody, rat anti-mouse CD11b (BD Bioscience, Drive Franklin Lakes, NJ,

USA) diluted 1:50 for 30 min at RT. FMO (Fluorescence Minus One) controls and the isotype control for the CD11b-PE antibody were performed. The specificity of the CD11b antibody signal and the gating strategy was subsequently controlled using APPPS1/CX3CR1/GFP$^{-/+}$ mice. Samples were measured using a BD FACSCanto™ II (BD Biosciences, Franklin, NJ, USA). Fifty thousands events were recorded and microglia was identified as CD11b+ expression. Results were analyzed using FlowJo software V10.2 (Ashland, OR, USA).

3.13 Statistical analysis

Data were analyzed using GraphPad Prism version 6 (GraphPad Software, La Jolla, CA) and presented by mean ± SEM. For systemic inflammation experiments differences among the groups were examined using one and two-way ANOVA followed by Tukey's post hoc test.

For ASC seeding experiments student-t test and one-way ANOVA followed by Tukey's post hoc test were used to analyze differences among the groups. For LC optogenetic modulation two-way ANOVA followed by Sidak's or Tukey's post hoc test were employed to analyze differences among the groups. Results were considered to be statistically significant if a $p<0,05$ was obtained.

4 Results: Systemic inflammation in AD

Besides aging, the major risk factor for developing AD, systemic inflammation has emerged as a possible risk factor as well. Considering the immune response taking place in the three different contexts, microglia rises as the natural link between them.

The aim of this chapter is to elucidate the role of microglial activation in the connection between systemic inflammation, aging and AD. In a mechanistically level, there is a particular focus on the NLRP3 inflammasome as microglial sensor for changes in brain homeostasis.

4.1 Systemic inflammation affects microglia in an age-dependent manner

Previous reports demonstrated that the peripheral administration of a single dose of LPS ranging from systemic inflammation (0,5-1mg/kg) to septic shock dosages (5-10mg/kg) cause an immune response in the CNS, characterized by neuroinflammatory changes (2, 99, 134, 135), identifying that microglia are affected by systemic immune challenge. Using *in-vivo* 2PLSM, it was sought to determine the microglial dynamics behind these observed changes. Hence, we performed cranial window surgery on 15 months old (mo) CX3CR1/GFP$^{-/+}$ mice and three weeks later injected them with a single dose of the bacterial cell wall component LPS (1mg/kg i.p). Following this peripheral challenge, microglial morphology was assessed within the first 48 hours post-LPS. Injected mice showed a 20% reduction in body weight within 48 hours as well as the characteristic sickness behavior, indicating a systemic response to the immune challenge. 2PLSM revealed that 24h after LPS injection, microglia cells showed morphological signs of activation, characterized by a significant reduction in the number, length and maximum order of the branches when compared to control mice (figure 7a,b). Moreover, it was found that changes in microglial morphology peaked at 48h, with a 50% reduction in all parameters measured (figure 7a,b).

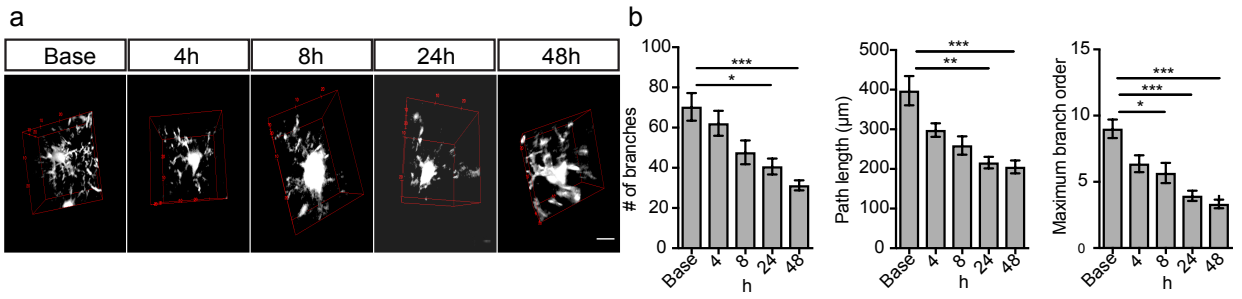

Figure 7. Systemic inflammation affects microglia morphology. a) Representative 2-photon microglia images showing morphological changes upon LPS injection within the first 48 hours. Scale bar: 10µm. b) Morphological parameters quantification within 48 hours after LPS injection (mean of 5-6±SEM; one-way ANOVA followed by Tukey's *post hoc* test, *p<0.05, **p<0.01, ***p<0.001).

To determine whether these changes were of a transient or permanent nature and whether aging, a major priming factor for microglial activation (4, 136, 137), influences these changes, 5 month and 15 month old CX3CR1/GFP$^{-/+}$ mice were analyzed longitudinally at 2 and 10 days post-LPS (figure 8). Comparison between 5 and 15mo showed that 15mo animals already presented signs of microglia activation (figure 8a,b,) prior to LPS administration, which was defined by a significant reduction in the number of processes as well as a reduction in the length of processes and maximum branch order (figure 8a,b). In addition, as a consequence of the above-described changes of the branches, the brain volume covered (total processes length/cell volume) was significantly reduced at 15mo compared to 5mo already in the absence of LPS challenge. This result suggests that aging compromises the capability of microglial to survey their environment. As shown for 15mo mice, 5mo animals had also a significant reduction in the morphological parameters analyzed upon LPS challenge, with full recovery observed by day 10 post-LPS (figure 8a,b). In 15mo mice, recovery was restricted to normalization of the branch number, suggesting that aging affects the dynamics of microglial activation.

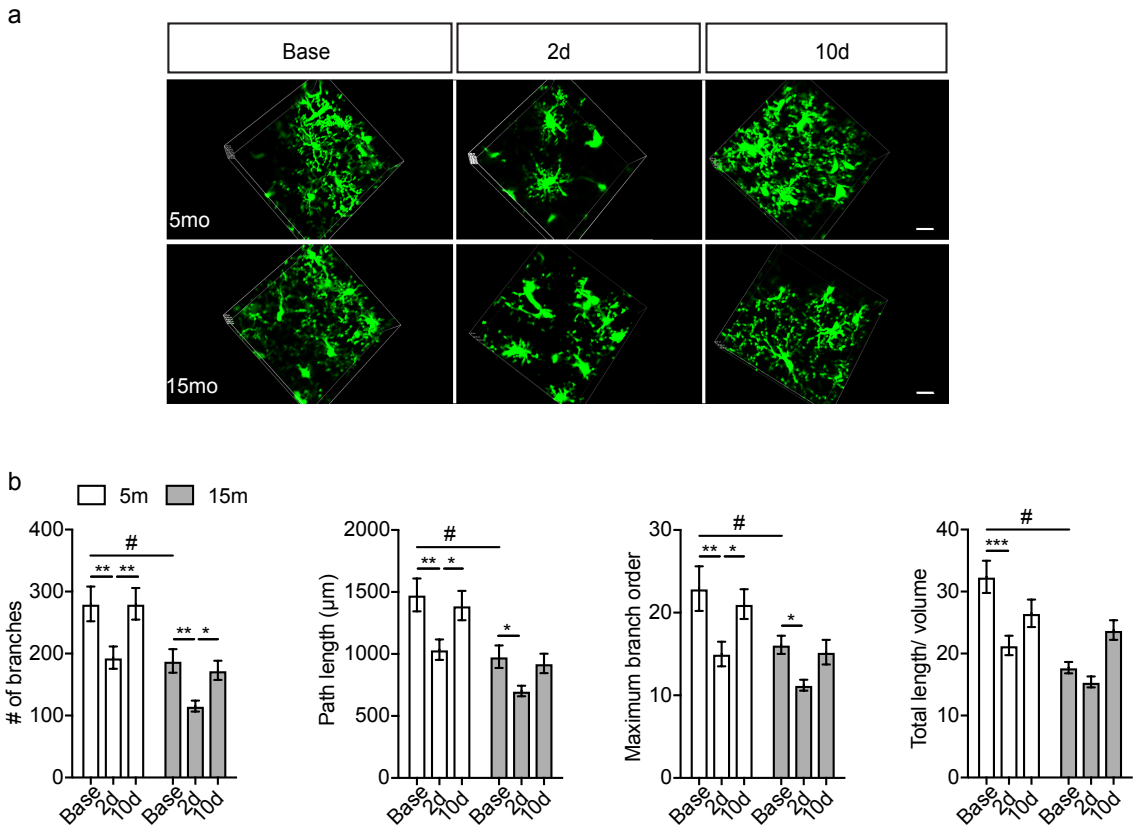

Figure 8. Systemic inflammation transiently affects microglia in an age-dependent manner. a). Representative two-photon images from 5 and 15 months old mice showing microglia changes 2 and 10 days post LPS injection. Scale bar: 20µm. b) Morphological parameters quantification for 5 and 15 months old mice after LPS injection (mean of 5-6±SEM; two-way ANOVA followed by Tukey's *post hoc* test, #*p<0.05, **p<0.01, ***p<0.001

4.2 NLRP3 ko mice are refractory to peripheral immune challenge and age-associated changes

Inflammasomes form in response to microbial or danger signals, which leads to the cleavage of pro-caspase-1 into the active caspase-1 enzyme. Active caspase-1 then cleaves the pro-forms of the inflammatory cytokines, IL-1β and IL-18, into their active forms (79, 138). To assess if the NLRP3 inflammasome is involved in the observed changes during aging and LPS challenge, *Nlrp3*$^{-/-}$ mice were crossed with CX3CR1/GFP$^{-/+}$ mice to assess microglial dynamics using 2PLSM (figure 9). No morphological differences between 5 and 15mo animals were observed at baseline for the assessed parameters, suggesting that NLRP3 deficiency protects against age-induced microglial alterations (figure 9a,b,c). Interestingly, microglia from NLRP3$^{-/-}$ mice were refractory to LPS injection (figure 9a,b,c) since no morphological changes were observed after LPS challenge.

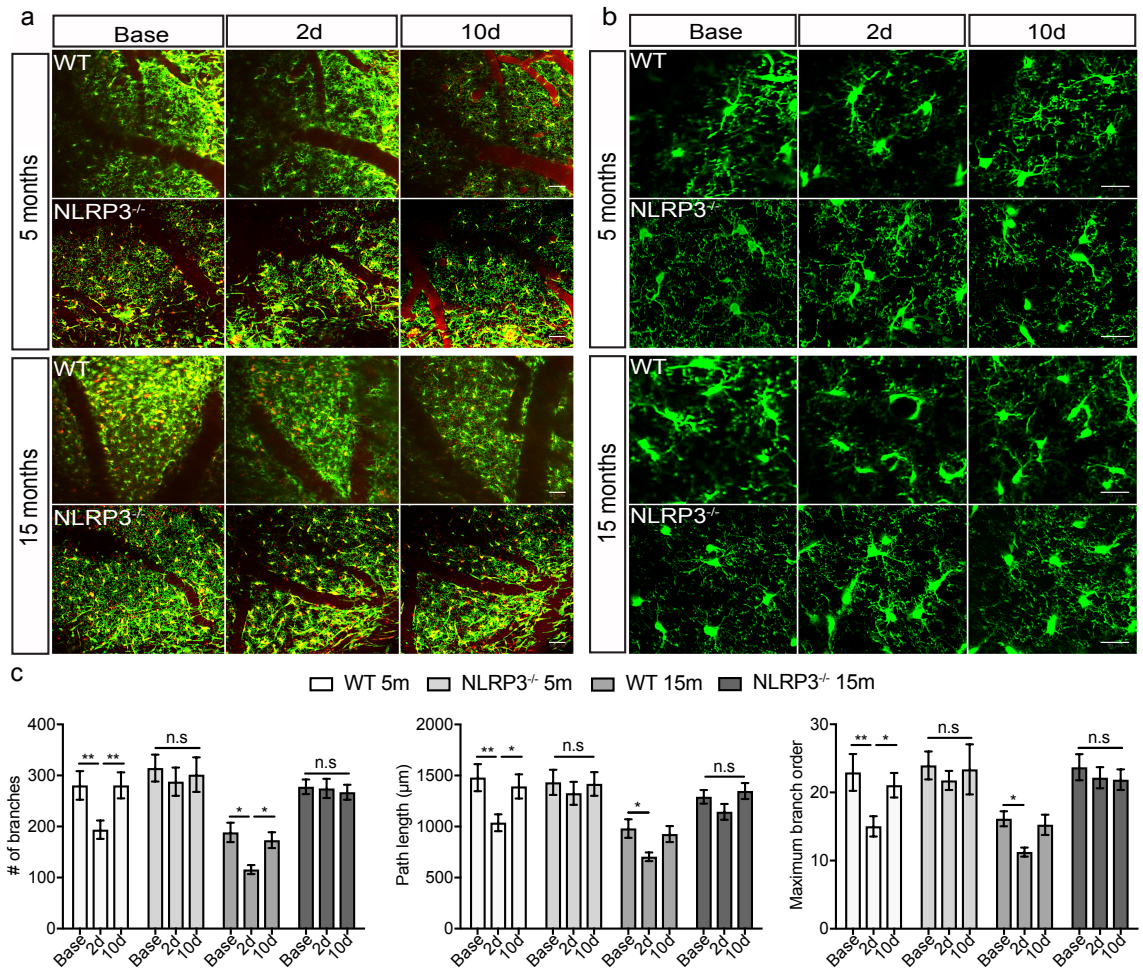

Figure 9. NLRP3 knock out mice are refractory to peripheral immune challenge or age-associated changes. a) Two-photon *in vivo* overview images from wild-type and NLRP3$^{-/-}$ mice (5 and 15 months old). Imaging was performed on the very same brain regions across the time-points evidenced by vasculature (Dextran red). Scale bar: 50µm. b) Two-photon representative images of wild-type and NLRP3$^{-/-}$ microglia (5 and 15 months old). Scale bar: 20µm. c) Quantification of morphological parameters for wild-type and NLRP3$^{-/-}$ mice after LPS injection.(mean of 5-6±SEM; two-way ANOVA followed by Tukey's *post hoc* test, *p<0.05, **p<0.01, ***p<0.001).

Accordingly, no changes in IL-1β levels were observed in NLRP3$^{-/-}$ mice after LPS injection (figure 10a), whereas wild-type mice exhibited an increase 2 days after peripheral challenge and then, 10 days later, a restoration to basal levels (figure 10a). When TNF-α levels were measured, it was found to increase in all the experimental groups, 2 days after peripheral challenge (figure 10b). Importantly, this increase was transient, since 10 days after LPS injection TNF-α levels dropped back down to basal condition (figure 10b).

Together these results suggest that the morphological changes observed in microglial morphology after LPS injection corresponds with changes in the inflammatory response, particularly with IL-1β secretion.

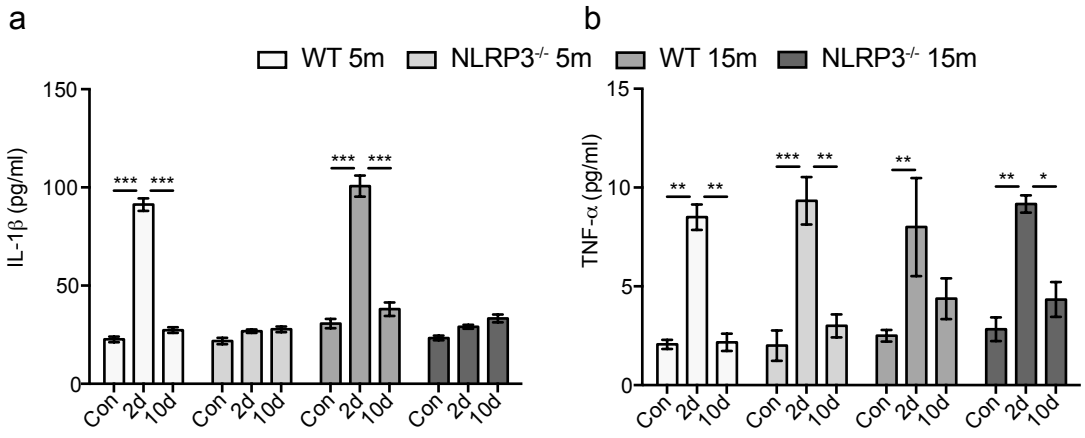

Figure 10. Brain inflammatory response after systemic inflammation. a) IL-1β ELISA measurement in brain lysates of wild-type and NLRP3$^{-/-}$. A significant IL-1β levels increase NLRP3-dependent was observed 2 days after LPS injection and then a return to control levels. b) TNF-α ELISA measurement in brain lysates of wild-type and NLRP3$^{-/-}$, all groups showed a transient increase in its levels (mean of 5-6±SEM; two-way ANOVA followed by Tukey's *post hoc* test, *p<0.05, **p<0.01, ***p<0.001).

4.3 Peripheral immune challenge affects amyloid deposition in APP/PS1 mice

Since systemic inflammation represents a risk for developing neurodegeneration particularly for AD (66), the effects of a peripheral immune challenge were analyzed on pathological hallmarks of AD using APP/PS1 mice. Additionally, it was tested whether these effects were mediated by the NLRP3 inflammasome. Therefore, APP/PS1 and APP/PS1/*Nlrp3*$^{-/-}$ mice underwent the same experimental protocols as described above for non-APP/PS1 mice (figure 4). While number and size of Aβ deposits were increased in APP/PS1 compared to APP/PS1/*Nlrp3*$^{-/-}$ mice (Figure 11a,b) at 15mo, APP/PS1 but not APP/PS1/*Nlrp3*$^{-/-}$, revealed a significant increase in Aβ deposition upon LPS challenge at both time points investigated (figure 11a,b). At 5mo, the time Aβ deposits evolve in this model, no apparent differences became detectable (139).

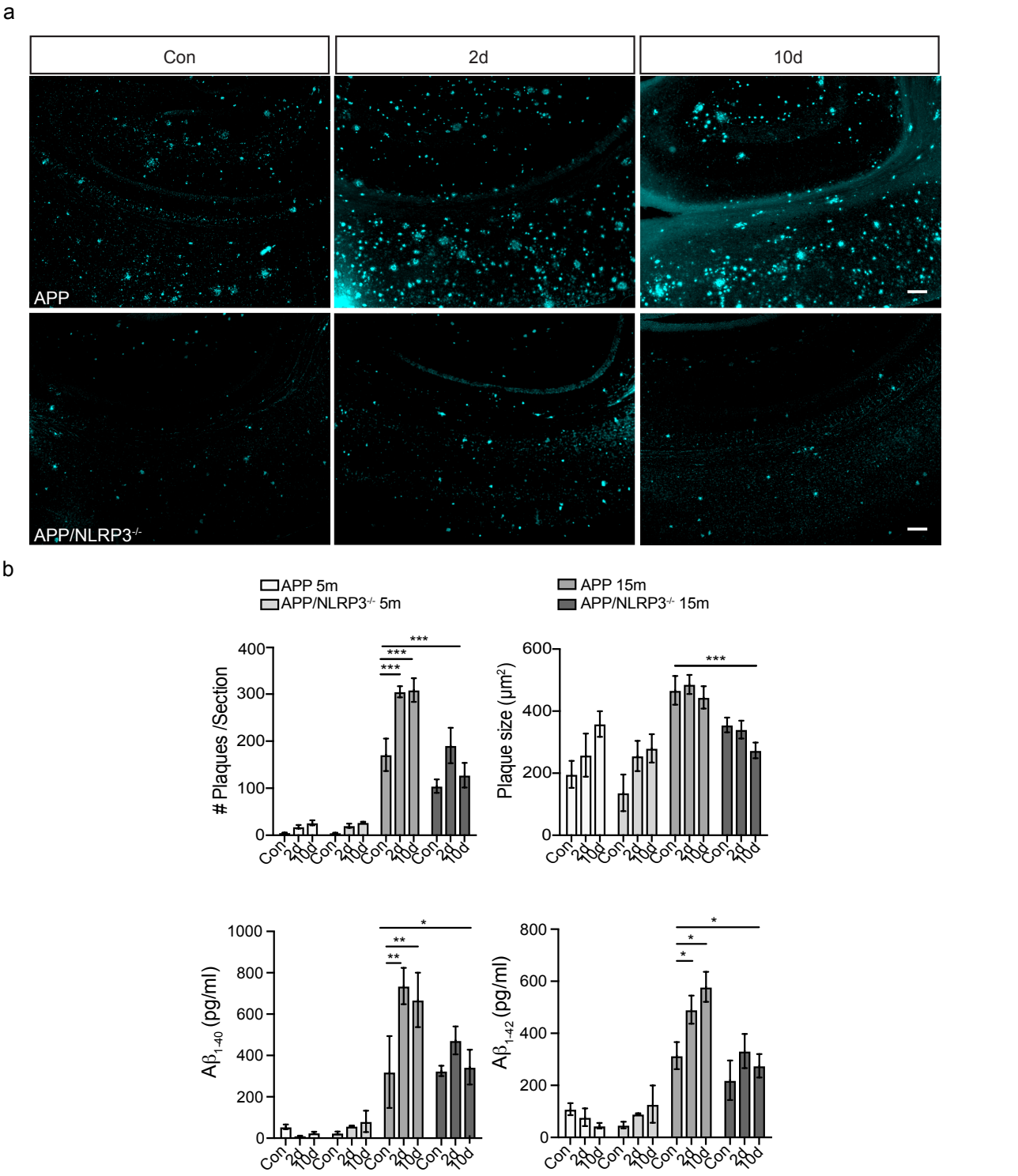

Figure 11. Peripheral immune challenge affects amyloid deposition in APP/PS1 mice. a) Representative images of MXO4 staining for APP and APPNLRP3$^{-/-}$ 15 months old mice. Scale bar: 20µm. b) Amyloid deposit number and size quantification, and Amyloid-beta$_{1-40}$ and $_{1-42}$ ELISA quantification for APP and APPNLRP3$^{-/-}$ mice (5 and 15 month old) mean of 5-6±SEM; two-way ANOVA followed by Tukey's *post hoc* test, *p<0.05, **p<0.01, ***p<0.001).

Additionally, these results were confirmed by ELISA measurements of $A\beta_{1-40}$ and $A\beta_{1-42}$ (figure 11b) and by Aβ specific antibody 6E10 inmunoblot (figure 12a,b). In case of 6E10 immunoblot, an increase in Aβ monomeric forms (10-15KDa) was observed in APP/PS1 mice after LPS immune challenge (figure 12a.b). Importantly, no changes were observed in APP/PS1/*Nlrp3*$^{-/-}$ mice after LPS injection (figure 12a,b)

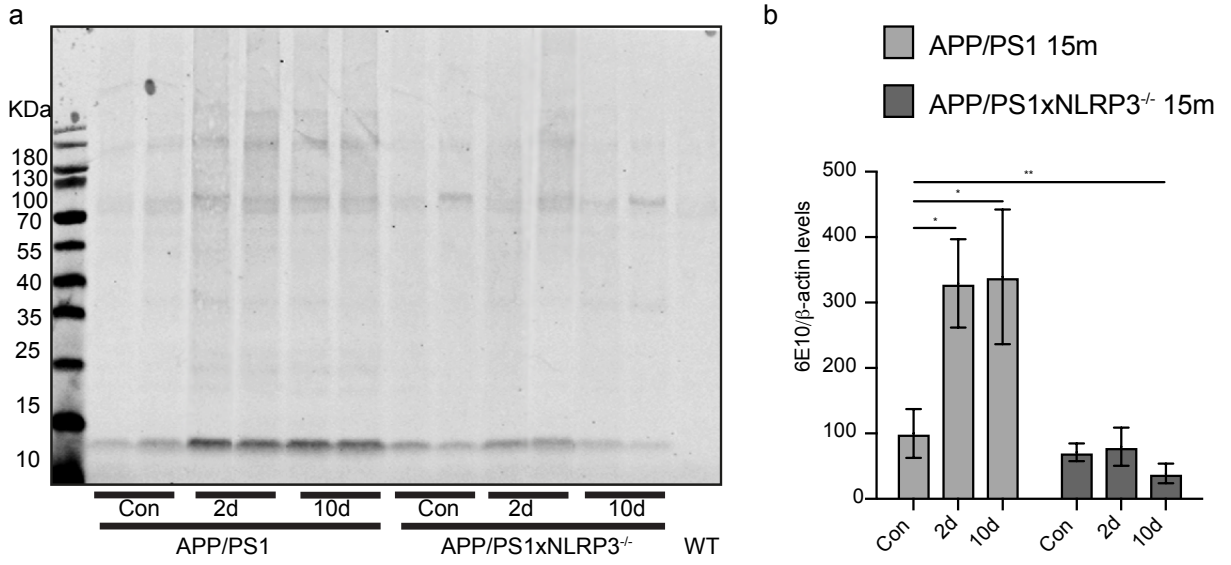

Figure 12. Peripheral immune challenge affects amyloid monomeric deposition in APP/PS1 mice. a) Western blot analysis of whole brain lysate from 15 months old APP and APPNLRP3$^{-/-}$ animals using 6E10 antibody b) Quantification of 6E10 levels (a) expression (mean of 2-5±SEM; two-way ANOVA followed by Tukey's *post hoc* test, *p<0.05, **p<0.01)

Of note, immunoblot analysis CT20 antibody (140), which detects the terminal fragments and the full length APP, determined that LPS challenge did not affect APP processing machinery since no changes in expression were observed in none of the groups analyzed (figure 13a,b).

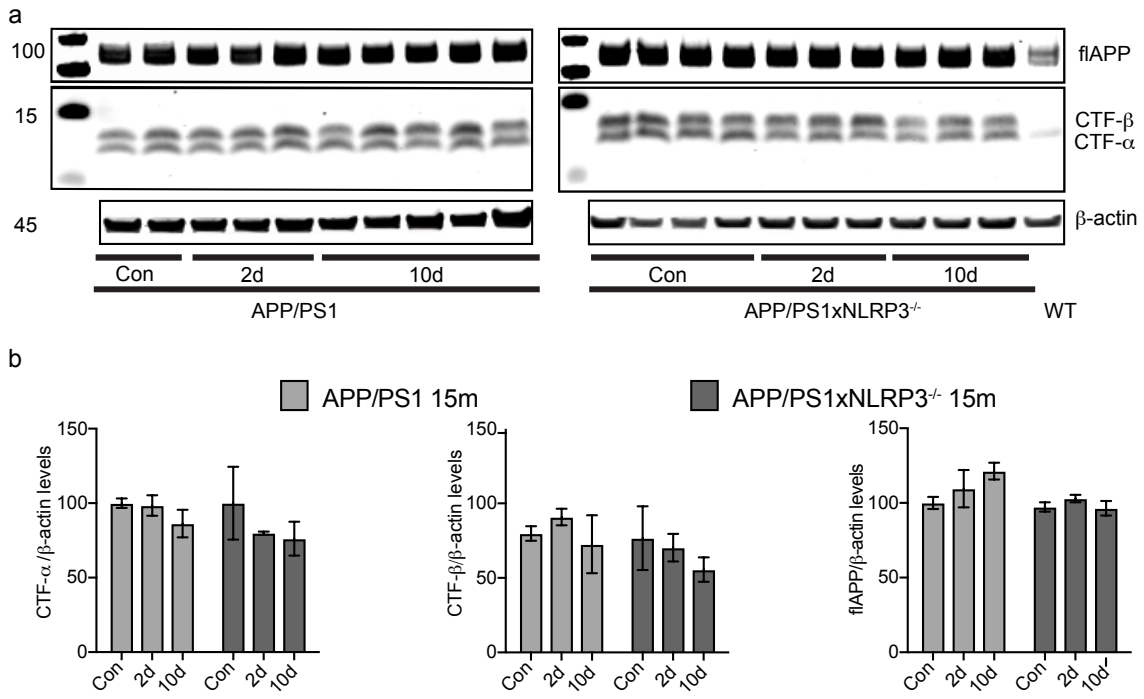

Figure 13. Peripheral immune challenge does not affect APP processing machinery. a) Western blot analysis of whole brain lysate from 15 months old APP and APPNLRP3$^{-/-}$ using CT20 antibody b) Quantification of CTF-α, CTF-β and full length APP

Concomitantly, IL-1β levels increased in APP/PS1 and APP/PS1/*Nlrp3*$^{-/-}$ mice (5 and 15mo) at 2 days, before decreasing 10 days later (figure 14a). For TNF-α levels, an increase was observed in APP/PS1 and APP/PS1/*Nlrp3*$^{-/-}$ (5mo) 2 days post LPS, which was back to baseline levels at 10 days. In 15mo mice, the rise in TNF-α was restricted to APP/PS1 and not detected in APP/PS1/*Nlrp3*$^{-/-}$ (figure 14b). Together, these results suggest that a LPS elicited peripheral immune challenge affects amyloid deposition in aged APP/PS1 mice in an NLRP3-dependent manner.

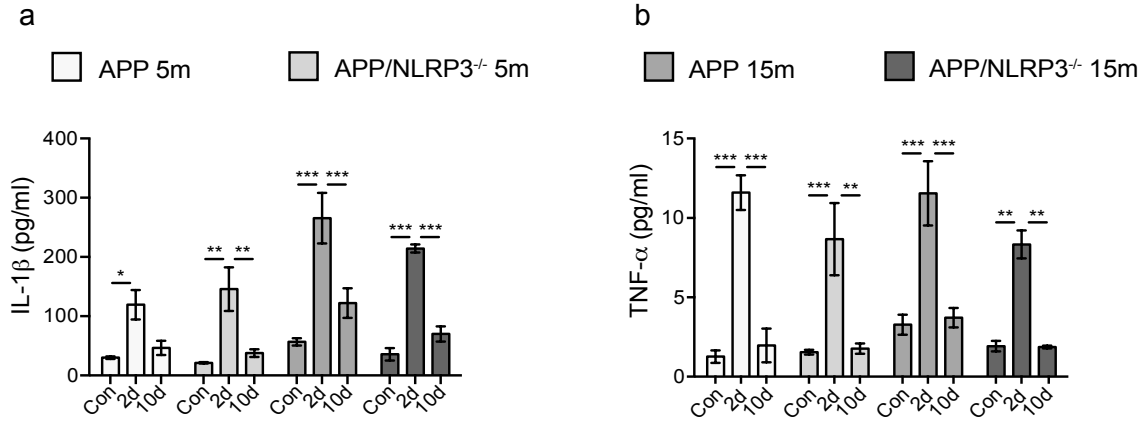

Figure 14. Systemic inflammation triggers an inflammatory response in APP/PS1 and APP/PS1/NLRP3$^{-/-}$. a,b) IL-1β and TNF-α ELISA measurement in brain lysates of APP and APPNLRP3$^{-/-}$. A significant IL-1β (a) and TNF-α (b) transient increase was observed 2 days after LPS injection and then a return to control levels (mean of 5-6±SEM; two-way ANOVA followed by Tukey's *post hoc* test, *p<0.05, **p<0.01, ***p<0.001)

4.4 Microglia dynamics depends on distance to Aβ deposition in APP/PS1 mice

Microglia cluster around amyloid deposits with their processes being retracted and less dynamic as compared to deposit-free areas (141). This suggests that on a morphological level at least two different populations of microglial cells have to be distinguished by location in murine AD models, those cells located near to Aβ and cells that are more distantly located. Analysis by 2PLSM revealed that LPS did not lead to further morphological changes in microglia located in the vicinity of Aβ deposits (figure 15a,b), most likely due to the already existing high-level of activation by Aβ itself (figure 16).

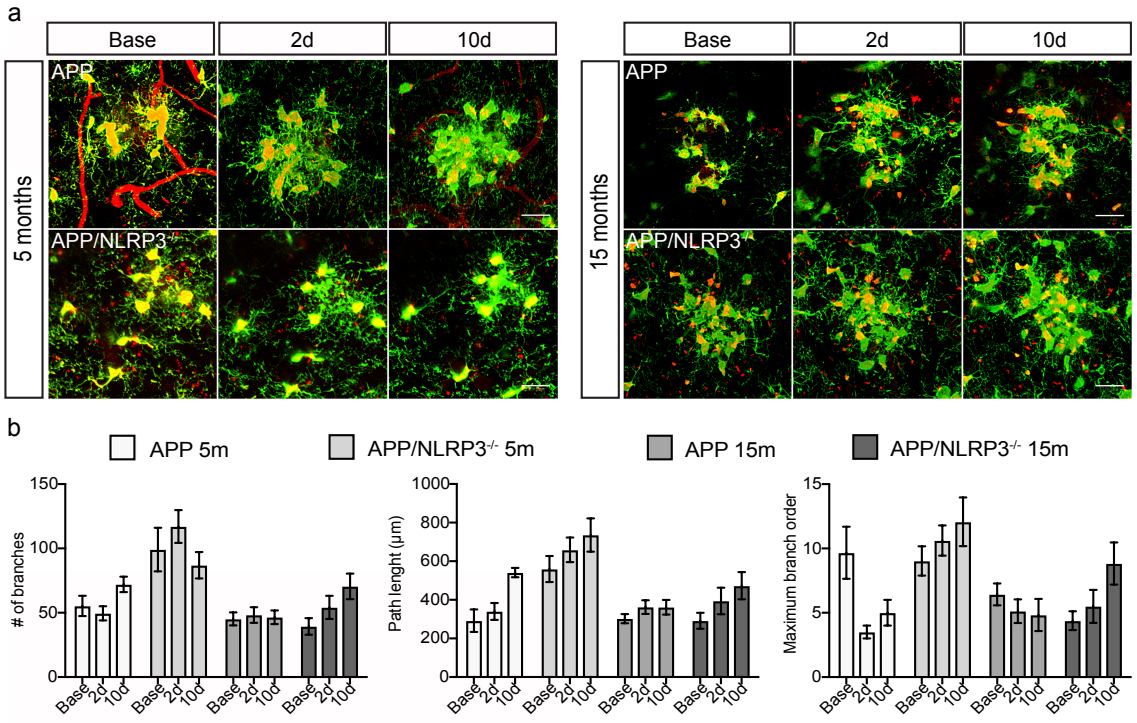

Figure 15. Microglia dynamics depends on distance to Aβ deposition. a) Two-photon images of microglia cells clustering around amyloid deposit for APP and APPNLRP3$^{-/-}$ (5 and 15 months old). Scale bar: 20µm b) Quantification of morphological parameters in (a) mean of 5-6±SEM; two-way ANOVA followed by Tukey's *post hoc* test, *p<0.05).

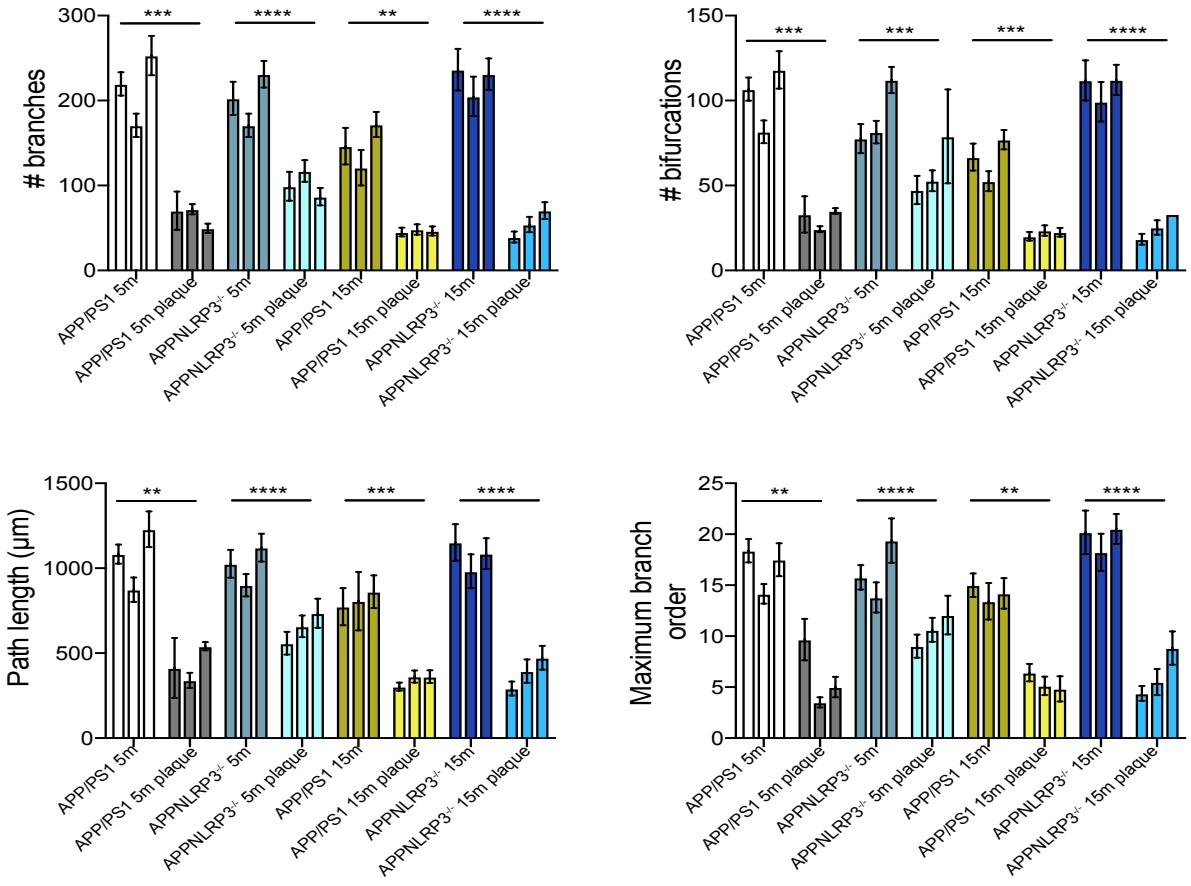

Figure 16. Amyloid deposit alters microglia morphology. Quantification of microglia morphological parameters for APP and APPNLRP3$^{-/-}$ mice (mean of 5-6±SEM; two-way ANOVA followed by Tukey's *post hoc* test, **p<0.01, ***p<0.001).

Considering the increase in amyloid deposition observed in APP/PS1 mice after LPS injection (figure 5), it is plausible to think that systemic inflammation functionally impairs this particular microglial population. With this aim, the ability of microglia to *in vivo* uptake Aβ was evaluated by FACS. Peripheral LPS challenge impaired microglial uptake of Aβ in APP/PS1 but not APP/PS1/*Nlrp3*$^{-/-}$ mice (figure 17a,b), suggesting that systemic inflammation affects the functional status particularly the Aβ clearance capacity of these cells.

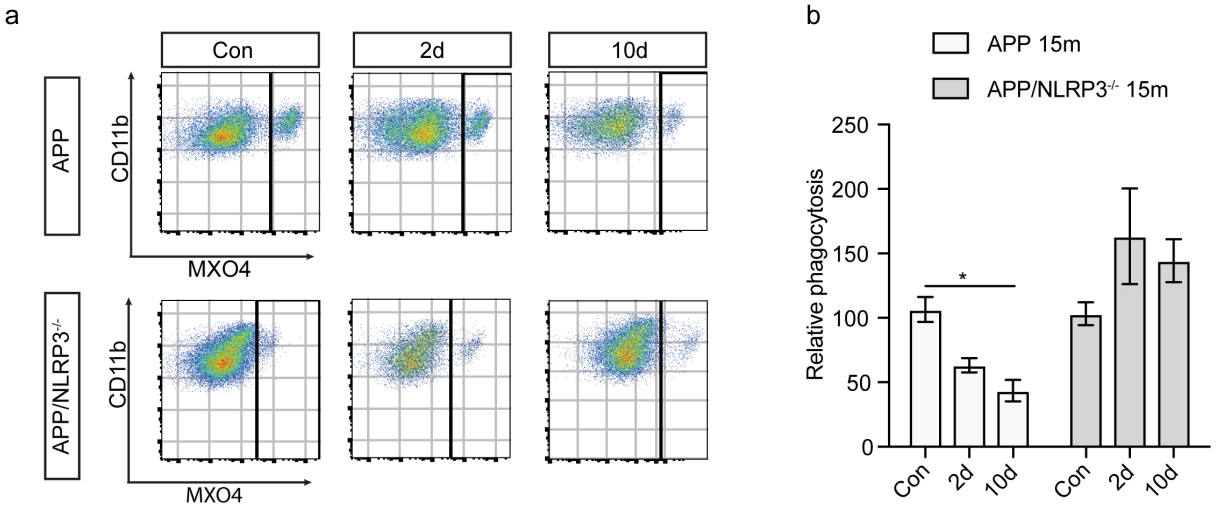

Figure 17. Systemic inflammation affects amyloid uptake by microglia in an NLRP3-dependent manner. a) Flow cytometry plots from APP and APPNLRP3$^{-/-}$ mice (15 months old); cells were gated on CD11b and MXO4 after microglia isolation. b) Relative Aβ microglia uptake quantification (mean of 5±SEM; two-way ANOVA followed by Tukey's *post hoc* test, *p<0.05)

In line with these findings, reduction in beclin-1 expression, a protein that is actively involved in protein degradation in AD (35), impaired Aβ phagocytosis (35). Therefore, beclin-1 expression was analyzed by immunoblot. Peripheral immune challenged reduced beclin-1 expression (figure 18a,b) in APP/PS1 mice but not in APP/PS1/*Nlrp3*$^{-/-}$, supporting the findings obtained with FACS analysis.

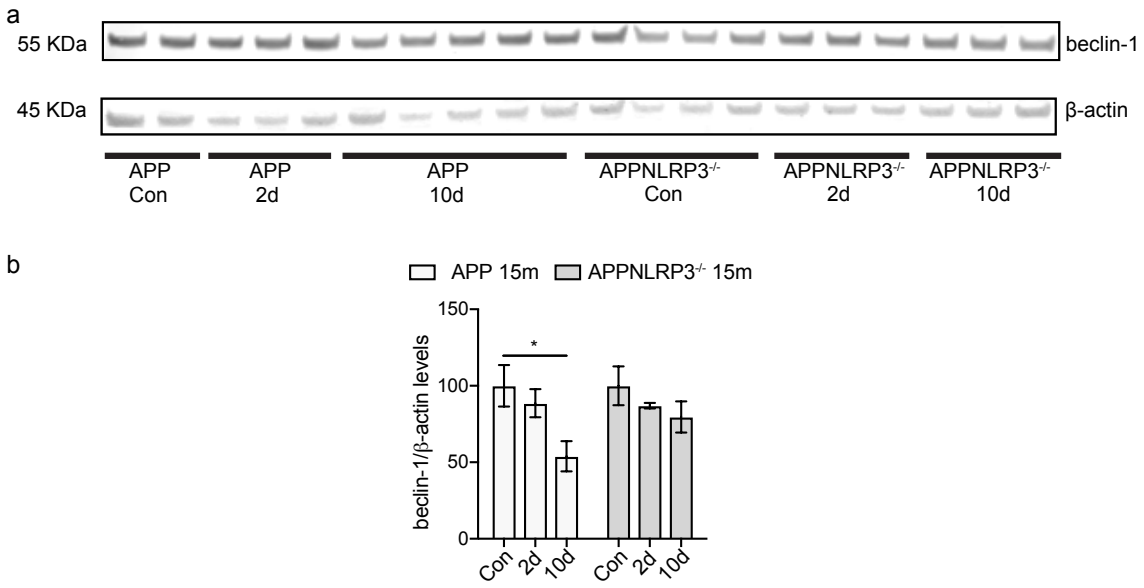

Figure 18. Systemic inflammation affects phagocytosis in an NLRP3-dependent manner. a) Western blot analysis of whole brain lysate from 15 months old APP and APPNLRP3$^{-/-}$ using beclin1 antibody. b) Quantification of beclin1 expression levels (mean of 2-5±SEM; two-way ANOVA followed by Tukey's *post hoc* test, *p<0.05)

In contrast to deposit-associated microglia, the morphological dynamics of deposit-distant microglia were more reminiscent to microglia of WT mice, with respect to their time-dependent morphological changes after peripheral immune challenge, age and presence of the NLRP3 inflammasome. In 5mo APP/PS1 mice the number of branches and the maximum branch order were reduced 2 days post-LPS, followed by a recovery in the number of branches by 10 days (figure 19). Of note, deposit distant microglial dynamics in aged APP/PS1 (15mo) mice, showed no changes upon peripheral immune challenge. These cells, despite not being in direct contact to Aβ deposits, already exhibited morphological signs of microglial activation (figure 16), likely to be caused by the presence of soluble Aβ species or inflammatory factors, which may render these cells less responsive to any further immune stimulation. In case of APP/PS1/*Nlrp3*$^{-/-}$ and in line with the results showed for NLRP3$^{-/-}$, we observed that these mice were largely refractory to peripheral immune challenge and aging, since no morphological changes were observed upon LPS challenge.

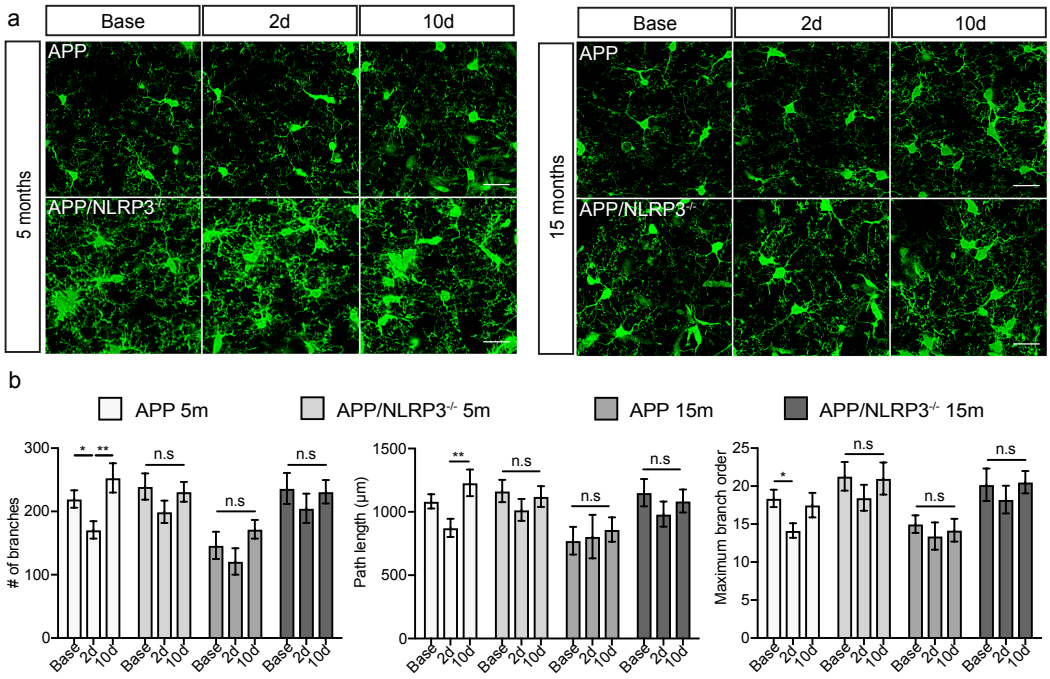

Figure 19. Microglial morphological dynamics depends on the distance to amyloid deposition. a) Two-photon microglia images from APP and APPNLRP3$^{-/-}$ animals in areas free of deposit (5 and 15 months old mice). Scale bar: 20µm b) Quantification of morphological parameters for microglia in areas free of deposit in APP and APPNLRP3$^{-/-}$ mice (mean of 5±SEM; two-way ANOVA followed by Tukey's *post hoc* test, *p<0.05, **p<0.01).

4.5 Peripheral myeloid cells infiltrate brains of APP/PS1 mice upon peripheral LPS challenge

Myeloid cell infiltration into the brain occurs in several models of inflammation (142–145). To investigate this phenomenon, cortex and hippocampal sections were immunohistologically stained for Iba-1 and the peripheral myeloid marker CD169 (146–148). Cortex and hippocampal sections were selected due to the fact that these brain regions are among the most affected areas in AD (88).

Analysis of young and aged WT and NLRP3$^{-/-}$ mice did not reveal myeloid cell infiltration into the brain upon LPS challenge (figure 20). Similarly, LPS did not induce myeloid cell infiltration in young or aged APP/PS1 or APP/PS1/*Nlrp3*$^{-/-}$ mice in brain areas free of Aβ deposits (figure 21a,b). Likewise, young APP/PS1 and APP/PS1/*Nlrp3*$^{-/-}$ mice showed no CD169 immunopositive cells in response to LPS. In strong contrast, CD169 positive cells became detectable in aged, 15mo APP/PS1 mice at 2 days after LPS, mostly located in close vicinity to Aβ deposits (figure 11c,d). Interestingly this was not found in APP/PS1/*Nlrp3*$^{-/-}$, whereby no CD169 positive cells became detectable (figure 21c,d). Together this may suggest that immunoattracting mediators, such as cytokines and chemokines are being produced close to Aβ deposits in aged APP/PS1 mice. Therefore, it is hypothesized that NLRP3 knockout may prevent the infiltration of Aβ-directed migration at several levels including the reduction of inflammatory mediators, the capability of peripheral immune cells to enter the brain and also by protecting the integrity of the blood brain barrier.

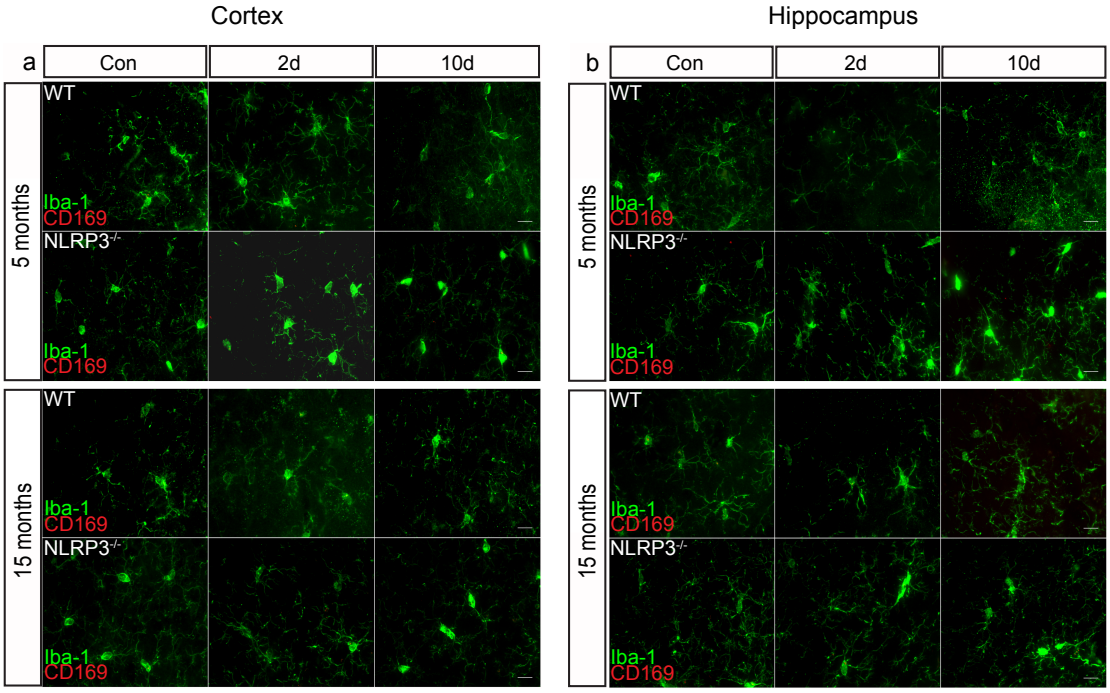

Figure 20. No peripheral myeloid cell infiltration was observed in non-APP mice upon LPS injection. a,b) Iba-1 (green) and CD169 (red) staining in cortex (left) and hippocampus (right) of 5 and 15 months old of wild-type and NLRP3$^{-/-}$ mice. Scale bar: 20μm

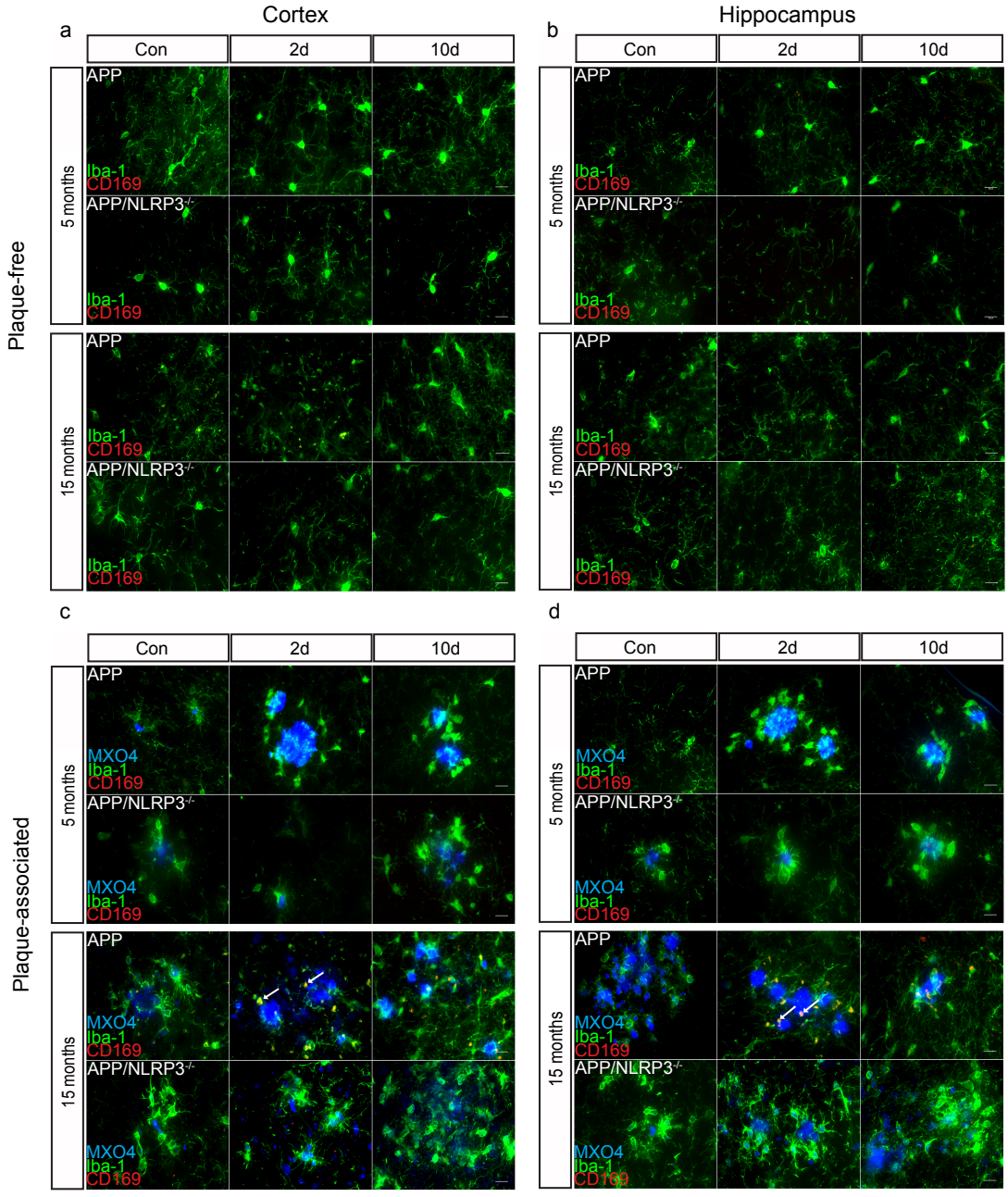

Figure 21. Peripheral myeloid cells infiltrates into APP/PS1 mice upon LPS injection. a,b) Iba-1 (green) and CD169 (red) staining in deposit-free areas (cortex and hippocampus) of 5 and 15 months old of APP and APPNLRP3$^{-/-}$. c,d) Iba-1 (green), CD169 (red) and MXO4 staining in deposit-associated areas (cortex and hippocampus) of 5 and 15 months old of APP and APPNLRP3$^{-/-}$. Note the colocalization between Iba-1 and CD169 (white arrows) in APP 15-month-old mice 2 days post LPS injection. Scale bar: 20μm

4.6 Microglia proliferate upon peripheral immune challenge

The microglial cell population renews physiologically by proliferation in mice and men (149, 150). In AD and related mouse models, microglial proliferation seems to be accelerated (151). To understand if a peripheral inflammatory stimulus further increases microglial proliferation, cortical and hippocampal sections were analyzed by immunostaining for Iba-1 and the proliferation marker Ki67. PBS-treated WT and NLRP3$^{-/-}$ animals showed only few proliferating microglia (figure 22a,c), except for 15mo WT mice, that revealed proliferating microglia in the hippocampus (figure 22b,c). Inter-group analysis revealed that in cortical areas, WT mice (5 and 15mo) had a higher proliferation rate as compared to Nlrp3$^{-/-}$ animals (figure 22). In the hippocampus, this difference was only observed when WT and NLRP3$^{-/-}$ animals were compared at 15mo. In contrast, APP/PS1 and APP/PS1/*Nlrp3*$^{-/-}$ mice already showed proliferating microglia in the cortex and hippocampus under control conditions mainly located at Aβ deposits (figure 23a,b). While there was no difference in the number of proliferating microglia between 5mo APP/PS1 and APP/PS1/*Nlrp*$^{-/-}$ mice, NLRP3 knockout substantially reduced the number of inflammation-induced proliferating microglia in aged, 15mo animals (figure 23c). This finding indicates that NLRP3 is involved in age- and Aβ-dependent microglial proliferation and therefore, blocking NLRP3 could be one solution of modifying pathological microglial proliferation.

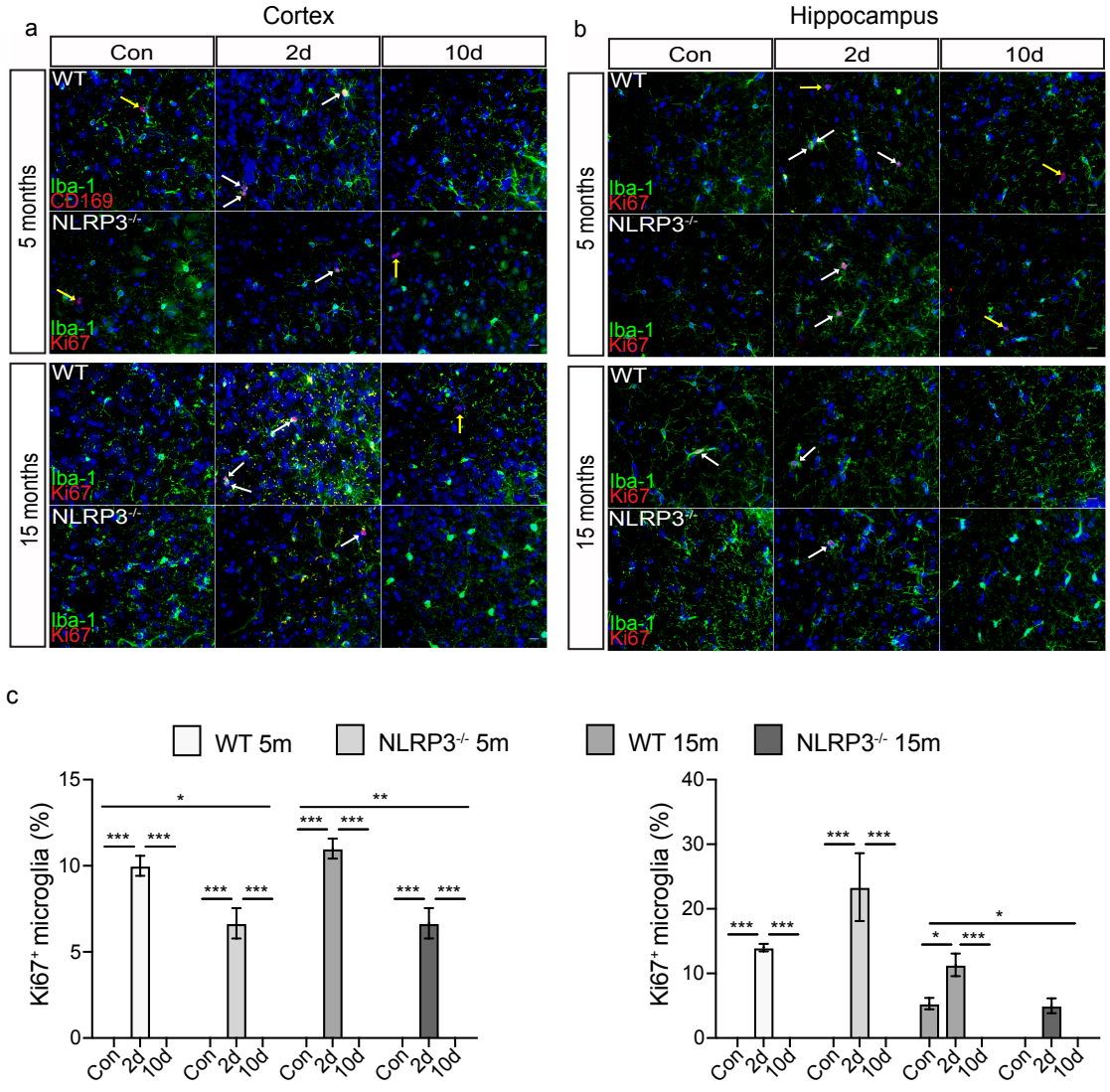

Figure 22. Microglia proliferates in non-APP mice upon peripheral immune challenge. a,b) Iba-1 and Ki67 staining in the cortex and hippocampus of wild-type and NLRP3$^{-/-}$ (5 and 15 months old). Microglia proliferates upon LPS injection (white arrows). Non-microglia cells proliferation was observed as well (yellow arrows) Scale bar: 20μm. c) Quantification of microglial proliferation in cortex (left panel) and hippocampus (right panel) (mean of 5±SEM; two-way ANOVA followed by Tukey's *post hoc* test, *p<0.05, **p<0.01, ***p<0.001).

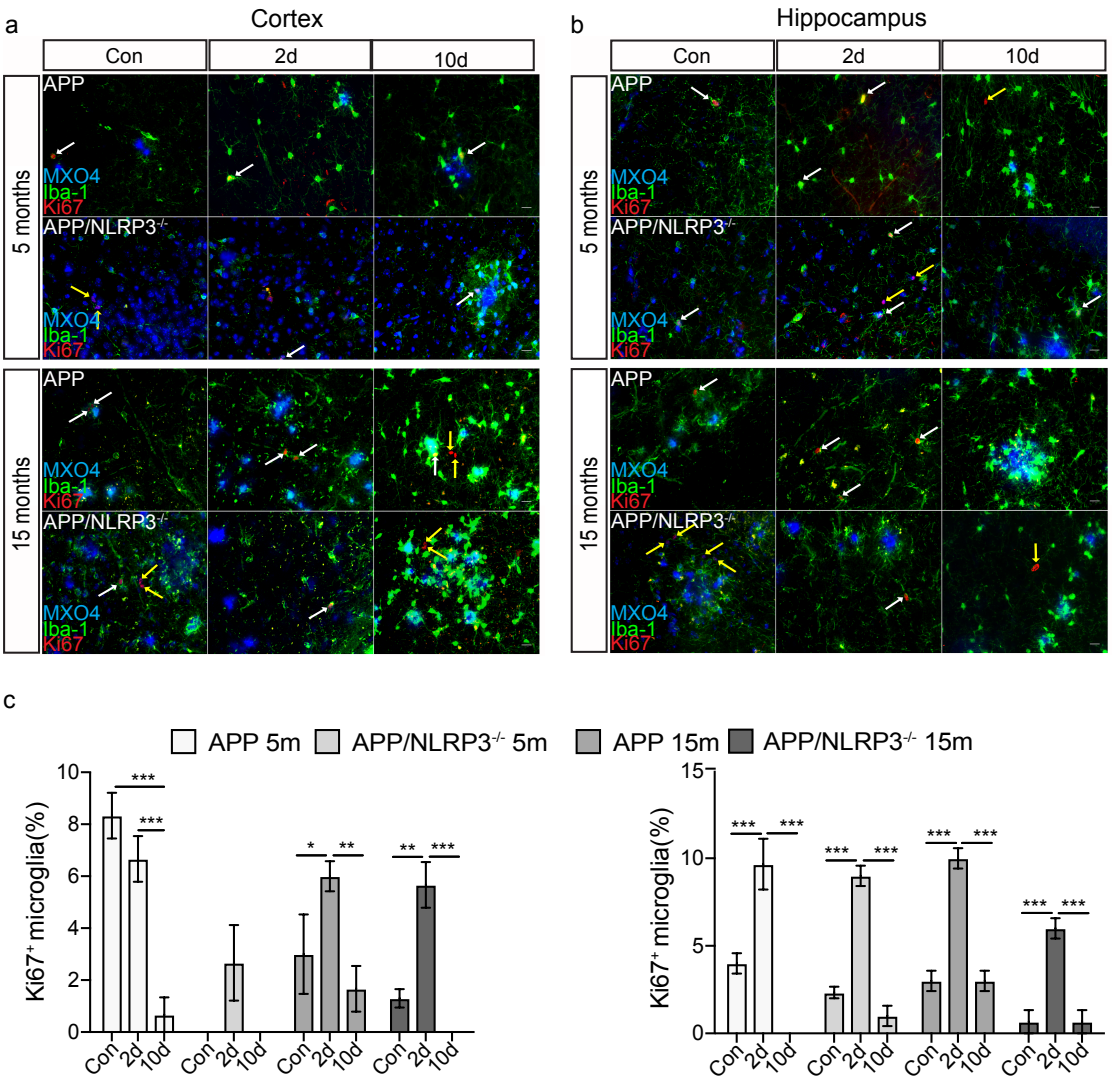

Figure 23. Microglia proliferates in APP/PS1 mice upon peripheral immune challenge. a,b) Iba-1, Ki67 and MXO4 staining in the cortex and hippocampus of APP and APPNLRP3$^{-/-}$ mice (5 and 15 months old). Microglia proliferates upon LPS injection (white arrows). Non-microglia cells proliferation was observed as well (yellow arrows). Scale bar: 20μm c) Quantification of microglial proliferation in cortex (left panel) and hippocampus (right panel) (mean of 5±SEM; two-way ANOVA followed by Tukey's *post hoc* test, *p<0.05, **p<0.01, ***p<0.001).

5 Discussion chapter 4

As the sentinels of the brain, microglia are designed to be extremely versatile to external stimuli. Physiologically, they exhibit a high order of ramification, but at the same time remain incredibly motile in order to continually survey and control their immediate environment. In the context of aging and neurodegeneration, however, their morphology and function drastically changes (152). Indeed, branches are retracted and their order reduced, while at the same time the soma volume increases (38). Functionally, these cells acquire a pro-inflammatory phenotype, releasing inflammatory cytokines and other neurotoxic mediators. In this part of the dissertation, microglial dynamics were assessed in the context of systemic inflammation and Aβ deposition by 2PLSM in wild-type and APP/PS1 transgenic mice, a murine model of AD, NLRP3 knockout and APPNLRP3$^{-/-}$ animals.

A 3-dimensonal analysis and quantification of microglia revealed that systemic inflammation: i) transiently affects microglia in an age-dependent manner, ii) worsens Aβ deposition by affecting microglia-mediated clearance and iii) increases microglial proliferation as a sign of disease acceleration. Most importantly, the activation of NLRP3 inflammasome has been identified as a key mediator of these effects.

To our knowledge, this is the first time that activation dynamics of microglia have been shown under *in vivo* imaging conditions. Microglial cell dynamics were strongly impaired at 48h after peripheral immune challenge in wild-type animals. This phenomenon was characterized by a 50% reduction in the number of branches, bifurcations, path length and maximum branch order. Together, these changes indicate a substantial loss of surveillance capacity in line with similar findings by previous immunohistochemical studies (2, 99, 153). Since microglia may undergo age-dependent changes affecting their reaction to external stimuli, mice were studied at 5 and 15 months (aged) of age. Aging itself also caused morphological changes in microglia, characterized by a reduction of all parameters assessed. This supports the hypothesis that age-associated brain changes may act as priming factors for microglia. In both, adult and aged wild-type animals, changes in microglia dynamics induced by systemic inflammation were of transient nature, peaking at 2 days and returning back to basal levels at 10 days after LPS challenge. In contrast to young animals, aged mice started from a primed, pre-activated level, but also returned completely back to baseline at 10 days, suggesting that aging affects the basal activation state, but not the capacity to fully recover, at least not at the time points and ages assessed in this dissertation. These findings from dynamic morphological *in vivo* imaging, parallel data from transcriptional analysis, which revealed age-related changes in genes

encoding for immune regulation, cytokine secretion, immune adhesion and chemotaxis (7). In addition, genes known as “off-signals” (154), including *Cd200* and *Cd300,* are downregulated in aged microglia. These results suggest that changes in microglial morphology are accompanied by functional responses, such as cytokine release as well as impaired cerebral metabolism (103) or iNOS expression (155).

Since systemic inflammation has been identified as a risk factor for persisting cognitive deficits in humans (100, 156, 157) and likewise for the development of neurodegenerative diseases such as AD (158), it was tested whether a single peripheral immune stimulus would affect neuropathological changes such as Aβ pathology and neuroinflammation in a murine AD model. A single LPS injection was sufficient to cause an increase in cerebral Aβ deposition in aged APP/PS1 transgenic mice. Since, no changes in APP processing were detectable, we hypothesized that microglia Aβ clearance might be affected by peripheral inflammation. In line with this assumption, LPS was found to reduce microglial Aβ uptake. In parallel, beclin-1, a factor involved in microglial Aβ phagocytosis (35), was reduced after peripheral immune challenge, supporting the hypothesis that dysfunctional microglia may account for the increase of Aβ deposition. These results are in accordance with previous reports showing that peripheral administration of LPS can increase amyloid deposition in transgenic murine models of beta-amyloidosis (159, 160).

Recent evidence suggests that the microglia population is not homogeneous within the AD brain (6, 161, 162). In concordance with these previous findings we have identified two different populations with regards to their distance to Aβ deposits. *In vivo* 2PLSM analysis showed that microglia located at the site of Aβ deposition did not show striking morphological changes upon peripheral immune stimulation as compared to microglia located at a greater distance from the deposits. Since microglia at the site of Aβ deposition already show substantial changes with reduction of branch number, length and order, it is suggested that these cells may not be “further” reacting, at least with respect to morphological measures. Instead, distant microglia showed dynamic changes of morphology, which were similar to WT mice. The process of microglia activation is frequently coupled with an expansion of the microglial population. In the context of neuroinflammation, this is almost exclusively upon proliferation of resident cells (149, 151). Here it was observed that systemic inflammation elicited microglial proliferation in cortex and hippocampus. Coincidentally, this increase in microglial proliferation was 2 days after LPS challenge, the time at which microglia become not only morphologically activated but also the time where an increase in the inflammatory response was observed. Importantly, for APP mice, microglia proliferation was already observed in absence of LPS challenge in concordance with

previous reports (151). Microglial proliferation decreased to basal levels in all experimental groups 10 days after immune challenge, the time where infection is resolved. These results support the hypothesis that expansion of microglial population occurs mainly due to proliferation of resident cells. Since the microglial population is regionally heterogeneous (7), it will be extremely important to characterize the identity of these proliferative cells in order to understand what their contribution to AD pathology could be.

In order to test the impact of innate immune signaling on the observed changes, mice carrying a genetic deletion of *Nlrp3* were analyzed, thus blocking NLRP3 inflammasome activation, a central pathway of peripheral and cerebral innate immunity. In general, inflammasomes are subcellular multiprotein complexes that play an important role in host defense against extracellular, vacuolar, and intracellular bacteria, fungi, and viruses (86, 163, 164). Given the fact that the NLRP3 inflammasome has been implicated in peripheral immune reactions upon bacterial challenge and also has been shown to contribute to neuroinflammatory changes (88, 165–167) makes it a prime candidate for the induced changes that occur upon LPS challenge during aging and Aβ deposition. Microglia from NLRP3 deficient animals were refractory to aging- and inflammation- induced morphological changes. This is consistent with a previous study showing that ablation of the NLRP3 inflammasome controls age-related inflammation (168).

Furthermore, the results presented here indicate that the NLRP3 inflammasome is involved in the changes of Aβ deposition observed upon peripheral immune challenge. In line with previous findings, APP/PS1/*Nlrp3*$^{-/-}$ mice showed significantly less Aβ deposition compared to APP/PS1 animals (88). Of note, peripheral immune challenge did not aggravate Aβ deposition in NLRP3 deficient mice. While this dissertation was not designed to analyze whether peripheral or central NLRP3 deficiency is mediating this beneficial effect, one contributing mechanism could be a preservation of Aβ clearance mechanisms as previously reported (88). This is supported by the observation that no changes in phagocytic capacity or beclin-1 were observed in APP/PS1/*Nlrp3*$^{-/-}$ after LPS injection unlike APP/PS1 mice. Thus NLRP3 inhibition may represent a novel therapeutic candidate for brain protection during systemic inflammation.

6 Results: ASC cross-seeding Aβ

Neuroinflammation, and particularly microglial activation has been extensively documented in AD patients and murine models. Amyloid deposition triggers NLRP3 activation in microglia cells, thus contributing to the neuroinflammatory process. However, the role of microglia cells spreading the disease has not been studied before. This chapter focuses on the role of the immune response, particularly the inflammasome complex protein ASC, in the spreading of Aβ pathology.

6.1 ASC specks enhances Aβ aggregation

It has been extensively documented that the innate immune system is involved in the initiation and progression of AD. This has been reflected by genetic (51, 52), epigenetics (169) and transcriptome (162) studies. Despite these advances, the connection between the immune system (particularly microglia cells) and the hallmarks of the disease is still unclear. Deposition and spreading of Aβ pathology is a phenomena that probably precedes the appearance of clinical symptoms by decades (170) and therefore the mechanisms involved in these processes are believed to hold therapeutic potential for AD. Once aggregated, Aβ is sensed by microglial pattern-recognition receptors leading to pathological innate immune activation and subsequent production of inflammatory mediators (66). Activation of the NLRP3 inflammasome, a central sensor for danger signals, has recently been documented in the brains of patients with AD and in APP/PS1 transgenic mice (88). Genetic deficiency in NLRP3 or caspase-1 both protect aged APP/PS1 mice against microglial IL-1β production, Aβ-related pathology and development of cognitive decline (88). Previous findings, which showed a very early and focal immune activation of IL-1β^{+} microglia in similar mouse models of AD, prompted the question whether activation of the NLRP3 inflammasome contributes to the progression and spreading of Aβ pathology. After NLRP3 activation, the adaptor protein ASC is recruited via interactions with its PYD domain, leading to the formation of an ASC speck. Indeed, in addition to causing pro-inflammatory IL-1β cytokine activation and release, NLRP3 inflammasome activity also results in the release of assembled ASC specks, which, once released into the intercellular space, can be taken up by neighboring myeloid cells to sustain the ongoing immune response (171). ASC specks were only visualized in brain sections of AD patients and in APP/PS1 transgenic mice (figure 24a-e). Neither age-matched controls nor wild-type brain sections showed any ASC immunopositive signals (figure 24b,c).

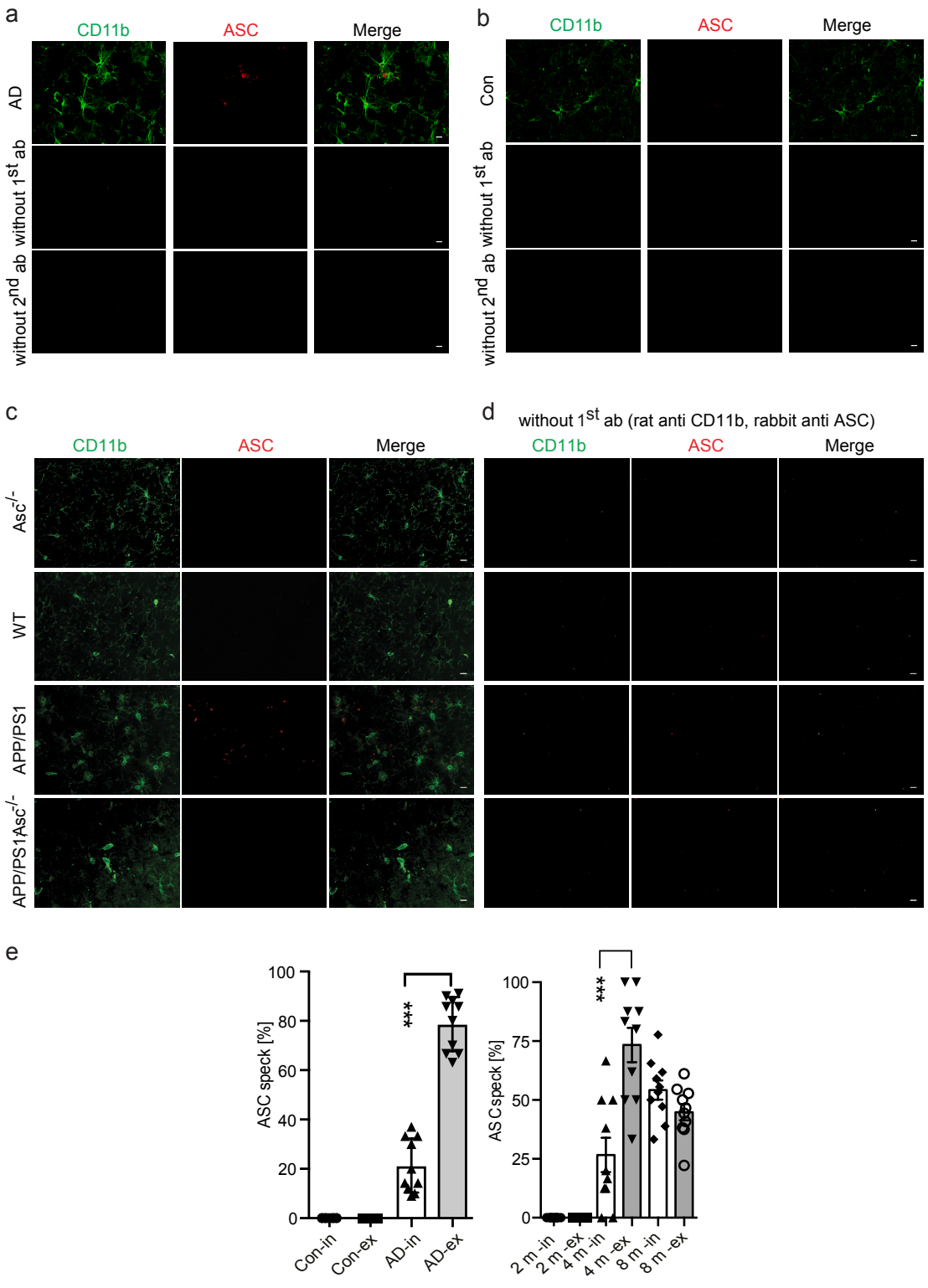

Figure 24. Characteristics of microglial ASC-speck formation in mice and humans
a,b) Immunohistochemistry of the microglial marker CD11b and ASC in sections derived from brains of patients with AD (a) or controls without dementia (Con) (b), and omitting either the primary (middle) or secondary (bottom) antibody. c) Hippocampal sections of 8-month-old wild-type (WT), Asc−/−, APP/PS1 and APP/PS1;Asc−/− mice were stained for the microglial marker CD11b and ASC in the presence of

primary and secondary antibodies (left) or in the absence of the respective primary antibody (right). d) Percentage of ASC specks detected by immunohistochemistry in- and outside (-in and -ex, respectively, on y axis) of microglial cells in sections derived from the hippocampus of APP/PS1 mice at the indicated ages given in months (m). (mean of 10±SEM. Two-tailed Student's t-test, ***P<0.0001

As an additional control, ASC was completely absent in brain sections of wild-type and APP/PS1 ASC knock-out mice (figure 24c,d). In brain sections where no amyloid deposition was present, ASC specks were mainly visualized intracellularly in $CD11b^+$ cells (figure 25a,b). ASC specks could also be found in the extracellular space although, in a minor proportion. ASC specks were visualized in the extracellular space; they were mainly bound to the core of the Aβ deposit (figure 25c-e). In line with these observations, it was found that ASC expression increases with age in APP/PS1, but not in wild-type, mice (3). This suggests that ASC-speck-mediated innate immune responses may result in cross-seeding of Aβ at an early stage of Aβ aggregation and deposition in vivo. In order to confirm these findings, thioflavin-T (ThT) assay (172) was employed. ThT is widely used for the identification and quantification of amyloid fibrils *in vitro*, and has become the premier technique used to monitor fibrillation kinetics in real-time (172). When ThT is added to samples containing β-sheet-rich structure of amyloid fibrils, it fluoresces strongly with excitation and emission maxima at approximately 440 and 490nm respectively (172). Interestingly, when using purified ASC specks generated by immunoprecipitation and enzymatic cleavage, analyses of ThT fluorescence assays further revealed that co-incubation with $A\beta_{1–42}$ accelerated Aβ aggregation in a time- and concentration-dependent manner. The decreased lag phase of aggregation in the presence of ASC indicates an increase in the formation of seeding nuclei (3). Moreover, this result was confirmed by western blot analysis, showing that ASC specks enhanced $A\beta_{1-42}$ oligomer formation (3)

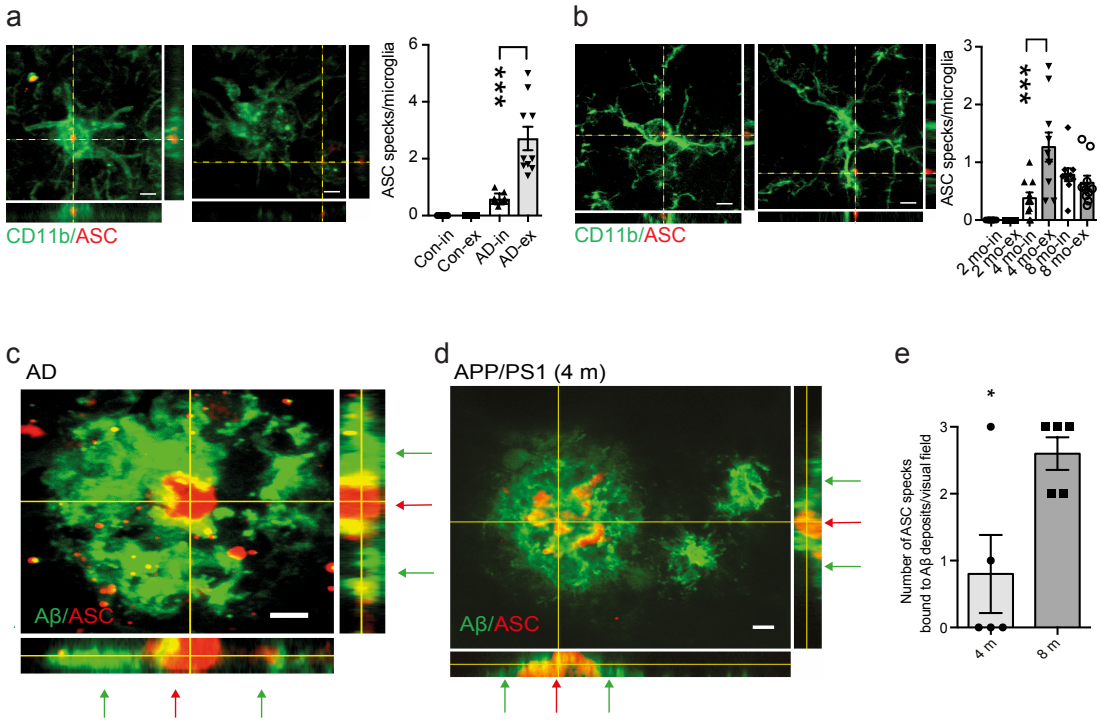

Figure 25. Microglia-released ASC specks bind to and cross-seed β-amyloid peptides
a) ASC specks detected in- and outside (ex) of microglia in hippocampal sections of brains of patients with AD and age-matched controls without dementia (mean of 10±SEM; one-way ANOVA followed by Tukey's *post hoc* test ***P<0.0001). Scale bar: 10μm. b) Microglia containing ASC specks and free ASC specks in the hippocampus of APP/PS1 mice and quantification at various ages (mean of 10±SEM; one-way ANOVA followed by Tukey's *post hoc* test ***P<0.0001). Scale bar: 10μm c) Co-immunohistochemistry of a deposit in the hippocampus of a patient with AD using ASC (AL177) and Aβ (6E10) antibodies. Arrows indicate AL177 (red) and 6E10 (green) immunoreactivity. Scale bar: 10μm. d) Co-immunohistochemistry of an early Aβ deposit in an APP/PS1 mouse at 4 months (4 m) using ASC (AL177) and Aβ (6E10) antibodies. Scale bar: 10μm. e) Number of ASC specks bound to Aβ deposits per visual field observed. n = 5 mice. Two-tailed Student's t-test, * P <0.05

7 Discussion chapter 6

Traditionally, neuroinflammation in the context of AD has been viewed as a consequence or bystander during the progression of the disease. Previous research showed that activation of the NLRP3 inflammasome by Aβ is essential for IL-1β maturation and the subsequent inflammatory cascade (85). In line with this, post-mortem analysis of brains from AD patients showed that NLRP3 was activated. This is reflected by the increased levels of caspase-1 in cortex and hippocampus of AD patients (88). Furthermore, APP/PS1 mice with *Nlrp3*

deficiency were largely protected from spatial memory loss and Aβ pathology (88). These observations led to the question of whether innate immunity is a consequence or a cause of AD. The data presented in this part of the dissertation showed that microglia cells are not only sensors for damage but also great contributors to AD progression. Particularly here, it has been shown that ASC specks released by microglia bind rapidly to Aβ and increase the formation of Aβ oligomers and aggregates acting as an inflammatory-driver for cross-seeding Aβ pathology. ASC specks are found exclusively in brains of AD patients or APP/PS1 transgenic mice (figures 24, 25). Moreover, ASC expression was increased in APP/PS1 mice but not in wild-type mice (figure 14f). Further research either *in vitro* or *in vivo* confirmed the interaction between ASC specks and Aβ (3). Using gradient centrifugation it has been shown that ASC-immunopositive material was located mainly in the core of the amyloid deposits (3). Importantly, the cross seeding activity of ASC has been corroborated *in vivo*. Intra-hippocampal injections of ASC specks increased the number and area of Aβ deposits without changes in expression of APP or APP-cleavage products (3). Finally, confirming these previous observations, treatment with an anti-ASC antibody reduced Aβ deposition without changes in APP expression or APP-cleavage products (3). Together, these data suggest that ASC specks contribute to Aβ aggregation and spreading. Previous experiments have reported that synthetic Aβ does not efficiently induce Aβ -deposit formation, suggesting that a co-factor driving Aβ assembly and deposition is necessary (173). ASC specks released after innate immune activation by pyroptotic microglia may represent such a cofactor, suggesting that inflammasome activation in the brain is connected to the progression of Aβ deposit formation in AD. Contrary to this putative mechanism, prion-related disease progression was unaffected by genetic deficiency of ASC or NLRP3 in a mouse model of scrapie (174), suggesting that mechanisms driving spreading differ between neurodegenerative disorders. The pathophysiological link between NLRP3 inflammasome responses and Aβ-deposit spreading suggests that pharmacological targeting of inflammasomes and in particular ASC specks could represent a novel treatment option for AD patients.

8 Results: optogenetic modulation of LC

The LC is the major source of NA for the brain. Its major projection areas comprise the cortex and the hippocampus. Besides of its function as a neurotransmitter, NA has been shown to have an immunosuppressive role on microglia cells. During aging and AD the neurons of LC region degenerate nonetheless. Currently there is a lack of animal models for LC degeneration in the context of aging or disease.

This chapter focuses on the generation of new tools to modulate LC activity and how this affects microglial activation

8.1 Generation of transgenic mouse lines for LC optogenetic modulation

LC-derived NA and β-adrenoceptors have been implicated in the physiological modulation of memory formation and retrieval. However, current rodent models of LC loss/NA deficiency are either based on the use of toxins, bearing the risk of potential effects on additional neurotransmitter systems (e.g. 6-hydroxydopamine (6OHDA), N-(2-chloroethyl)-N-ethyl-2-bromobenzylamine hydrochloride (DSP4). Alternatively, genetic knockout strategies have been implemented. These strategies involve dopamine beta hydroxylase ($DBH^{-/-}$), the enzyme on charge of noradrenaline production and Ear2 ($Ear2^{-/-}$), a nuclear receptor essential for the devolvement of LC neurons. However, it is important to mention that these approaches could potentially induce compensatory mechanisms (121, 124). The recent development of optogenetic tools has provided a valuable opportunity to inhibit or stimulate activity in genetically targeted neural populations with high spatial and temporal precision. Optogenetics involve the combination of optical and genetic methods to achieve activation or inhibition of specific cells in living tissues (175).

Therefore we established an inducible murine model that allows for transient silencing of LC activity in response to optogenetic modulation. In order to achieve optical silencing of LC neurons, the bacterial opsin halorodopsin (NpHR) was employed. The bacterial opsins are retinal-binding proteins that combine a light-sensitive domain with an ion channel or pump; providing light-dependent ion transport, membrane potential alteration, and sensory functions to bacteria. The third-generation halorhodopsin eNpHR3.0 is an expression-optimized, yellow-to-red light-driven (~580-680 nm), inward chloride ion pump that causes hyperpolarization and prevents action potentials. For example, illumination of NpHR-expressing neurons leads to reversible photoinhibition of action potential firing/neural activity in these cells (176). Particularly for the LC, it has been demonstrated that continuous photoinhibition of NpHR-expressing

neurons in the LC significantly decreased cortical levels of NA (130). Together these results indicate that NpHR could be employed to successfully inhibit neuronal activity.

In this dissertation LC optogenetic modulation was performed using transgenic mice (see material and methods section), which afford important advantages such as stable and heritable transgene expression patterns across experimental cohorts, precluding the challenges associated to a viral gene delivery system and intraparenchymal irritation. Since NpHR is coupled to the YFP (figure 26a), its expression was restricted to TH positive neurons at the LC when NpHR mice were backcrossed with the TH-cre mice (figure 26b). In addition, no positive immunoreactivity was observed neither for YFP nor for TH when motor and pre-frontal cortex were analyzed (figure 26b). Together these results suggest that LC neurons specifically express NpHR and that this mouse is suitable for optogenetic inhibition.

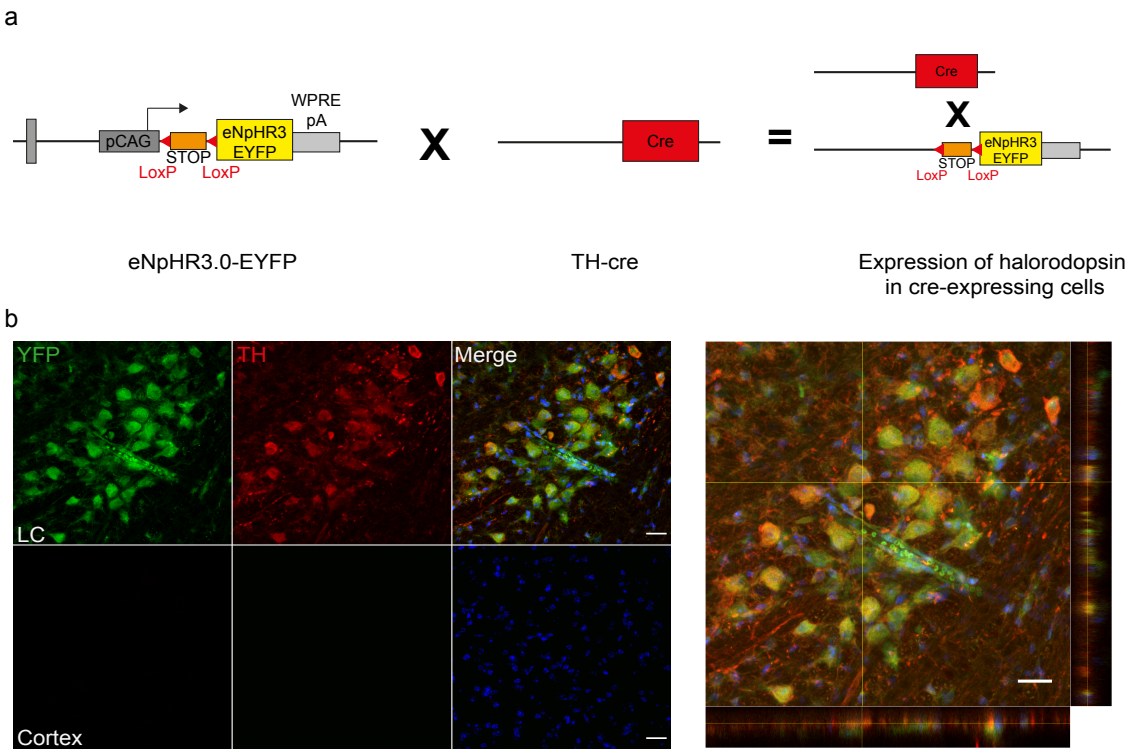

Figure 26. LC optogenetic modulation in transgenic mouse lines. a) Halorodopsin mouse was crossed with TH-cre mouse resulting in halorodopsin expression in cre-expressing cells. b) Representative microscopy images from LC and cortex showing halorodopsin expression restricted to TH neurons in LC. Scale bar 20μm.

8.2 Optogenetic inhibition decreases neuronal activity in LC but not in cortex

In order to confirm that optogenetic modulation of LC was successful, c-fos immunoreactivity was measured as a cellular correlate of neuronal activity (177). C-fos is commonly used as a

neuronal activity marker (178), therefore it was hypothesized that changes in c-fos immunoreactivity should be observed in the LC upon optogenetic modulation.

After 1-hour of continuous LC inhibition, a significant decrease in c-fos immunoreactivity was observed in LC of TH-cre/H-ROSA mice but not in H-ROSA mice (figure 27). In addition, when motor cortex from the very same animals was evaluated for c-fos immunoreactivity, no differences were observed between TH-cre/H-ROSA and H-ROSA mice (figure 27). These results suggest that LC optogenetic modulation was successfully achieved, since a decrease in neuronal activity restricted to the LC was observed.

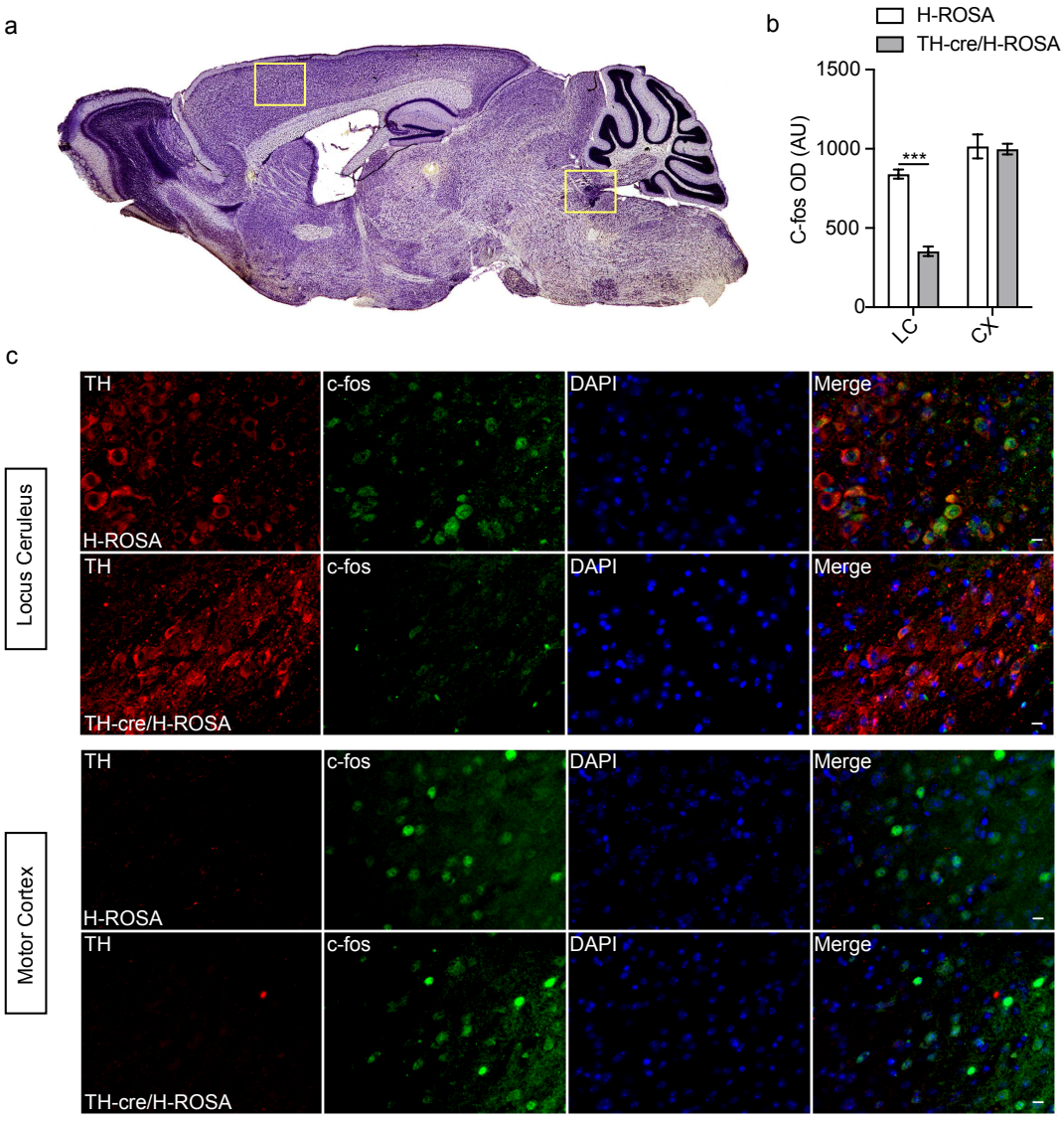

Figure 27. LC optogenetic modulation reduced c-fos immunoreactivity. a) Images were acquired in the LC and motor cortex. b) A significant reduction in C-fos immunoreactivity (green) was observed in the LC of TH-cre/ H-ROSA after 1h inhibition in comparison to control (H-ROSA) mice but not in motor cortex (mean of 3±SEM; two-way ANOVA followed by Sidak's *post hoc* test, ***p<0.001). c) Representative

pictures after 1h inhibition of TH and c-fos staining in the LC (top) and motor cortex (bottom) for H-ROSA and TH-cre/H-ROSA mice. Scale bar 25µm

8.3 LC optogenetic inhibition morphologically activates microglia

Microglia are changing their activation state in response to sustained noradrenergic depletion by the noradrenergic toxin DSP4 (116, 179). However, the dynamics of this change has not been studied so far. Therefore, microglial changes in the motor cortex were assessed by 2PLSM upon optogenetic LC silencing. The latter caused reductions of the number of microglia branches, bifurcations and length of processes, which became detectable 3h post LC silencing and were strongest at 24h (figure 28). Importantly, it was found that these microglial morphological changes were transient in nature. One-week post LC silencing, microglial morphology was back to preinhibition values. It is important to mention that these changes were observed just for the TH-cre/H-ROSA mice while H-ROSA mice remained refractory to photoinhibition. Given the fact that microglial process retraction is a sign of activation, this microglial change may also indicate an increased release of immune mediators, or a decrease in providing trophic factors to neurons. Furthermore, since microglia processes are intimately involved in the maintenance of dendritic spines, it seems likely that process shortening and reduction of branch numbers compromises these microglial actions thereby affecting neuronal network functions.

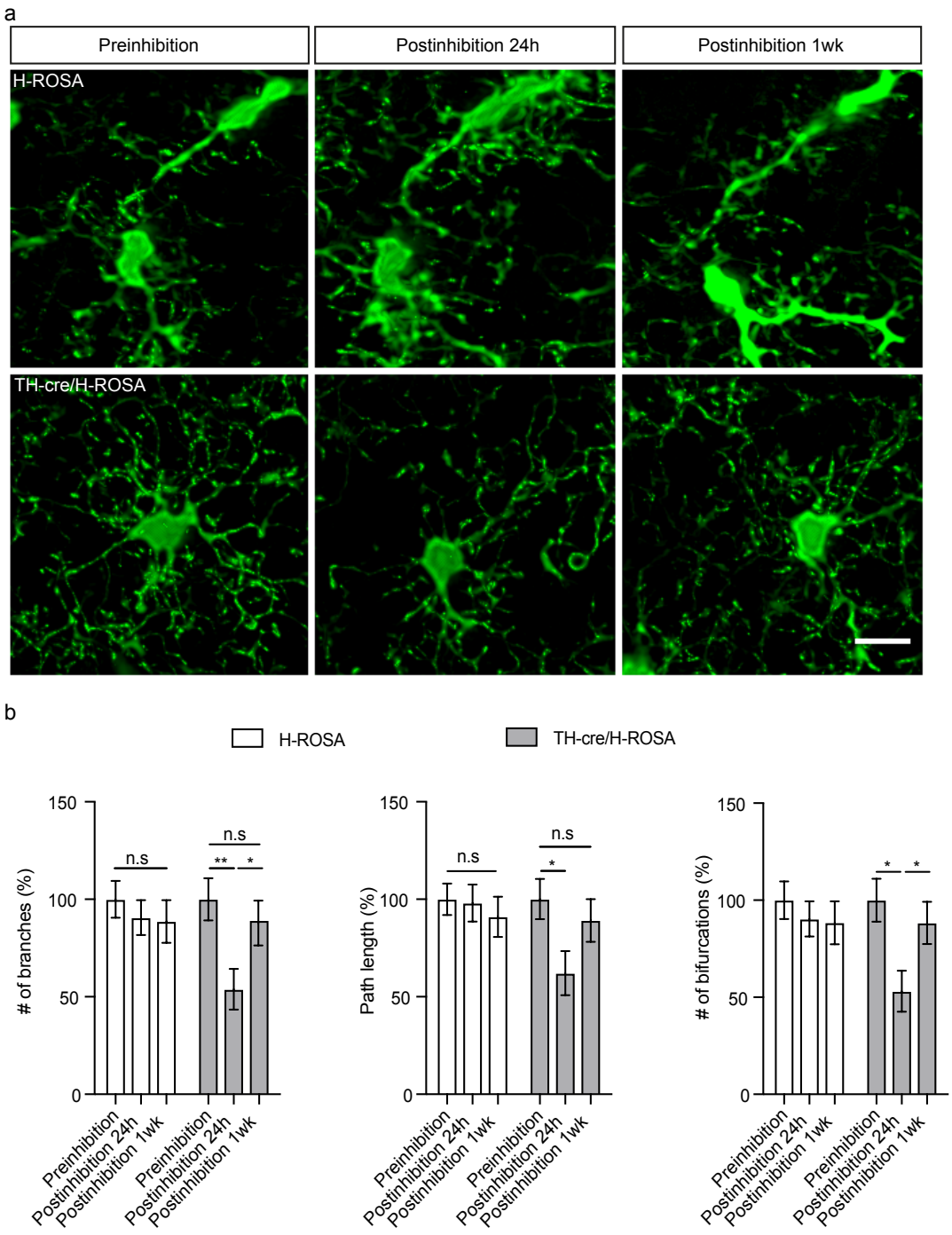

Figure 28. LC optogenetic modulation morphologically activates microglia in motor cortex. a) Representative two-photon images from motor cortex of H-ROSA and TH-cre/H-ROSA before, 24 hours and 1 week after LC inhibition. Scale bar 25µm. b) Quantification of morphological parameters from (a) (mean of 4±SEM; two-way ANOVA followed by Tukey's *post hoc* test, *p<0.05, **p<0.01)

9 Discussion chapter 8

The LC noradrenergic nucleus was the first neuromodulatory system to be delineated anatomically and specified neurochemically (180). As a result, it is the most intensely investigated of these systems. The tiny nucleus LC is situated deep in the pons and sends projections to most other brain regions, including the brainstem, the cerebellum, the diencephalon and the paleo- and neocortex. These noradrenergic projections from the LC to virtually all brain regions (with the notable exception of the basal ganglia) is the sole source of noradrenaline in the forebrain, and a single neuron can innervate diverse regions (105). Notably, due to its great extent of innervation, the LC-NA system has been shown to be involved in behavioral and cognitive functions (e.g. arousal, attention, affective behavior, learning and memory) (105, 121). Histologically and electrophysiologically, identified NA neurons within the LC-NA system of both lightly anesthetized and freely moving rodents, felines, and primates exhibit three distinct activation profiles as follows: (1) low tonic, (2) high tonic, and (3) phasic activity. It has been proposed that these neurons fire differently to determine behavioral flexibility to various environmental challenges. Low-tonic LC discharge (1–2 Hz) is consistent with an awake state, whereas phasic burst activity results from distinct sensory stimuli, such as flashes of light, auditory tones or brief touch. Stressful events and stimuli shift LC activity toward a high-tonic mode of firing (3–8 Hz) (130, 181). Importantly, besides as its role as neurotransmitter, NA has been shown to act as a potent modulator of the micro- and astroglial immune response in the brain (116, 179, 182). However, in the context of normal aging and neurodegeneration (e.g. AD) LC degeneration and therefore NA depletion, is an ubiquitous event years before neurocognitive signs (117, 124). It is worth mentioning that currently there is no single model that mimics LC degeneration in the context of aging and neurodegeneration. So far, the strategies to target LC degeneration rely on the use of genetic knockout mice or the use of toxins. Despite both approaches, effectively targeting LC neurons, neither of them mimics progressive LC degeneration. The use of knockout mice ($DBH^{-/-}$ and $Ear2^{-/-}$) has been shown to induce compensatory mechanisms since they are lacking both the peripheral and central noradrenergic systems (117). On the other hand, the use of neurotoxins such as DSP4 could bare the risk of affecting other neurotransmitter systems such as the dopaminergic and cholinergic systems (121, 124). To overcome these issues, LC was optogenetically silenced in transgenic mice expressing NpHR specifically in LC neurons (figure 16). The use of transgenic

mouse lines to perform optogenetics has a number of advantages over virus-driven optogenetic modulation. These involve stable and heritable transgene expression patterns across experimental cohorts, precluding the challenges associated to a viral gene delivery system and intraparenchymal irritation. Another important advantage of the transgene stable expression is the possibility to longitudinally study the effects of LC modulation. It has been previously shown that inhibition of LC neurons using designer receptor exclusively activated by designer drug (DREADD), triggered a significant decrease of c-fos^{+} neurons (181). C-fos is an immediate early gene expressed in the brain by neurons (183) and has been used as a marker of changing the neuronal activity (177). In concordance with these observations, the decrease observed in c-fos immunoreactivity (figure 27) after LC illumination is an indicator of a successful LC inhibition. Besides its role as neurotransmitter, NA has been shown to possess immunosuppressive activity. Originally described in 1988, NA has been shown to inhibit Interferon-γ expression. In addition, it was demonstrated that this effect was mediated via β-adrenergic receptors (184). Later work confirmed that microglia stimulated either with NA or β-adrenergic agonists suppressed inflammatory-induced responses (111, 182, 185, 186). The fact that LC degeneration is observed in aging and AD, has led to the hypothesis that neuroinflammation is exacerbated due to the lack of NA. This is reflected by findings showing that LC pharmacological ablation increased Aβ and Tau-induced neuroinflammation. In line with these observations, NA depletion also led to increased amyloid and tau pathology (116, 123, 124, 187). Supporting this hypothesis, supplementation with the NA precursor L-threo-DOPS, reverted these effects (116). In consonance with these observations, the results presented in this dissertation showed for the first time microglial activation upon LC optogenetic inhibition *in vivo* (figure 28). Importantly, the changes in microglial morphology, as a measurement of microglial activation, were transient in nature. This observation opens the opportunity to repeatedly inhibit LC optogenetically and observed microglial dynamics. It is worth to mention that future work will be needed in order to discriminate the involvement of NA and LC neuronal activity for the regulation of microglial activation and subsequent neuronal changes in the respective target regions.

10 Conclusions

Collectively the results presented in this dissertation suggest the following:

1) Systemic inflammation transiently activates microglia in an age and NLRP3-dependent manner.
2) Systemic inflammation increases amyloid deposition in an NLRP3-dependent manner by reducing microglial clearance capacity.
3) Systemic inflammation increases microglia proliferation.
4) Inflammasome activation and particularly ASC specks release is connected to seeding and spreading of amyloid-β pathology in patients with AD.
5) Optogenetical modulation of LC transiently activates microglia in projection areas.

11 Future directions

Over the past decade neuroinflammation has emerged as a central component for cerebral aging and the pathogenesis of neurodegenerative diseases. The traditional vision of the brain as an immune-privileged organ has already been overcome. Along this dissertation, many aspects of microglial activation, some of them novel, have been unveiled. However, the deeper we penetrate into our knowledge of microglial activation, the more complex the situation becomes. Far from being discouraging, this is extremely exciting and constructive. Proof of this is the great advance in many areas, traditionally not related to the neuroinflammation field. This is the case of the "omics" revolution. The knowledge acquired during the last years from transcriptomics, metabolomics and connectomics regarding microglial activation, is without any doubts extremely valuable. Despite the progress on the development and generation of new techniques and knowledge, the very same three questions remain. Microglial activation: when, where and how. These three questions are defined based on the high versatility of these cells. Regarding the "when", it seems likely that microglial activation is rigorously timed. Clearly, the microglial activation in the developing brain, -shaping our synaptic circuitry is not the same as during neurodegeneration, albeit similar receptor systems and signaling cascades may be involved. Regarding neurodegenerative disease, while most patients present for diagnosis at 65 years of age and above, evidence suggests that the underlying pathological processes begin years, if not decades, before clinical symptoms appear. Hence, aging may not be the common primary risk factor for developing neurodegenerative disease, but other factors, which initiate the pathological processes in the early adulthood or during the midtime of our lives. Therefore, understanding the changes microglia cells undergo during very early is of utmost interest for future research. With respect to the "where", nowadays we know that microglia populations are heterogeneous within the brain. In line with this observation, it has been demonstrated that certain brain regions show higher vulnerability to neurodegenerative disease. For the future we need focus our efforts to understand how microglial activation could be influenced by neuronal activity and vice versa.

Additionally, in the last decade we have witnessed a paradigm shift regarding the "where". This is reflected by the presence of the novel "gut-brain" axis. It is substantial the amount of evidence suggesting that gut microbiota and immune reactions in the gut, trigger an immune

response in the brain that could lead to neurodegeneration. Thus, we need to incorporate these new sets of data, understanding that microglia actions can be in response to changes in the local environment but also the consequence of processes taking place in distant regions of the very same organism.

Current research points that immune reactions in the brain, particularly microglia activation hold an enormous therapeutic potential for the future. Therefore, clarifying the “how” is an imperative for the future.

Finally, I do not know whether we are going to be able to reveal the many faces of microglial activation, but for sure I know that worth my life as a scientist trying to decipher it.

12 References

1. Heneka MT, Kummer MP, Latz E (2014) Innate immune activation in neurodegenerative disease. *Nat Rev Immunol* 14(7):463–477.
2. Gyoneva S, et al. (2014) Systemic inflammation regulates microglial responses to tissue damage in vivo. *Glia* 62:1345–1360.
3. Venegas C, et al. (2017) Microglia-derived ASC specks cross-seed amyloid-β in Alzheimer's disease. *Nature* 552(7685):355–361.
4. Cunningham C (2013) Microglia and neurodegeneration: The role of systemic inflammation. *Glia* 61(1):71–90.
5. Block ML, Zecca L, Hong J (2007) Microglia-mediated neurotoxicity: uncovering the molecular mechanisms. *Nat Rev Neurosci* 8(January):57–69.
6. Baron R, Babcock A a, Nemirovsky A, Finsen B, Monsonego A (2014) Accelerated microglial pathology is associated with Aβ plaques in mouse models of Alzheimer's disease. *Aging Cell* (January):1–12.
7. Grabert K, et al. (2016) Microglial brain region − dependent diversity and selective regional sensitivities to aging. *Nautre Neurosci* (January). doi:10.1038/nn.4222.
8. Winblad B, et al. (2016) Defeating Alzheimer's disease and other dementias: a priority for European science and society. *Lancet Neurol* 15(5):455–532.
9. Sasaguri H, et al. (2017) APP mouse models for Alzheimer's disease preclinical studies. *EMBO J* 36(17):2473–2487.
10. Baruch K, et al. (2016) PD-1 immune checkpoint blockade reduces pathology and improves memory in mouse models of Alzheimer's disease. *Nat Med* 22(2):135–7.
11. Heneka MT, et al. (2015) Neuroinflammation in Alzheimer's disease. *Lancet Neurol* 14(4):388–405.
12. De Strooper B, Karran E (2016) The Cellular Phase of Alzheimer's Disease. *Cell* 164(4):603–615.
13. Campion D, et al. (1999) Early-Onset Autosomal Dominant Alzheimer Disease: Prevalence, Genetic Heterogeneity, and Mutation Spectrum. *Am J Hum Genet* 65(3):664–670.
14. Ameen-Ali KE, et al. (2017) Review: Neuropathology and behavioural features of transgenic murine models of Alzheimer's disease. *Neuropathol Appl Neurobiol*

43(7):553–570.

15. Eriksen JL, Janus CG (2007) Plaques, tangles, and memory loss in mouse models of neurodegeneration. *Behav Genet* 37(1):79–100.
16. Wild-Bode C, et al. (1997) Intracellular generation and accumulation of amyloid beta-peptide terminating at amino acid 42. *J Biol Chem* 272(26):16085–8.
17. Baker M, et al. (2006) Mutations in progranulin cause tau-negative frontotemporal dementia linked to chromosome 17. *Nature* 442(7105):916–919.
18. He Z, et al. (2018) Amyloid-β plaques enhance Alzheimer's brain tau-seeded pathologies by facilitating neuritic plaque tau aggregation. *Nat Med* 24(1):29–38.
19. Saito T, Matsuba Y, Yamazaki N, Hashimoto S, Saido TC (2016) Calpain Activation in Alzheimer's Model Mice Is an Artifact of APP and Presenilin Overexpression. *J Neurosci* 36(38):9933–9936.
20. Ginhoux F, et al. (2010) Fate mapping analysis reveals that adult microglia derive from primitive macrophages. *Science* 330(6005):841–5.
21. Goldmann T, et al. (2016) Origin, fate and dynamics of macrophages at central nervous system interfaces. *Nat Immunol* advance on(August 2015). doi:10.1038/ni.3423.
22. Prinz M, Erny D, Hagemeyer N (2017) Ontogeny and homeostasis of CNS myeloid cells. *Nat Immunol* 18(4):385.
23. Lawson LJ, Perry VH, Dri P, Gordon S (1990) Heterogeneity in the distribution and morphology of microglia in the normal adult mouse brain. *Neuroscience* 39(1):151–70.
24. Hughes V (2012) Microglia: The constant gardeners. *Nature* 485(7400):570–572.
25. Davalos D, et al. (2005) ATP mediates rapid microglial response to local brain injury in vivo. *Nat Neurosci* 8(6):752–8.
26. Tremblay M-È, et al. (2011) The role of microglia in the healthy brain. *J Neurosci* 31(45):16064–9.
27. Kettenmann H, Kirchhoff F, Verkhratsky A (2013) Microglia: new roles for the synaptic stripper. *Neuron* 77(1):10–8.
28. Schafer DP, et al. (2012) Microglia sculpt postnatal neural circuits in an activity and complement-dependent manner. *Neuron* 74(4):691–705.
29. Tremblay M-È, Lowery RL, Majewska AK (2010) Microglial interactions with synapses are modulated by visual experience. *PLoS Biol* 8(11):e1000527.
30. Parkhurst CN, et al. (2013) Microglia Promote Learning-Dependent Synapse Formation through Brain-Derived Neurotrophic Factor. *Cell* 155(7):1596–1609.
31. Schafer DP, et al. (2012) Microglia sculpt postnatal neural circuits in an activity and

complement-dependent manner. *Neuron* 74(4):691–705.

32. Paolicelli RC, et al. (2011) Synaptic Pruning by Microglia Is Necessary for Normal Brain Development. *Science (80-)* 333:1456–1458.
33. Erion JR, et al. (2014) Obesity elicits interleukin 1-mediated deficits in hippocampal synaptic plasticity. *J Neurosci* 34(7):2618–31.
34. d'Avila JC, et al. (2012) Microglial activation induced by brain trauma is suppressed by post-injury treatment with a PARP inhibitor. *J Neuroinflammation* 9(1):31.
35. Lucin KM, et al. (2013) Microglial beclin 1 regulates retromer trafficking and phagocytosis and is impaired in Alzheimer's disease. *Neuron* 79(5):873–86.
36. Prinz M, Priller J (2014) Microglia and brain macrophages in the molecular age: from origin to neuropsychiatric disease. *Nat Rev Neurosci* 15(5):300–12.
37. Tejera D, Heneka MT (2016) Microglia in Alzheimer ' s Disease : The Good , the Bad and the Ugly. *Curr alzheimer Res*:370–380.
38. Kreutzberg GW (1995) Microglia: a sensor for pathological events in the CNS. *Trends Neurosci* 19(8):312–318.
39. Hickman SE, et al. (2013) The microglial sensome revealed by direct RNA sequencing. *Nat Neurosci* 16(12):1896–1905.
40. Martinez FO, Sica A, Mantovani A, Locati M (2008) Macrophage activation and polarization. *Front Biosci* 13:453–61.
41. Lavin Y, et al. (2014) Tissue-Resident Macrophage Enhancer Landscapes Are Shaped by the Local Microenvironment. *Cell* 159(6):1312–1326.
42. Gosselin D, et al. (2014) Environment Drives Selection and Function of Enhancers Controlling Tissue-Specific Macrophage Identities. *Cell* 159(6):1327–1340.
43. Johnson WJ, Marino PA, Schreiber RD, Adams DO (1983) Sequential activation of murine mononuclear phagocytes for tumor cytolysis: differential expression of markers by macrophages in the several stages of development. *J Immunol* 131(2):1038–43.
44. Perry VH, Teeling J (2013) Microglia and macrophages of the central nervous system: The contribution of microglia priming and systemic inflammation to chronic neurodegeneration. *Semin Immunopathol* 35(5):601–612.
45. Mosher KI, Wyss-Coray T (2014) Microglial dysfunction in brain aging and Alzheimer's disease. *Biochem Pharmacol* 88(4):594–604.
46. Streit WJ (2004) Microglia and Alzheimer's disease pathogenesis. *J Neurosci Res* 77(1):1–8.
47. Mackenzie IR (2000) Anti-inflammatory drugs and Alzheimer-type pathology in aging.

Neurology 54(3):732–4.

48. Weggen S, et al. (2001) A subset of NSAIDs lower amyloidogenic Abeta42 independently of cyclooxygenase activity. *Nature* 414(6860):212–6.
49. Hickman SE, Allison EK, El Khoury J (2008) Microglial dysfunction and defective beta-amyloid clearance pathways in aging Alzheimer's disease mice. *J Neurosci* 28(33):8354–60.
50. Rubio-Perez JM, Morillas-Ruiz JM (2012) A review: inflammatory process in Alzheimer's disease, role of cytokines. *ScientificWorldJournal* 2012:756357.
51. Guerreiro R, et al. (2013) TREM2 variants in Alzheimer's disease. *N Engl J Med* 368(2):117–27.
52. Bradshaw EM, et al. (2013) CD33 Alzheimer's disease locus: altered monocyte function and amyloid biology. *Nat Neurosci* 16(7):848–50.
53. Jiang T, et al. (2014) CD33 in Alzheimer's disease. *Mol Neurobiol* 49(1):529–35.
54. Lajaunias F, Dayer J-M, Chizzolini C (2005) Constitutive repressor activity of CD33 on human monocytes requires sialic acid recognition and phosphoinositide 3-kinase-mediated intracellular signaling. *Eur J Immunol* 35(1):243–51.
55. Hollingworth P, et al. (2011) Common variants at ABCA7, MS4A6A/MS4A4E, EPHA1, CD33 and CD2AP are associated with Alzheimer's disease. *Nat Genet* 43(5):429–35.
56. Griciuc A, et al. (2013) Alzheimer ' s Disease Risk Gene CD33 Inhibits Microglial Uptake of Amyloid Beta. *Neuron* 78:631–643.
57. Rosenthal SL, Kamboh MI (2014) Late-Onset Alzheimer's Disease Genes and the Potentially Implicated Pathways. *Curr Genet Med Rep* 2:85–101.
58. Wang Y, et al. (2016) TREM2-mediated early microglial response limits diffusion and toxicity of amyloid plaques. *J Exp Med*:jem.20151948.
59. Hamerman JA, et al. (2006) Cutting edge: inhibition of TLR and FcR responses in macrophages by triggering receptor expressed on myeloid cells (TREM)-2 and DAP12. *J Immunol* 177(4):2051–5.
60. Turnbull IR, et al. (2006) Cutting edge: TREM-2 attenuates macrophage activation. *J Immunol* 177(6):3520–4.
61. Takahashi K, Rochford CDP, Neumann H (2005) Clearance of apoptotic neurons without inflammation by microglial triggering receptor expressed on myeloid cells-2. *J Exp Med* 201(4):647–57.
62. Heneka MT, O'Banion MK (2007) Inflammatory processes in Alzheimer's disease. *J Neuroimmunol* 184(1–2):69–91.

63. Hickman SE, El Khoury J (2014) TREM2 and the neuroimmunology of Alzheimer's disease. *Biochem Pharmacol* 88(4):495–8.
64. Wang Y, et al. (2015) TREM2 Lipid Sensing Sustains the Microglial Response in an Alzheimer's Disease Model. *Cell*. doi:10.1016/j.cell.2015.01.049.
65. Ulland TK, et al. (2017) TREM2 Maintains Microglial Metabolic Fitness in Alzheimer's Disease. *Cell* 170(4):649–663.e13.
66. Heneka MT, Golenbock DT, Latz E (2015) Innate immunity in Alzheimer's disease. *Nat Immunol* 16(3):229–36.
67. Dinarello CA (1997) Interleukin-1. *Cytokine Growth Factor Rev* 8(4):253–65.
68. Akiyama H, et al. (2000) Inflammation and Alzheimer's disease. *Neurobiol Aging* 21(3):383–421.
69. Lucin KM, Wyss-Coray T (2009) Immune activation in brain aging and neurodegeneration: too much or too little? *Neuron* 64(1):110–22.
70. Paranjape GS, Gouwens LK, Osborn DC, Nichols MR (2012) Isolated amyloid-β(1-42) protofibrils, but not isolated fibrils, are robust stimulators of microglia. *ACS Chem Neurosci* 3(4):302–11.
71. Lim GP, et al. (2000) Ibuprofen suppresses plaque pathology and inflammation in a mouse model for Alzheimer's disease. *J Neurosci* 20(15):5709–14.
72. Sabio G, Davis RJ (2014) TNF and MAP kinase signalling pathways. *Semin Immunol*:1–9.
73. Guerrini MM, et al. (2015) Inhibition of the TNF Family Cytokine RANKL Prevents Autoimmune Inflammation in the Central Article Inhibition of the TNF Family Cytokine RANKL Prevents Autoimmune Inflammation. *Immunity* 43:1–12.
74. Rubio-Perez JM, Morillas-Ruiz JM (2012) A review: inflammatory process in Alzheimer's disease, role of cytokines. *ScientificWorldJournal* 2012:1–16.
75. Perry RT, Collins JS, Wiener H, Acton R, Go RCP (2001) The role of TNF and its receptors in Alzheimer ' s disease. *Neurobiol Aging* 22:873–883.
76. Mehlhorn G, Hollborn M, Schliebs R (2000) Induction of cytokines in glial cells surrounding cortical beta-amyloid plaques in transgenic Tg2576 mice with Alzheimer pathology. *Int J Dev Neurosci* 18(4–5):423–31.
77. Krabbe G, et al. (2013) Functional impairment of microglia coincides with Beta-amyloid deposition in mice with Alzheimer-like pathology. *PLoS One* 8(4):e60921.
78. He P, et al. (2007) Deletion of tumor necrosis factor death receptor inhibits amyloid beta generation and prevents learning and memory deficits in Alzheimer's mice. *J Cell Biol*

178(5):829–41.

79. Vanaja SK, Rathinam VAK, Fitzgerald KA (2015) Mechanisms of inflammasome activation : recent advances and novel insights. *Trends Cell Biol* 25(5):308–315.
80. Franchi L, Eigenbrod T, Muñoz-Planillo R, Nuñez G (2009) The inflammasome: a caspase-1-activation platform that regulates immune responses and disease pathogenesis. *Nat Immunol* 10(3):241–247.
81. Fink SL, Cookson BT (2006) Caspase-1-dependent pore formation during pyroptosis leads to osmotic lysis of infected host macrophages. *Cell Microbiol* 8(11):1812–25.
82. Walsh JG, Muruve D a., Power C (2014) Inflammasomes in the CNS. *Nat Rev Neurosci* 15(February). doi:10.1038/nrn3638.
83. Lu A, et al. (2014) Unified polymerization mechanism for the assembly of ASC-dependent inflammasomes. *Cell* 156(6):1193–1206.
84. Masumoto J, et al. (1999) ASC, a novel 22-kDa protein, aggregates during apoptosis of human promyelocytic leukemia HL-60 cells. *J Biol Chem* 274(48):33835–8.
85. Halle A, et al. (2008) The NALP3 inflammasome is involved in the innate immune response to amyloid-beta. *Nat Immunol* 9(8):857–65.
86. Cassel SL, Joly S, Sutterwala FS (2009) The NLRP3 inflammasome: a sensor of immune danger signals. *Semin Immunol* 21(4):194–8.
87. Latz E, Xiao TS, Stutz A (2013) Activation and regulation of the inflammasomes. *Nat Rev Immunol* 13(6):397–411.
88. Heneka MT, et al. (2013) NLRP3 is activated in Alzheimer's disease and contributes to pathology in APP/PS1 mice. *Nature* 493(7434):674–8.
89. Mélik-Parsadaniantz S, Rostène W (2008) Chemokines and neuromodulation. *J Neuroimmunol* 198(1–2):62–8.
90. White FA, et al. (2005) Excitatory monocyte chemoattractant protein-1 signaling is up-regulated in sensory neurons after chronic compression of the dorsal root ganglion. *Proc Natl Acad Sci U S A* 102(39):14092–7.
91. Kim JS, et al. (1995) Expression of monocyte chemoattractant protein-1 and macrophage inflammatory protein-1 after focal cerebral ischemia in the rat. *J Neuroimmunol* 56(2):127–34.
92. Che X, Ye W, Panga L, Wu DC, Yang GY (2001) Monocyte chemoattractant protein-1 expressed in neurons and astrocytes during focal ischemia in mice. *Brain Res* 902(2):171–7.
93. El Khoury J, et al. (2007) Ccr2 deficiency impairs microglial accumulation and accelerates

progression of Alzheimer-like disease. *Nat Med* 13(4):432–8.

94. Fuhrmann M, et al. (2010) Microglial Cx3cr1 knockout prevents neuron loss in a mouse model of Alzheimer's disease. *Nat Neurosci* 13(4):411–3.
95. Lee S, et al. (2010) CX3CR1 deficiency alters microglial activation and reduces beta-amyloid deposition in two Alzheimer's disease mouse models. *Am J Pathol* 177(5):2549–62.
96. Krauthausen M, et al. (2015) CXCR3 promotes plaque formation and behavioral deficits in an Alzheimer ' s disease model. *J Clin Invest* 125(1):365–378.
97. Widmann CN, Heneka MT (2014) Long-term cerebral consequences of sepsis. *Lancet Neurol* 13(June):630–636.
98. Hoogland ICM, Houbolt C, Westerloo DJ Van, Gool WA Van, Beek D Van De (2015) Systemic inflammation and microglial activation : systematic review of animal experiments. *J Neuroinflammation* 12:1–13.
99. Qin L, et al. (2007) Systemic LPS Causes Chronic Neuroinflammation and Progressive Neurodegeneration. *Glia* 462(October 2006):453–462.
100. Walker KA, et al. (2017) Midlife systemic inflammatory markers are associated with late-life brain volume: The ARIC study. *Neurology* 89(22):2262–2270.
101. Combrinck MI, Perry VH CC (2002) Peripheral infection evokes exaggerated sickness behaviour in pre-clinical murine prion disease. *Neuroscience* 112:7–11.
102. Matt SM, Lawson MA, Johnson RW (2016) Aging and peripheral lipopolysaccharide can modulate epigenetic regulators and decrease IL-1?? promoter DNA methylation in microglia. *Neurobiol Aging* 47:1–9.
103. Semmler A, et al. (2008) Sepsis causes neuroinflammation and concomitant decrease of cerebral metabolism. *J Neuroinflammation* 5:38.
104. Kandel ER, Schwartz james H, Jessell TM, Siegelbaum SA, Hudspeth AJ (2013) *Principles of Neural Science* (McGraw Hill). Fifth Edit.
105. Sara SJ (2009) The locus coeruleus and noradrenergic modulation of cognition. *Nat Rev Neurosci* 10(3):211–23.
106. Moore RY, Bloom FE (1979) Central catecholamine neuron systems: anatomy and physiology of the norepinephrine and epinephrine systems. *Annu Rev Neurosci* 2:113–68.
107. Trillo L, et al. (2013) Ascending monoaminergic systems alterations in Alzheimer ' s disease . Translating basic science into clinical care. *Neurosci Biobehav Rev* 37:1363–1379.

108. Shepard KN, Liles LC, Weinshenker D, Liu RC (2015) Norepinephrine Is Necessary for Experience-Dependent Plasticity in the Developing Mouse Auditory Cortex. *J Neurosci* 35(6):2432–2437.
109. O'Dell TJ, Connor SA, Gelinas JN, Nguyen P V (2010) Viagra for your synapses: Enhancement of hippocampal long-term potentiation by activation of beta-adrenergic receptors. *Cell Signal* 22(5):728–36.
110. Pocock JM, Kettenmann H (2007) Neurotransmitter receptors on microglia. *Trends Neurosci* 30(10):527–35.
111. Feinstein DL, et al. (2002) Noradrenergic regulation of inflammatory gene expression in brain. *Neurochem Int* 41(5):357–65.
112. Murchison CF, et al. (2004) A distinct role for norepinephrine in memory retrieval. *Cell* 117(1):131–43.
113. Murchison CF, Schutsky K, Jin S-H, Thomas SA (2011) Norepinephrine and ß$_1$-adrenergic signaling facilitate activation of hippocampal CA1 pyramidal neurons during contextual memory retrieval. *Neuroscience* 181:109–16.
114. Ramos BP, et al. (2005) The beta-1 adrenergic antagonist, betaxolol, improves working memory performance in rats and monkeys. *Biol Psychiatry* 58(11):894–900.
115. Zheng J, Luo F, Guo N, Cheng Z, Li B (2015) β1-and β2-adrenoceptors in hippocampal CA3 region are required for long-term memory consolidation in rats. *Brain Res* 1627:109–18.
116. Heneka MT, et al. (2010) Locus ceruleus controls Alzheimer's disease pathology by modulating microglial functions through norepinephrine. *Proc Natl Acad Sci U S A* 107(13):6058–63.
117. Jardanhazi-Kurutz D, et al. (2011) Distinct adrenergic system changes and neuroinflammation in response to induced locus ceruleus degeneration in APP/PS1 transgenic mice. *Neuroscience* 176:396–407.
118. Iversen LL, et al. (1983) Loss of pigmented dopamine-beta-hydroxylase positive cells from locus coeruleus in senile dementia of Alzheimer's type. *Neurosci Lett* 39(1):95–100.
119. Bondareff W, et al. (1987) Neuronal degeneration in locus ceruleus and cortical correlates of Alzheimer disease. *Alzheimer Dis Assoc Disord* 1(4):256–62.
120. Vijayashankar N, Brody H (1979) A quantitative study of the pigmented neurons in the nuclei locus coeruleus and subcoeruleus in man as related to aging. *J Neuropathol Exp Neurol* 38(5):490–7.
121. Chalermpalanupap T, et al. (2013) Targeting norepinephrine in mild cognitive impairment

and Alzheimer's disease. *Alzheimers Res Ther* 5(2):21.

122. Grudzien A, et al. (2007) Locus coeruleus neurofibrillary degeneration in aging, mild cognitive impairment and early Alzheimer's disease. *Neurobiol Aging* 28(3):327–35.
123. Heneka MT, et al. (2002) Noradrenergic Depletion Potentiates NL -Amyloid-Induced Cortical Inflammation: Implications for Alzheimer's Disease. 22(7):2434–2442.
124. Chalermpalanupap T, et al. (2017) Locus coeruleus ablation exacerbates cognitive deficits, neuropathology, and lethality in P301S tau transgenic mice. *J Neurosci* 38(1):1483–17.
125. Jung S, et al. (2000) Analysis of Fractalkine Receptor CX 3 CR1 Function by Targeted Deletion and Green Fluorescent Protein Reporter Gene Insertion Analysis of Fractalkine Receptor CX 3 CR1 Function by Targeted Deletion and Green Fluorescent Protein Reporter Gene Insertion. *Mol Cell Biol* 20(11):4106–4114.
126. Jankowsky JL, et al. (2001) Co-expression of multiple transgenes in mouse CNS: a comparison of strategies. *Biomol Eng* 17(6):157–65.
127. Kanneganti T-D, et al. (2006) Bacterial RNA and small antiviral compounds activate caspase-1 through cryopyrin/Nalp3. *Nature* 440(7081):233–6.
128. Holtmaat A, et al. (2009) Long-term, high-resolution imaging in the mouse neocortex through a chronic cranial window. *Nat Protoc* 4(8):1128–44.
129. Paxinos G, Watson C (1985) *The Rat Brain in Stereotaxic Coordinates* (Academic Press, San Diego, CA). 3rd Ed.
130. Carter ME, et al. (2010) Tuning arousal with optogenetic modulation of locus coeruleus neurons. *Nat Neurosci* 13(12):1526–33.
131. Bolmont T, et al. (2008) Dynamics of the Microglial/Amyloid Interaction Indicate a Role in Plaque Maintenance. *J Neurosci* 28(16).
132. Scorcioni R, Polavaram S, Ascoli G a (2008) L-Measure: a web-accessible tool for the analysis, comparison and search of digital reconstructions of neuronal morphologies. *Nat Protoc* 3(5):866–76.
133. Bolte S, Cordelieres FP (2006) A guided tour into subcellular colocalization analysis in light microscopy. *J Microsc* 224(3):213–232.
134. Semmler A, Okulla T, Sastre M, Dumitrescu-Ozimek L, Heneka MT (2005) Systemic inflammation induces apoptosis with variable vulnerability of different brain regions. *J Chem Neuroanat* 30(2–3):144–157.
135. Semmler A, et al. (2007) Long-term cognitive impairment, neuronal loss and reduced cortical cholinergic innervation after recovery from sepsis in a rodent model. *Exp Neurol*

204(2):733–740.

136. Raj DDA, et al. (2014) Priming of microglia in a DNA-repair deficient model of accelerated aging. *Neurobiol Aging* 35(9):2147–2160.
137. Fonken LK, et al. (2016) The Alarmin HMGB1 Mediates Age-Induced Neuroinflammatory Priming. *J Neurosci* 36(30):7946–7956.
138. Man SM, et al. (2016) IRGB10 Liberates Bacterial Ligands for Sensing by the AIM2 and Caspase-11-NLRP3 Inflammasomes. *Cell* 167(2):382–396.e17.
139. Maia LF, et al. (2013) Changes in Amyloid- and Tau in the Cerebrospinal Fluid of Transgenic Mice Overexpressing Amyloid Precursor Protein. *Sci Transl Med* 5(194):194re2-194re2.
140. Varvel NH, et al. (2008) A Oligomers Induce Neuronal Cell Cycle Events in Alzheimer's Disease. *J Neurosci* 28(43):10786–10793.
141. Condello C, Yuan P, Schain A, Grutzendler J (2015) Microglia constitute a barrier that prevents neurotoxic protofibrillar abeta42 hotspots around plaques around plaques. *Nat Commun* (May 2014):1–14.
142. Wattananit S, et al. (2016) Monocyte-Derived Macrophages Contribute to Spontaneous Long-Term Functional Recovery after Stroke in Mice. *J Neurosci* 36(15):4182–4195.
143. Lévesque SA, et al. (2016) Myeloid cell transmigration across the CNS vasculature triggers IL-1β–driven neuroinflammation during autoimmune encephalomyelitis in mice. *J Exp Med* 213(6):929–949.
144. Jay TR, et al. (2015) TREM2 deficiency eliminates TREM2+ inflammatory macrophages and ameliorates pathology in Alzheimer's disease mouse models. *J Exp Med* 212(3):2–10.
145. Wohleb ES, et al. (2014) Knockdown of Interleukin-1 Receptor Type-1 on Endothelial Cells Attenuated Stress-Induced Neuroinflammation and Prevented Anxiety-Like Behavior. *J Neurosci* 34(7):2583–2591.
146. Rice RA, et al. (2015) Elimination of Microglia Improves Functional Outcomes Following Extensive Neuronal Loss in the Hippocampus. *J Neurosci* 35(27):9977–9989.
147. Perez OA, et al. (2017) CD169 $^{+}$ macrophages orchestrate innate immune responses by regulating bacterial localization in the spleen. *Sci Immunol* 2(16):eaah5520.
148. Shinde P V., et al. (2017) TNF-mediated survival of CD169 $^{+}$ cells promotes immune activation during vesicular stomatitis virus infection. *J Virol*:JVI.01637-17.
149. Askew K, et al. (2017) Coupled Proliferation and Apoptosis Maintain the Rapid Turnover of Microglia in the Adult Brain. *Cell Rep* 18(2):391–405.

150. Réu P, et al. (2017) The Lifespan and Turnover of Microglia in the Human Brain. *Cell Rep* 20(4):779–784.
151. Olmos-Alonso A, et al. (2016) Pharmacological targeting of CSF1R inhibits microglial proliferation and prevents the progression of Alzheimer's-like pathology. *Brain* 139(3):891–907.
152. Ransohoff RM, Perry VH (2009) Microglial physiology: unique stimuli, specialized responses. *Annu Rev Immunol* 27:119–45.
153. Jo M, et al. (2017) Astrocytic orosomucoid-2 modulates microglial activation and neuroinflammation. *J Neurosci* 37(11):2534–16.
154. Biber K, Neumann H, Inoue K (2007) Neuronal 'On' and 'Off' signals control microglia. *Trends Neurosci* 30(11):596–602.
155. Weberpals M, et al. (2009) NOS2 gene deficiency protects from sepsis-induced long-term cognitive deficits. *J Neurosci* 29(45):14177–84.
156. Semmler A, et al. (2013) Persistent cognitive impairment, hippocampal atrophy and EEG changes in sepsis survivors. *J Neurol Neurosurg Psychiatry* 84(1):62–69.
157. Iwashyna TJ, Ely EW, Smith DM, Langa KM (2010) Long-term Cognitive Impairment and Functional Disability Among Survivors of Severe Sepsis. *JAMA* 304(16):1787.
158. Widmann CN, Heneka MT (2014) Long-term cerebral consequences of sepsis. *Lancet Neurol* 13(6):630–6.
159. Lee JW, et al. (2008) Neuro-inflammation induced by lipopolysaccharide causes cognitive impairment through enhancement of beta-amyloid generation. *J Neuroinflammation* 5(1):37.
160. Joshi YB, Giannopoulos PF, Chu J, Praticò D (2014) Modulation of lipopolysaccharide-induced memory insult, γ-secretase, and neuroinflammation in triple transgenic mice by 5-lipoxygenase. *Neurobiol Aging* 35(5):1024–1031.
161. Gyoneva S, Swanger SA, Zhang J, Weinshenker D, Traynelis SF (2016) Altered motility of plaque-associated microglia in a model of Alzheimer's disease. *Neuroscience* (June). doi:http://dx.doi.org/10.1016/j.neuroscience.2016.05.061.
162. Keren-shaul H, et al. (2017) Article A Unique Microglia Type Associated with Restricting Development of Alzheimer ' s Disease Article A Unique Microglia Type Associated with Restricting Development of Alzheimer ' s Disease. *Cell*:1–15.
163. Song L, Pei L, Yao S, Wu Y, Shang Y (2017) NLRP3 Inflammasome in Neurological Diseases, from Functions to Therapies. *Front Cell Neurosci* 11(March). doi:10.3389/fncel.2017.00063.

164. Lamkanfi M, Dixit VM (2014) Mechanisms and Functions of Inflammasomes. *Cell* 157(5):1013–1022.
165. Yin J, et al. (2017) NLRP3 Inflammasome Inhibitor Ameliorates Amyloid Pathology in a Mouse Model of Alzheimer's Disease. *Mol Neurobiol*. doi:10.1007/s12035-017-0467-9.
166. Lee H-M, Kang J, Lee SJ, Jo E-K (2013) Microglial activation of the NLRP3 inflammasome by the priming signals derived from macrophages infected with mycobacteria. *Glia* 61(3):441–52.
167. Grace PM, et al. (2016) Morphine paradoxically prolongs neuropathic pain in rats by amplifying spinal NLRP3 inflammasome activation. *Proc Natl Acad Sci U S A*:1–10.
168. Youm YH, et al. (2013) Canonical Nlrp3 inflammasome links systemic low-grade inflammation to functional decline in aging. *Cell Metab* 18(4):519–532.
169. Gjoneska E, et al. (2015) Conserved epigenomic signals in mice and humans reveal immune basis of Alzheimer's disease. *Nature* 518(7539):365–9.
170. Jack CR, et al. (2013) Tracking pathophysiological processes in Alzheimer's disease: an updated hypothetical model of dynamic biomarkers. *Lancet Neurol* 12(2):207–16.
171. Baroja-Mazo A, et al. (2014) The NLRP3 inflammasome is released as a particulate danger signal that amplifies the inflammatory response. *Nat Immunol* 15(8):738–748.
172. Hudson SA, Ecroyd H, Kee TW, Carver JA (2009) The thioflavin T fluorescence assay for amyloid fibril detection can be biased by the presence of exogenous compounds. *FEBS J* 276(20):5960–5972.
173. Meyer-Luehmann M, et al. (2006) Exogenous induction of cerebral beta-amyloidogenesis is governed by agent and host. *Science* 313(5794):1781–4.
174. Nuvolone M, Sorce S, Schwarz P, Aguzzi A (2015) Prion pathogenesis in the absence of NLRP3/ASC inflammasomes. *PLoS One* 10(2):e0117208.
175. Deisseroth K (2011) Optogenetics. *Nat Methods* 8(1):26–29.
176. Zhang F, et al. (2007) Multimodal fast optical interrogation of neural circuitry. *Nature* 446(7136):633–639.
177. Gabanyi I, et al. (2016) Neuro-immune Interactions Drive Tissue Programming in Intestinal Macrophages Article Neuro-immune Interactions Drive Tissue Programming in Intestinal Macrophages. *Cell* 164:378–391.
178. Abiega O, et al. (2016) Neuronal Hyperactivity Disturbs ATP Microgradients, Impairs Microglial Motility, and Reduces Phagocytic Receptor Expression Triggering Apoptosis/Microglial Phagocytosis Uncoupling. *PLOS Biol* 14(5):e1002466.
179. Rey NL, et al. (2012) Locus coeruleus degeneration exacerbates olfactory deficits in

APP/PS1 transgenic mice. *Neurobiol Aging* 33(2):426.e1-426.e11.

180. Maeda T (2000) The locus coeruleus: history. *J Chem Neuroanat* 18(1–2):57–64.
181. Mccall JG, et al. (2015) Article CRH Engagement of the Locus Coeruleus Noradrenergic System Mediates Stress-Induced Anxiety Article CRH Engagement of the Locus Coeruleus Noradrenergic System Mediates Stress-Induced Anxiety. *Neuron* 87:605–620.
182. Mori K, Ozaki E, Zhang B, Yang L, Yokoyama A (2002) Effects of norepinephrine on rat cultured microglial cells that. 43:1026–1034.
183. Bullitt E (1990) Expression ofC-fos-like protein as a marker for neuronal activity following noxious stimulation in the rat. *J Comp Neurol* 296(4):517–530.
184. Frohman EM, Vayuvegula B, Gupta S, van den Noort S (1988) Norepinephrine inhibits gamma-interferon-induced major histocompatibility class II (Ia) antigen expression on cultured astrocytes via beta-2-adrenergic signal transduction mechanisms. *Proc Natl Acad Sci U S A* 85(4):1292–6.
185. Kong Y, Ruan L, Qian L, Liu X, Le Y (2010) Norepinephrine promotes microglia to uptake and degrade amyloid beta peptide through upregulation of mouse formyl peptide receptor 2 and induction of insulin-degrading enzyme. *J Neurosci* 30(35):11848–57.
186. Färber K, Pannasch U, Kettenmann H (2005) Dopamine and noradrenaline control distinct functions in rodent microglial cells. *Mol Cell Neurosci* 29(1):128–38.
187. Kummer MP, et al. (2014) Ear2 Deletion Causes Early Memory and Learning Deficits in APP/PS1 Mice. *J Neurosci* 34(26):8845–8854.